5-2022

Electrically Conductive Bearing Adapter Polymer Pad for Use in Freight Railcar Service Applications

Jesse M. Aguilera
The University of Texas Rio Grande Valley

ELECTRICALLY CONDUCTIVE BEARING ADAPTER POLYMER PAD FOR USE IN FREIGHT RAILCAR SERVICE APPLICATIONS

A Thesis

by

JESSE M. AGUILERA

Submitted in Partial Fulfillment of the

Requirement for the Degree of

MASTER OF SCIENCE IN ENGINEERING

Major Subject: Mechanical Engineering

The University of Texas Rio Grande Valley
May 2022

ELECTRICALLY CONDUCTIVE BEARING ADAPTER POLYMER PAD

FOR USE IN FREIGHT RAILCAR SERVICE APPLICATIONS

A Thesis
by
JESSE M. AGUILERA

COMMITTEE MEMBERS

Dr. Constantine Tarawneh, Ph.D.
Co-Chair of Committee

Dr. Robert E. Jones, Ph.D.
Co-Chair of Committee

Dr. Arturo Fuentes, Ph.D.
Committee Member

May 2022

ABSTRACT

Aguilera, Jesse M., Electrically Conductive Bearing Adapter Polymer Pad for Use in Freight Railcar Service Applications. Master of Science in Engineering (MSE), May, 2022, 98 pp., 3 tables, 89 figures, references, 17 titles.

Many freight railcars rest on polymer adapter pads made of injection-molded Thermoplastic Polyurethane (TPU) polymers which feature two copper studs to provide electrical conductivity through the adapter pads, which power onboard systems. In service, pads experience impact and cyclic loading, resulting in wear and plastic compression of the copper studs. This leads to signal interruptions and periodic replacement of the polymer pads, which results in downtime due to maintenance and reduced reliability since pad failure is unpredictable. These limitations in the current design are the impetus to create an electrically conductive polymer adapter pad that does not rely on the inclusion of metal components that are susceptible to wear. Therefore, the University Transportation Center for Railway Safety (UTCRS) has been developing a conductive composite blend of TPU and Carbon Nanofibers (CNF) to create injection-molded polymer composite inserts. The work presented in this thesis focused on fiber alignment that would produce consistent conductivity at all railcar loads. Test results were successful and show that the newly created composite inserts with proper fiber orientation provide approximately double the needed conductivity required for a 24-Volt railcar valve to actuate when tested under the minimum load conditions an adapter would experience in field service.

DEDICATION

To my parents.

ACKNOWLEDGMENTS

To the faculty and staff of the School of Engineering at UTRGV. To all my professors who continue to push me and other students as we are guided towards academic success. To the members of this committee, thank you for taking the time to review this work and for believing in my success. To Dr. Tarawneh, for taking a chance on me when there are hundreds of other students that would do anything for the opportunity that I have been given. Through his mentorship, I acquired knowledge and expertise that will serve me for the rest of my professional career. His constant guidance and encouragement have allowed me to break barriers and reach out for the stars. I can honestly say that I would not be the professional I am today if it were not for him pushing me and guiding me every step of the way.

I would also like to acknowledge the tremendous help and support I received from my fellow research assistant, Mr. Harry Siegel. Thank you for all your help in the lab.

To these people and more, thank you.

Finally, this study was made possible by funding provided by the University Transportation Center for Railway Safety (UTCRS) and the USDOT through the Dwight David Eisenhower Transportation Fellowship Program (DDETFP) through Grant No. 693JJ32145214.

TABLE OF CONTENTS

Page

LIST OF TABLES

Page

LIST OF FIGURES

Page

CHAPTER I

INTRODUCTION, BACKGROUND, AND LITERATURE REVIEW

1.1 Introduction and Background

Despite technological advancements in air, sea, and ground-based transportation, freight rail continues to be the most efficient method of transporting cargo on land in the freight industry. There are a vast number of components and procedures involved in ensuring the safe continuous operation of freight railcars, where any malfunctioning equipment or component can provide a threat to safety, and in extreme cases, cause a derailment which results in massive damage to infrastructure and as a worst outcome, the loss of human life.

Derailments, and other rail incidents and accidents, can arise from mechanical failures stemming from axle-bearing defects. These defects may originate from commonly documented causes for bearing failures such as roller misalignment, contact rolling fatigue (RCF), spalls, water contamination, subsurface inclusions, improper lubrication, lubricant deterioration, and damaged seals [1].

These journal bearings are critical for railcar service. To mitigate bearing component failures, wayside monitoring systems like the Hot Box Detectors (HBDs) and the Trackside Acoustic Detector Systems (TADS®) detect at-risk bearings and flag them for removal from service. However, over the last two decades, technological advancements have led to the development of many onboard systems and devices used for continuous condition monitoring of railcar components to ensure the safe operation of freight trains. Some of these systems require

an electrical signal to be transmitted from the rail tracks to the devices located on the railcar body. For these applications, the electrical signal needs to be transmitted through the railcar's suspension system which includes the wheel, axle, bearing, bearing adapter, and side frame. Although the majority of these components are made from steel, which permits electrical signals to be transmitted, a design modification to the bearing adapter has resulted in some electrical conductivity issues.

The first-generation bearing adapter is an all-metal adapter which permits electrical signals to be transmitted to the side frame and the railcar body. However, the steel-on-steel contact between the adapter and the side frame resulted in excessive wear brought on by the metal-on-metal compressive shear generated during railcar steering.

To combat that, a new bearing adapter design manufactured by Amsted Rail and labeled the AdapterPlus™ [2], pictured in Figure 1, was introduced into the market. The AdapterPlus™ design features a Thermoplastic Polyurethane (TPU) polymer pad (green polymer pad shown in Figure 1) that is meant to improve the axle-to-rail wheelset alignment and prolong the roller bearing service life. The stated performance improvements are predicated on the assumption that the adapter pad absorbs some of the lateral forces and vertical impacts experienced by the bearing, while also providing improved curving and rolling resistance and reducing the wear on the side frame pedestal roof. The manufacturer claims that these features help mitigate the potential for train derailments [2].

Yet, one of the current issues associated with this design is its electrical conductivity. The AdapterPlus™ relies on two copper studs inserted in the polymer pad, as seen in Figure 1, to provide the electrical conductivity needed to power onboard electronics such as gate openers. However, the shear wear and plastic deformation damage dealt to the two copper studs over time

by the high-capacity loads and impacts experienced in freight railcar service tend to compress the studs, as illustrated in the pictures of Figure 2. When these copper studs deform, contact is broken between the side frame and the adapter, which interrupts signal transmission to the automated onboard systems. The replacement procedure is arduous as it involves sidelining the train, isolating the specific railcar with the pad issue, lifting the railcar chassis, and replacing the faulty pad. This process is costly, inefficient, and results in unnecessary delays.

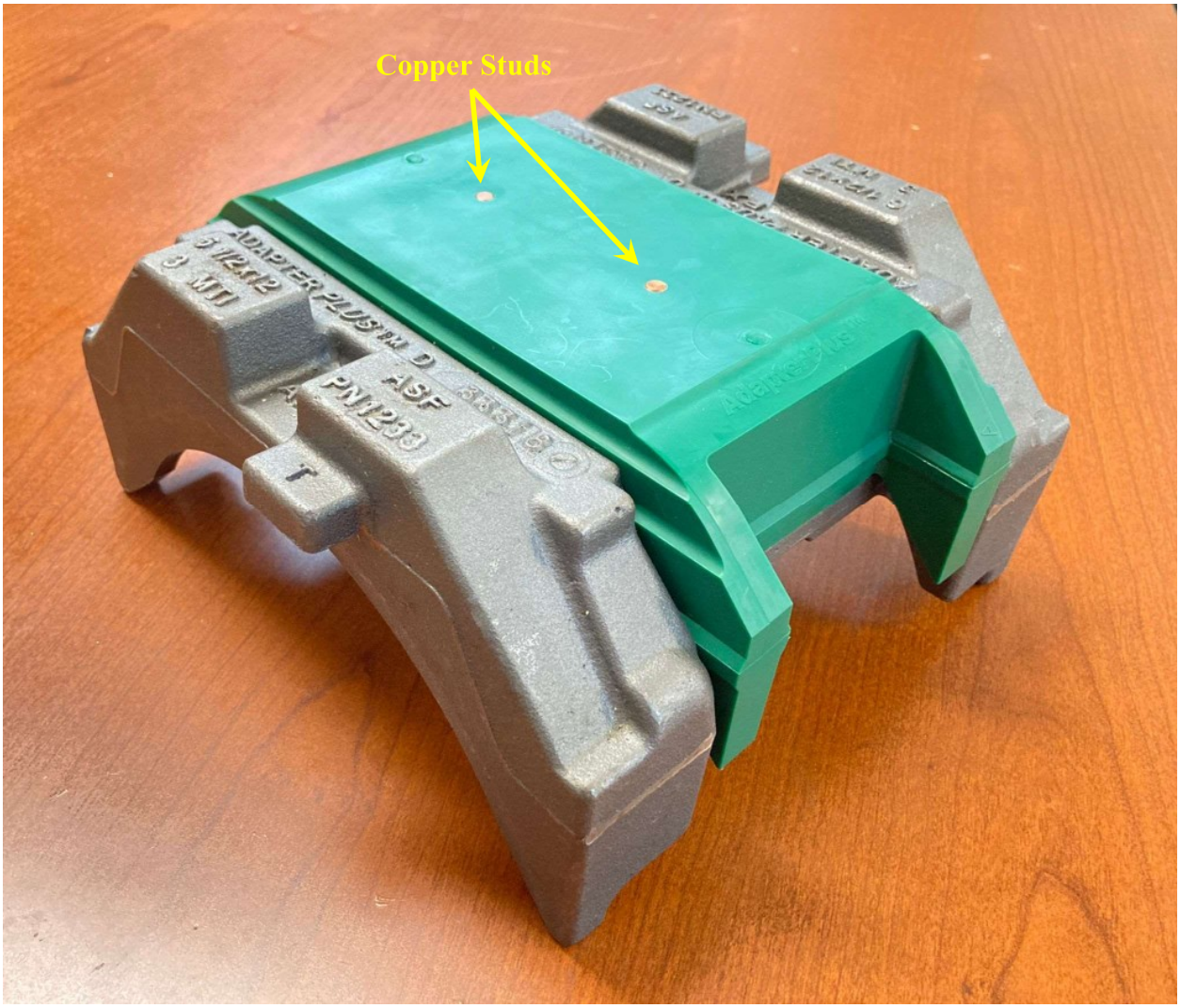

Figure 1. Amsted Rail AdapterPlus™ featuring the Thermoplastic Polyurethane (TPU) green polymer pad with the two-copper stud design

Figure 2: (left to right) New copper stud compared to the plastically deformed copper stud [3]

Motivated by this design oversight, The University Transportation Center for Railway Safety (UTCRS) at The University of Texas Rio Grande Valley (UTRGV) proceeded to explore ways to make the polymer pad electrically conductive without the need to embed the copper studs in the pad. The approach involved mixing additives with the Thermoplastic Polyurethane (TPU) polymer to make it electrically conductive. Initial efforts focused on mixing Carbon Black with the TPU polymer, but the final product did not adhere to the required mechanical properties needed for the polymer pad to survive the harsh conditions seen in rail service [3]. The latter conclusion led to the team shifting focus to Thermoplastic Polyurethane-Carbon Nanofiber (TPU-CNF) composites.

The TPU-CNF composite was selected because of its potential to enhance the mechanical and electrical properties of the adapter polymer pad, currently in service, by providing compressive shear resistance and low electrical resistivity. The composite borrows properties from the carbon nanofibers which include high electrical conductivity, chemical and corrosion

resistance, high thermal conductivity, high elastic modulus, and improved tensile strength.

Elastollan® 1195a, the polymer matrix surrounding the fibers, features abrasion resistance, toughness, transparency, low-temperature flexibility, hydrolytic stability, fungus resistance, damping characteristics, and resistance to tearing propagation [4]. The composite nanofiber blend was offered to the UTCRS in a pelletized form, which was then used to create adapter pad inserts via injection molding. A brief literature review on TPU and CNF is provided hereafter.

1.2 Literature Review

1.2.1 Thermoplastic Polyurethane (TPU)

The polymer adapter pads, currently in service, are manufactured via injection molding using Elastollan® 1195a. This specific TPU (schematically represented in Figure 3) was selected as the matrix for the composite blend because of its favorable characteristics like abrasion resistance, elasticity, and superior mechanical performance which were reliably proven in previous work [3]. Thermoplastic polyurethane is a melt-processable thermoplastic elastomer (TPE) which belongs to a class of copolymers that consist of an elastomeric segment and a thermoplastic segment, allowing for manufacturing processes like injection molding, blow-molding, and extrusion.

One of the main benefits of using TPE is its elastic ability to tolerate moderate elongations and return to its original shape, resulting in a longer service life and sustained physical performance when compared to other materials. TPUs consist of a linear block copolymers composed of segments of variable hardness [5]. This is seen in the schematic diagram of Figure 3.

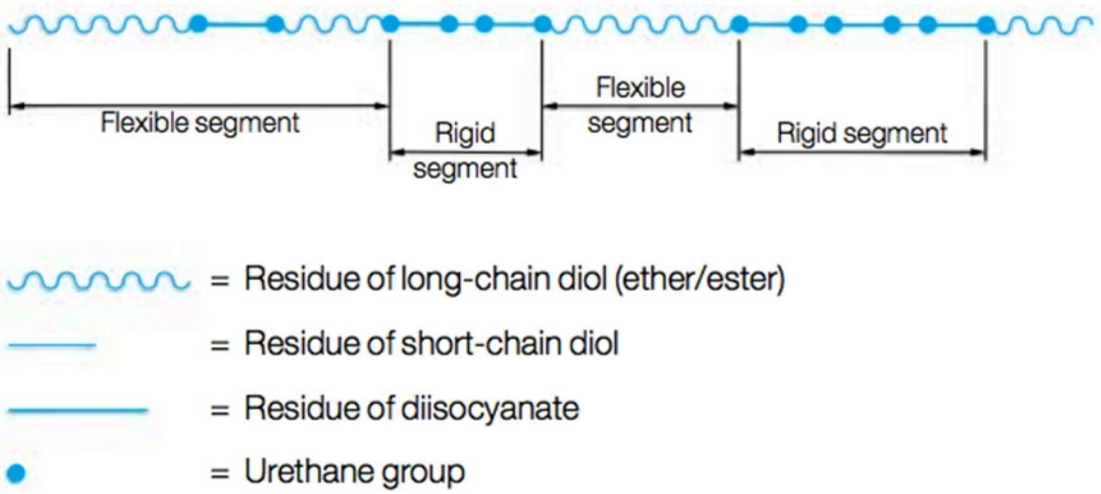

Figure 3: Schematic representation of TPU [6]

The soft segments are built from polyol and diisocyanate, providing flexibility and toughness. The rigid segments are constructed from a chain extender and diisocyanate, providing strength and hardness [6]. These differing segments are not compatible at room temperature, but when melted, they combine and produce favorable material properties such as good wear performance, toughness, and high tensile strength [7]. TPUs are used in the automotive, extruded film, sporting goods, medical, and freight transportation fields. TPUs are also found in simple day-to-day life products like shoe soles, protective phone cases, and power tools.

1.2.2 Carbon Nanofibers (CNF)

The structure of the CNFs used for this research is the ‘stacked cups’ formation, demonstrated in Figure 4, as this structural shape allows extremely high length-to-diameter ratios and provides an excellent surface-area-to-volume ratio. These cylindrical, one-dimensional nanostructures are composed of arranged graphene layers stacked on top of each other as cups, cones, or plates [8].

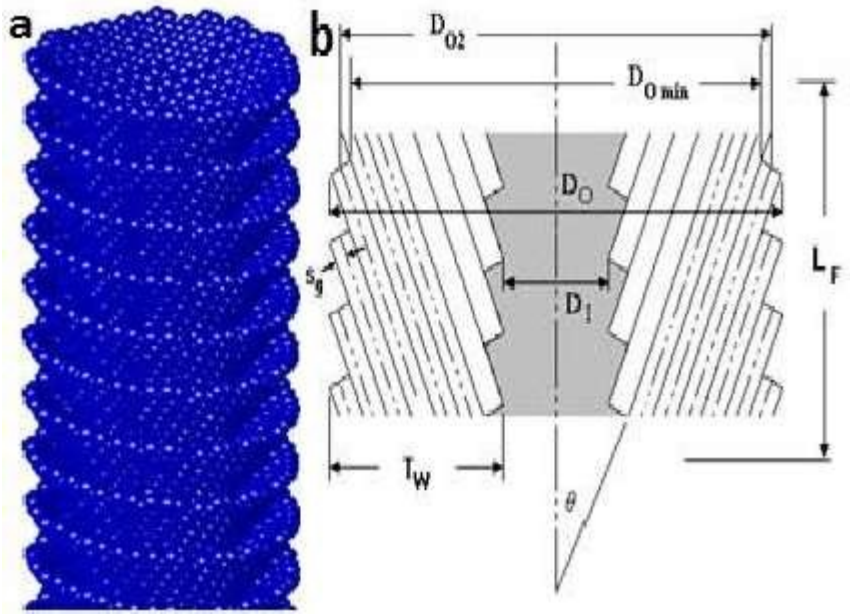

Figure 4: Stacked-cup carbon nanofiber [5]

CNFs are ideal for a polymer matrix because they do not add any additional stress to the polymer backbone, which allows the mechanical properties to be maintained and ensures efficient load transfer between the matrix and the fibers [8]. The fibers are composed of graphene, which is a highly ordered structure that allows excellent mechanical properties in the CNFs, high electrical conductivity, and high thermal conductivity; qualities which will benefit the composite adapter pad inserts.

The fibers are composed of graphene, which is a highly ordered structure that allows excellent mechanical properties in the CNFs, high electrical conductivity, and high thermal conductivity; qualities which will benefit the composite adapter pad inserts.

Direct contact (DC) and quantum tunneling (QT) are two methods of electrical conduction that work in tandem to allow current through the nanofiber composite. DC occurs when the fibers within the matrix directly touch each other, creating a conductive contact fiber chain through the matrix. The fiber chains allow electrons to travel to the lower potential side to pass through the system. DC allows for low fiber percentages to achieve desired conductivity.

The disadvantage of direct contact is the need for physical contact between fibers that could lead to undesirable agglomerates - a mass or collection of nanofibers. These formations have the potential to function like cracks and reduce the mechanical and electrical properties of the fibers. The fiber distribution achieved in these materials is evaluated in Section 4.4 of this thesis.

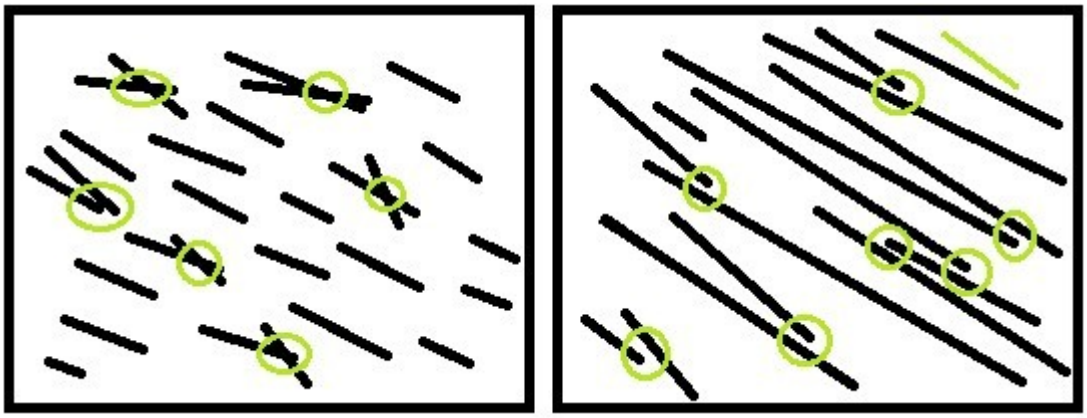

Figure 5: (left to right), Conductivity via direct contact, conductivity via quantum tunneling

Quantum tunneling is a phenomenon that allows electrons to ‘jump’ between fibers within approximately 10 nm of each other but requires a higher concentration of fibers compared to DC. However, QT improves electrical properties and does not provide the potential for cracks or a reduction in mechanical properties. Both conduction mechanisms are illustrated schematically in Figure 5.

These two mechanisms work in tandem to successfully conduct electrical current through the polymer pad, however, the distribution or concentration of one method over the other is largely unintentional, difficult to determine, and a direct result of the injection mold. With that in mind, the work presented in this thesis focusses on the alignment of the carbon nanofibers, which is the most critical factor for consistent conductivity in the fabricated TPU-CNF inserts, and the mold design modifications implemented to ensure an optimized fiber orientation.

In Chapter 2, a summary of the previous work done by the UTCRS team to produce an electrically conductive adapter polymer pad will be presented as well as the motivation behind

the current study. Chapter 3 provides a detailed description on the mold design process and selection which was based on simulations performed using the Mold Flow Advisor software by AutoDesk®. In Chapter 4, an overview of the equipment used to manufacture and test the composite inserts is given along with a description of the methodology and instrumentation utilized. Chapter 5 summarizes the thermal hysteretic properties and creep behavior of the fabricated inserts, and the results regarding resistivity, laboratory validation testing, and polymer pad insert optimization. Lastly, Chapter 6 discusses the main conclusions and findings of the work performed for this thesis.

CHAPTER II

PREVIOUSLY PERFORMED WORK

This chapter outlines the previous work carried out by the UTCRS team which eventually led to the creation of electrically conductive polymer pad inserts through the work presented in this thesis. The chapter summarizes the initial work done by Suarez [3] which focused on the use of Thermoplastic Polyurethane-Carbon Black (TPU-CB) composite blend to manufacture the polymer pad. Following this, research conducted by Basaldua [9] explored the use of Vapor Grown Nanofibers on Thermoplastic Polyurethane to create a puck design by means of transfer molding manufacturing. Third iteration of this project involved the work done by Villarreal [10] who used a Thermoplastic Polyurethane-Carbon Nanofiber (TPU-CNF) composite blend to fabricate inserts for the interlock portions of the polymer pad since these areas of the pad remain under load at both empty and fully loaded railcar conditions. Finally, the motivation behind the current work presented in this thesis is explained at the end of the chapter.

2.1 Thermoplastic Polyurethane–Carbon Black (TPU-CB) Composite

Suarez [3] set out to create an entire freight railcar adapter polymer steering pad that was electrically conductive. He proposed a new composite of TPU blended with a specified weight-percent (wt%) of Carbon Black (CB) that would be used to fabricate an electrically conductive polymer steering pad, as shown in Figure 6, thus eliminating the need for the two copper stud inserts used in the current design.

CB presented many advantages such as affordability, electrical conductivity, and increased thermal conductivity, but it required relatively high additive loading to achieve the desired conductivity. Suarez [3] tested three different CB (1) Columbian N-339 – which is a high conductivity CB, (2) Cabot Vulcan XC72R, which was optimized for high conductivity at low loading levels, and provided good chemical and physical cleanliness and processability, and (3) Ensaco 250 G. which had excellent dispersion and surface quality in polymers, as well as good electrical and thermal conductivity and mechanical properties.

Figure 6: Bearing adapter polymer steering pad manufactured entirely from a TPU-CB composite blend [3]

In his thesis, Suarez [3] concluded that 17 wt% of dispersed CB would provide adequate electrical conductivity to actuate an onboard railcar solenoid valve. Laboratory results showed that undermixing or overmixing the Carbon Black (CB) in the Thermoplastic Polyurethane (TPU) results in loss of conductivity. Full pads were molded from commercially blended TPU-CB composite, but the resulting full pads did not have the desired electrical conductivity. More

importantly, the molded full pads had poor mechanical durability as evidenced by the catastrophic failure of the TPU-CB pad, shown in Figure 7., when subjected to impact testing at cold temperatures (< 0°C).

Figure 7: Fractured TPU-CB molded full pad when subjected to impact testing at cold temperatures (<0°C) [3]

Because the TPU-CB molded full pads did not meet the manufacturer's mechanical requirements, the decision was made to evaluate pad inserts made from CB modified TPU as an alternative approach. Consequently, Suarez [3] tested three insert designs: a large rectangular insert, two smaller rectangular inserts, and a cylindrical "puck" insert shown in Figure 8 and Figure 9.

Figure 8: (left to right) Large rectangular insert and two smaller rectangular inserts [3]

Suarez [3] found that the large rectangular insert provided the highest resulting electrical conductivity at the lowest applied load of 10% of the maximum rated load for class F and K bearings, but unfortunately, it failed mechanical testing. Note that the maximum rated load for class F and class K bearings is 153 kN or 34.4 kips per bearing. The two smaller rectangular inserts passed the mechanical testing but had a lower electrical conductivity than the puck insert.

Lastly, the cylindrical puck insert passed both the mechanical and the initial electrical testing conducted at the full rated load of 153 kN (34.4 kips). However, when service life tests were carried out on the pad with the puck insert, it was revealed that the polymer pad deformed resulting in loss of contact between the electrically conductive puck insert and the metal plate (shown in Figure 9) that simulates the pedestal roof of the side frame when the lowest load of 10% was applied.

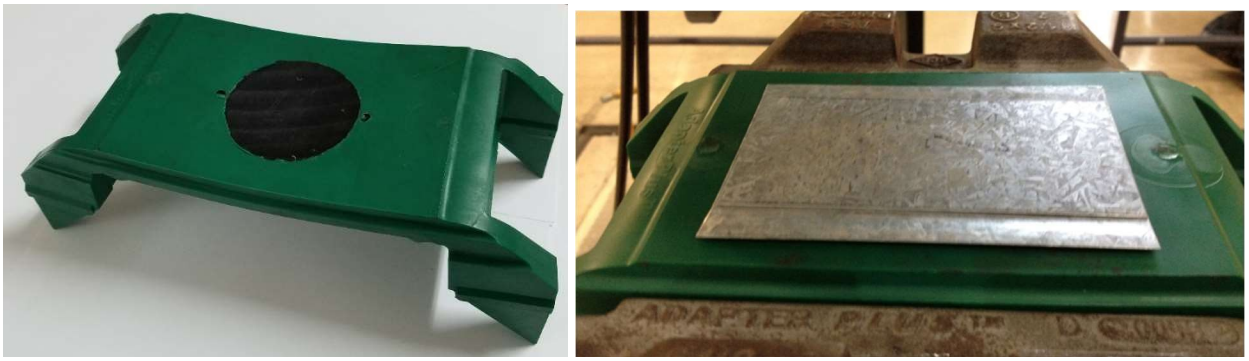
Figure 9: (left to right) circular puck design which was tested with metal plate to simulate pedestal roof of the side frame [3]

2.2 Vapor Grown Carbon Nanofibers in Thermoplastic Elastomer

Following the work of Suarez [3], Basaldua [9] proposed the development of a vapor-grown carbon nanofiber (VGCNF) thermoplastic polyurethane (TPU) composite by means of a melt-mixing process. The goal set out by Basaldua [9] was to create a CNF-TPU composite material and study its mechanical, thermal, and electrical properties to evaluate its potential in railcar service.

Basaldua [9] examined the dispersion and distribution of carbon nanofibers inside the TPU matrix by utilizing scanning electron microscopy to determine homogeneity. The composite material underwent durometer testing, thermal gravimetric analysis, differential scanning calorimetry, heat transfer analysis, hysteresis, dynamic modulus, creep, tensile, abrasion, and electrical conductivity testing to characterize its properties and predict its behavior.

The results of the compression (shown in Figure 10) and injection-molded pucks (shown in Figure 11) indicated that carbon nanofiber additives can potentially enhance the electrical and thermal properties of the composite material but with certain limitations like reduced toughness. The primary concern stemming from the work by Basaldua [9] was balancing the decrease in toughness that accompanied the increased hardness and strength. He proposed that carbon nanofiber reinforced polymers could create a strong material with high elasticity, but the ideal material required further investigation. Basaldua [9] noted temperature effects, alternative-mixing methods, scale-up procedures, and field implementation as potential research areas that could produce the desired qualities [9].

Figure 10: Compression mold [9]

Figure 11: Injection molded composite puck [9]

2.3 Conductive TPU-CNF Composite Steering Adapter Pad for Freight Railcar Service

Villarreal [10] used the previous research conducted by Basaldua [9] regarding transfer molding manufacturing to create a conductive composite insert (aluminum mold shown in Figure

12) made of a Thermoplastic Polyurethane-Carbon Nanofiber blend for the purpose of replacing the interlock portions of the polymer adapter pad, as shown in Figure 13. This design was developed based on the fact that these areas remain under compressive load at both empty and fully loaded railcar conditions.

Figure 12: Machine manufactured aluminum mold for composite insert [10]

Figure 13: Underside view of the prototype pad with TPU-CNF interlock insert [10]

A pressure film study performed by UTCRS in 2012 determined that the main load-bearing portion of the steering pad in unloaded freight railcar conditions was the interlock

portion, represented by the darker shaded regions of Figure 14. For this reason, it was decided to create a conductive insert with the same profile as the interlocks to ensure that the conductive portion of the prototype pad was constantly under compressive load [10].

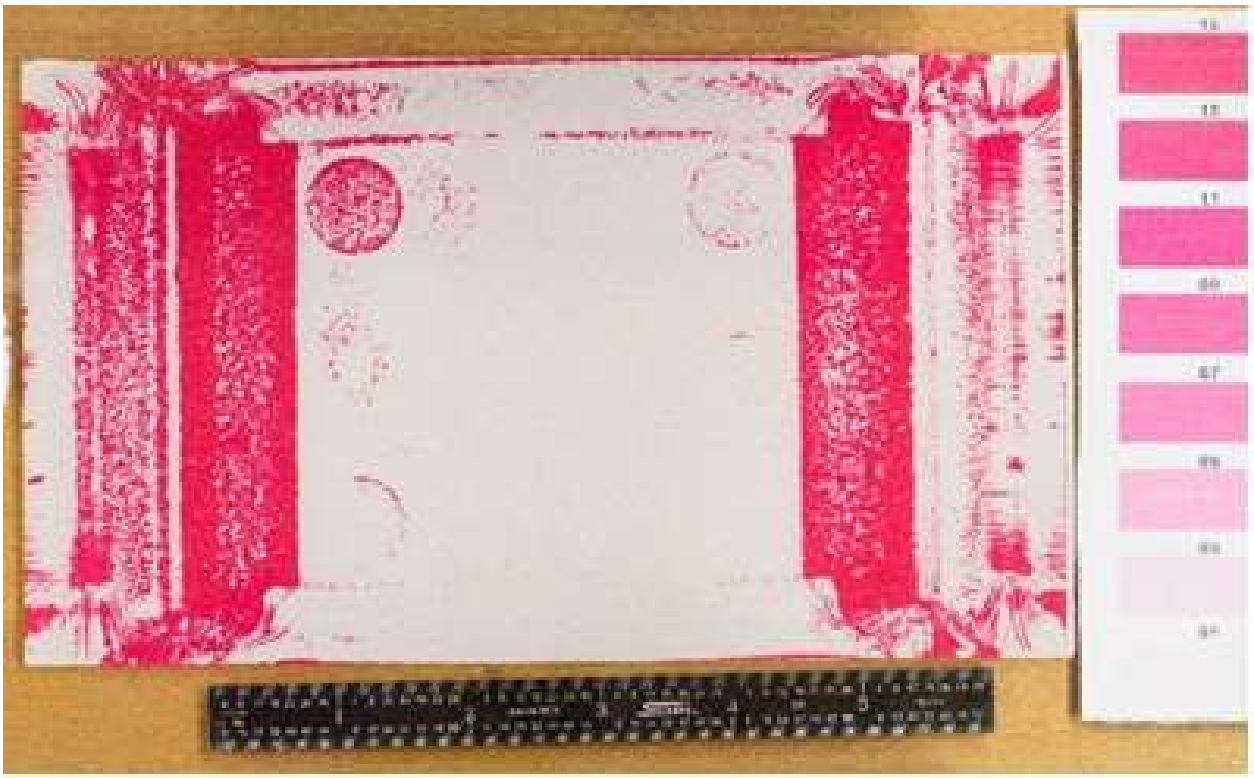

Figure 14: Pressure film load study [10]

The primary goal set out by Villarreal was to create a homogeneous conductive material by blending CNFs with TPU and using the new combined composite to replace part of the current TPU. It was found that using Elastollan® 1195a TPU in a blend of 15 wt% of carbon nanofibers and 85 wt% polymer could produce the desired electrical, mechanical, and thermal properties required for railcar service.

Electrical resistivity tests showed that increasing the applied pressure on the polymer adapter pad between 0 and 926 kPa caused a reduction in resistivity. Note that resistivity is the inverse of conductivity, i.e., a low resistivity implies a high conductivity. Applied stresses greater than 926 kPa affected resistivity to an exponentially lesser degree. Villarreal [10] also

presented a non-linear relationship between resistance and voltage dependence, meaning, as the applied potential difference increased, the resistance of the material decreased [10].

Further resistivity test results showed a noticeable reduction in resistivity when samples were measured horizontally as compared to those measured in the vertical direction. Villarreal concluded that the alignment of the carbon nanofibers played a critical role in the conductivity of the material and future designs needed to optimize this orientation to achieve the desired level of conductivity.

In turn, Villarreal [10] recommended improving the conductivity of future prototypes by optimizing gate placement to cause the nanofibers within the injection molded part to align in the direction of the desired electrical current flow [10].

These previous efforts are the motivation behind the work performed in this study, which is aimed towards bringing this project into conclusion by fabricating TPU-CNF composite inserts with an optimized fiber orientation that provides consistent and reliable electrical conductivity at all operating conditions experienced by the polymer pad in freight rail service.

To achieve the desired fiber alignment, a redesigned model of the interlock portion of the polymer adapter pad was created using AutoDesk® Moldflow Adviser software to simulate the flow of plastic injection into the mold cavity. This software allowed for iterative refinement of the orientation of the short-length carbon nanofibers by optimizing a multi-gate design. The final design was then manufactured to begin molding inserts for testing. The details of the mold design and selection are discussed at length in Chapter 3.

CHAPTER III

MOLD DESIGN PROCESS AND SELECTION

As emphasized at the conclusion of the previous chapter, the proper alignment of the carbon nanofibers during the molding of the adapter pad inserts is the key factor behind ensuring consistent electrical conductivity. The inserts are responsible for allowing the electrical current to flow through them to the onboard systems of the railcars. As explained earlier, the previous work conducted by Villarreal [10] failed to control fiber direction and alignment, which results in inconsistent conductivity, especially at the lower loads simulating an empty railcar load. Therefore, one of the main challenges in this thesis was designing and building a mold that would deliver optimal carbon nanofiber orientation in the fabricated pad inserts to produce the desired electrical conductivity. This chapter describes the work done to arrive at an optimized mold design for the conductive polymer pad inserts.

3.1 Background

Autodesk® Moldflow Advisor software was used to create the final optimized mold design by simulating flow of the liquid TPU-CNF composite into different hypothetical mold designs and predicting fiber alignment and distribution. A stereolithographic model of the interlock section of an AdapterPlus™ polymer steering pad was created using the computer aided design (CAD) software SolidWorks® and imported into Moldflow Advisor where more than 40 different mold designs were developed. Figure 15 is a rendering of the pad insert which

shows the interlock and arm regions as well as the current flow direction of the liquid TPU-CNF composite into the mold.

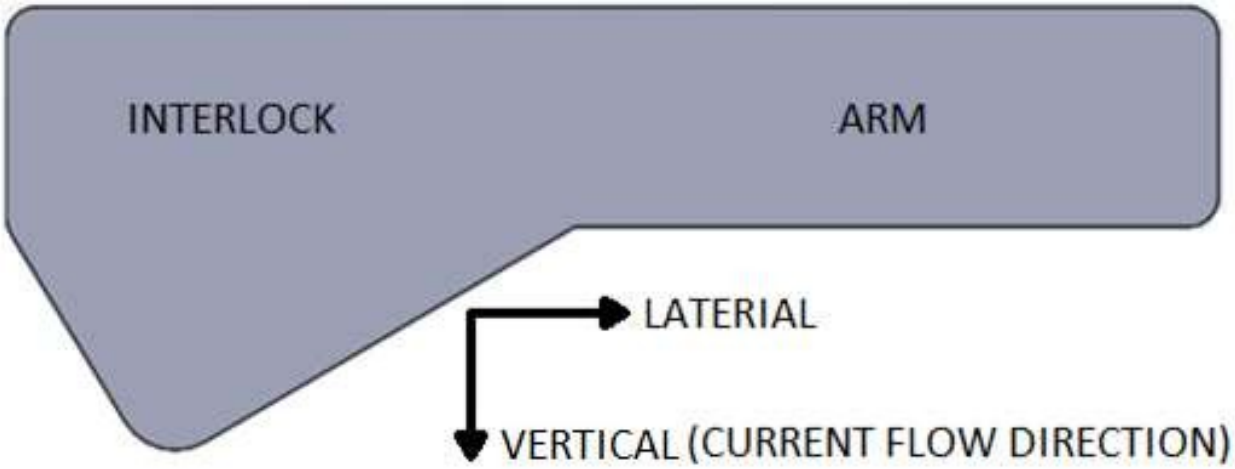

Figure 15: Insert model, front face view with general direction nomenclature, region references, and designated current flow direction

In the mold designs, the three major gate and runner designs explored were: branch, fan, and direct configurations. All designs featured a rectangular gate due to its simplicity and because it allows for a precise gate size. Gate locations vary based on design type. Figure 16 is a pictorial representation of the different injection mold terminology used in this thesis. Note that the commercial software Autodesk® Moldflow Advisor used here does not include flow data for nanofiber systems. Hence, the mold flow simulation modeling performed for this study was done using data for standard short fibers. The models and simulations which guided the final optimized mold design provided an overall map of fiber alignment within the pad insert and predicted high levels of alignment in certain regions.

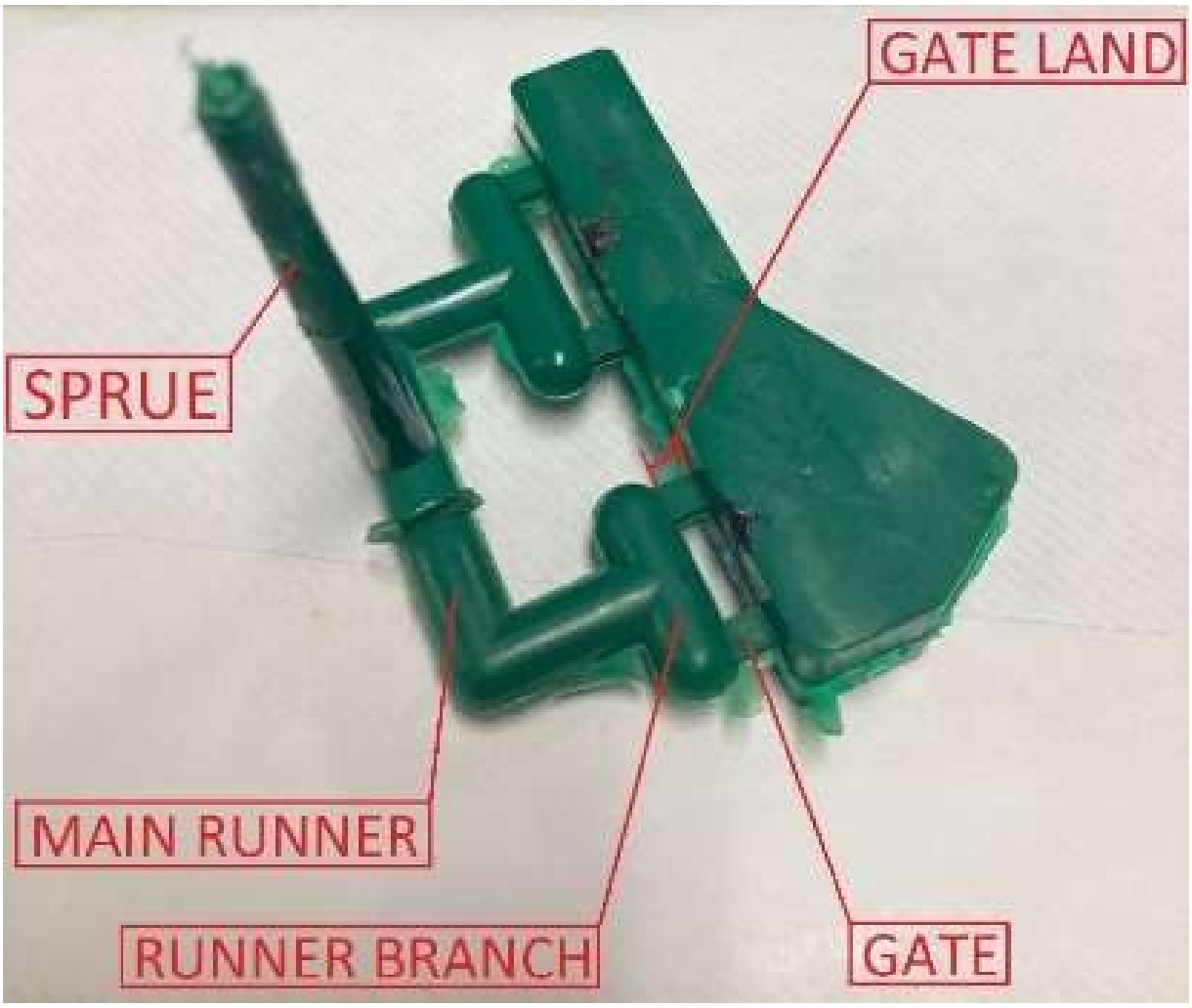

Figure 16: Injection mold terminology

Figure 17 is the simulated fiber alignment of the mold design created by Villarreal [10], which shows the areas near the gate to have the greatest fiber alignment, in the lateral direction, perpendicular to the gate. The simulation results of Figure 17 are in line with the results of his work which showed poor electrical conductivity in the vertical direction.

Note that, the legend in Figure 17 represents the fiber orientation tensor result, which indicates the degree of orientation of fibers at the end of the molding process. The probability of fiber orientation being in the displayed direction is reported. A high probability is indicated in red, represented by a value close to 1. Values indicated in blue, which are closer to 0, indicate the possibility of a more random arrangement of fibers in the finished product [12].

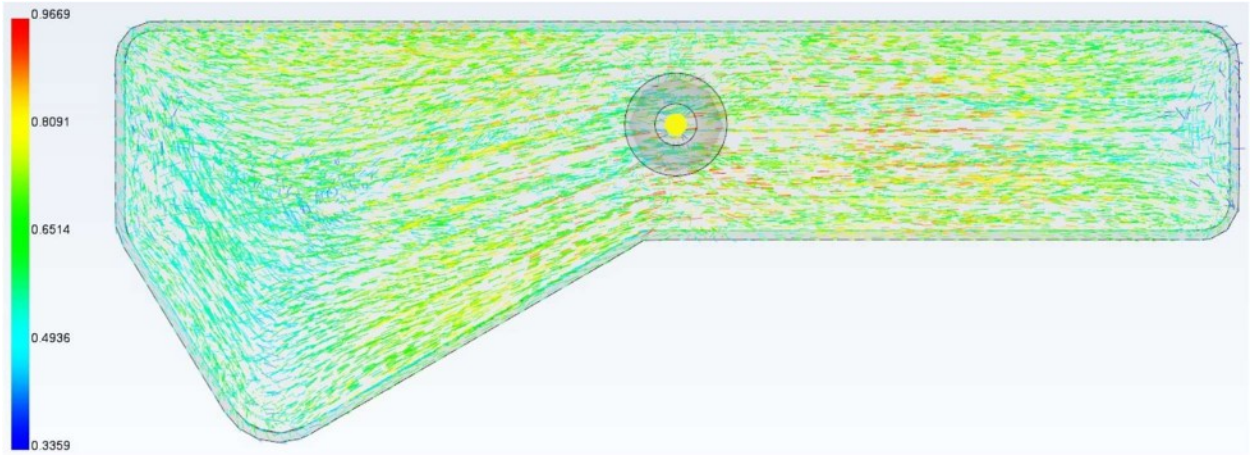

Figure 17: Fiber orientation of the previous mold design [11]

3.2 Direct Design

The direct configuration flow mold design features no runners. Instead, it only has a sprue and gate that feed the liquid plastic into the mold but features no way to manage the fiber alignment. The sprue can be located on any surface of the mold design. The previous work done by Villarreal [10] is based on this design configuration, with the sprue normal to the front surface of the insert, as demonstrated in Figure 17.

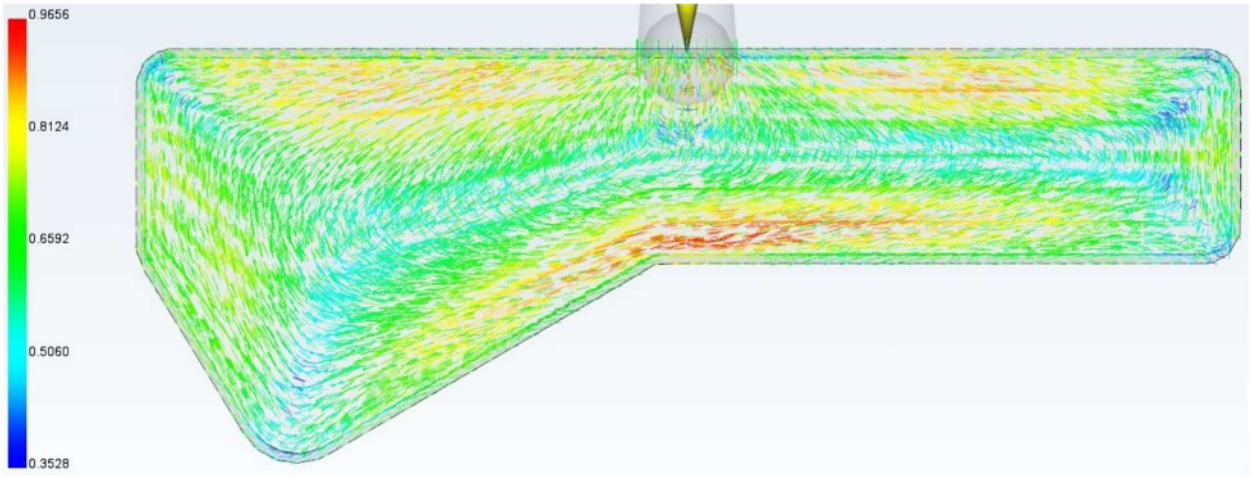

Figure 18: Fiber orientation in direct configuration, injected from top surface [11]

However, these direct configuration designs produced poor fiber alignment results, as seen in Figure 17 and Figure 18, which show that only a few regions exhibited favorable fiber

orientation in the vertical direction. As stated before, the main area of focus is the interlock section of the insert because this section is always under load and in constant contact with the bearing adapter and the side frame roof pedestal. Therefore, it is crucial that the fiber alignment in the interlock section of the insert is mostly in the vertical direction to achieve consistent electrical conductivity. Overall, this configuration offers low fiber alignment throughout the insert and particularly in the interlock region, which is a direct result of the volume of the mold cavity occupied by the interlock. The turbulence that takes place in the large interlock mold cavity while the liquid polymer mixture is being fed through the gate results in poor fiber alignment and electrical conductivity of the composite insert. That is why the direct configuration design was not chosen for manufacturing of the pad inserts. Additional direct gate designs that were simulated can be found in APPENDIX B; all showed a similar, poor fiber orientation.

3.3 Fan Design

Figure 19 illustrates the fiber alignment of the fan configuration injected from the top of the mold cavity. This design produced greater fiber alignment vertically when compared to the previous direct configuration design shown in Figure 18. Nevertheless, despite the better fiber alignment results throughout the insert, there was still significant turbulence of the liquid plastic flow in the interlock section in all the fan configuration simulations that were explored. Additional fan designs can be found in APPENDIX B.

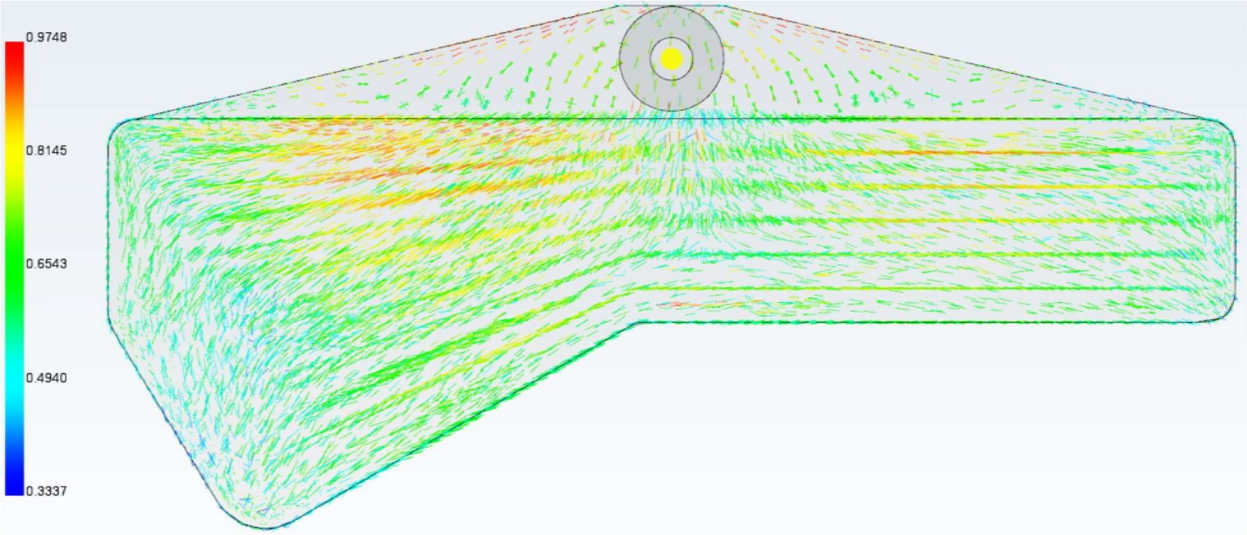

Figure 19: Fiber orientation of the fan configuration, injected from top surface [11]

3.4 Branch Design

After several design iterations, the branch configurations showed great promise. Higher levels of fiber alignment in certain areas were visible compared to the previous iterations, but the two-gate design simulation exhibited turbulence in the interlock portion of the insert. As demonstarted thus far, turbulence of the liquid plastic flow in the interlock region results in poor fiber alignment and unsatisfactory electrical conductivity. These results suggested the use of more gates to improve fiber alignment.

Figure 20 and Figure 21 feature two different mold designs with two equal-sized and three equal-sized gates, evenly spaced across the top surface of the mold insert, respectively. These two designs did not produce great fiber alignment in the interlock section, and turbulence can be seen in the center of the insert. Hence, these two designs were also discarded as they would have resulted in poor electrical conductivity.

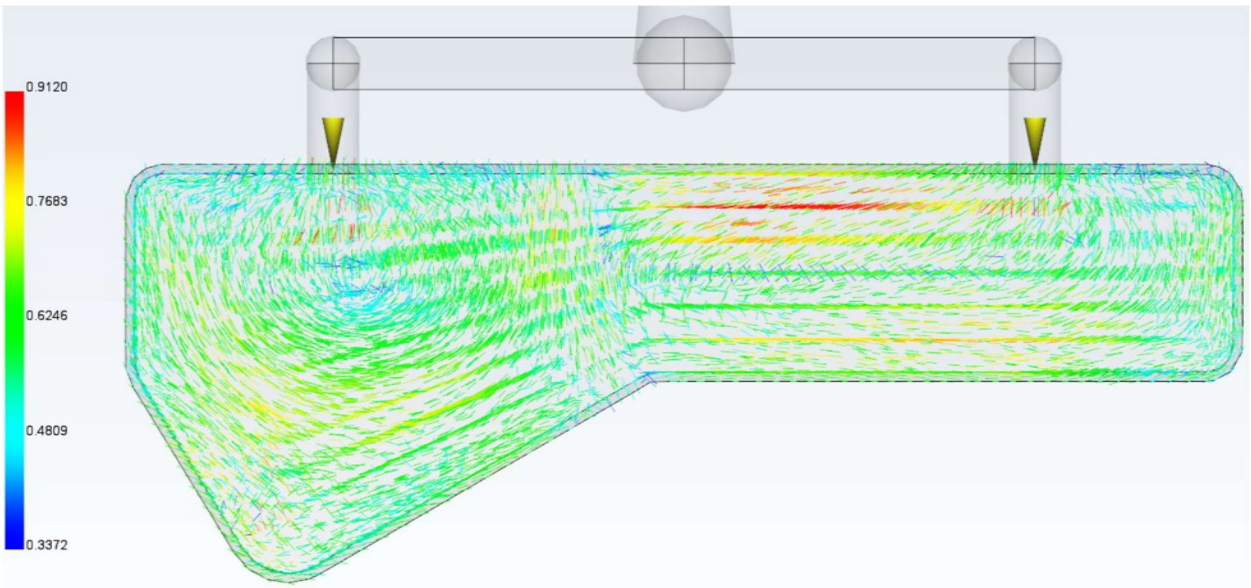

Figure 20: Fiber orientation in a branch configuration with two equal sized gates [11]

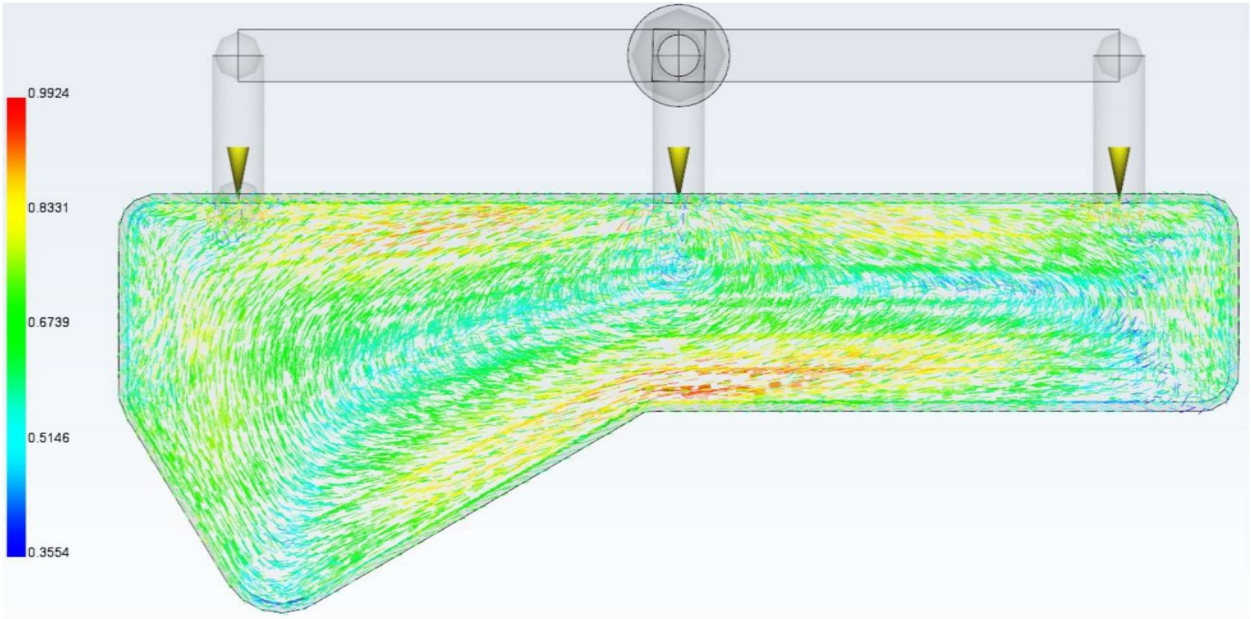

Figure 21: Fiber orientation in a branch configuration with three equal sized gates [11]

Figure 22 displays the results of the four-gate, branch design which produced favorable fiber alignment in the vertical direction throughout the insert with better management of the turbulence in the interlock section. This result was achieved by the runners, which were divided into two sections; an interlock section and the arm section (i.e., the remaining rectangular area of the insert), while maintaining an even flow from all gates, as required by the mold design.

However, the gates were not evenly spaced but rather the locations of the gates were determined by dividing the total volume of the insert by the four gates.

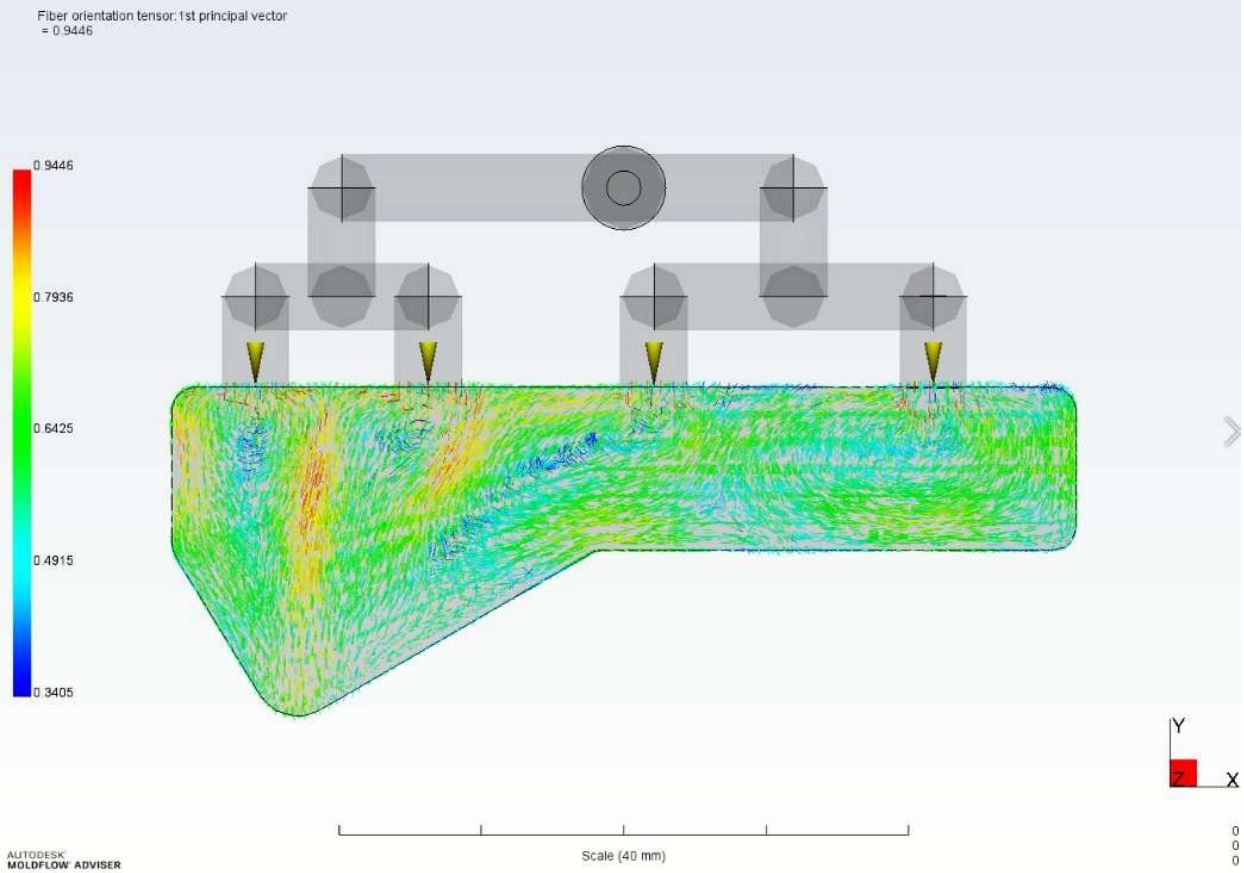

Figure 22: Fiber orientation in final branch configuration with four equal sized gates [11]

Despite the presence of some turbulence in the center of the insert, the interlock region clearly exhibits three individual patches of high fiber alignment in the vertical direction, which extend from the top of the insert to the bottom of the interlock area. Additionally, the top surface of the pad insert displays excellent fiber alignment. For these reasons, this mold design was chosen for manufacturing. The molded parts were examined using a Scanning Electron Microscope, and fiber alignment was found to correlate with the model simulation predictions. These results are presented in Chapter 5 A three-dimensional rendering of the final runner and gate design used to build the mold for the polymer pad inserts is provided in Figure 23.

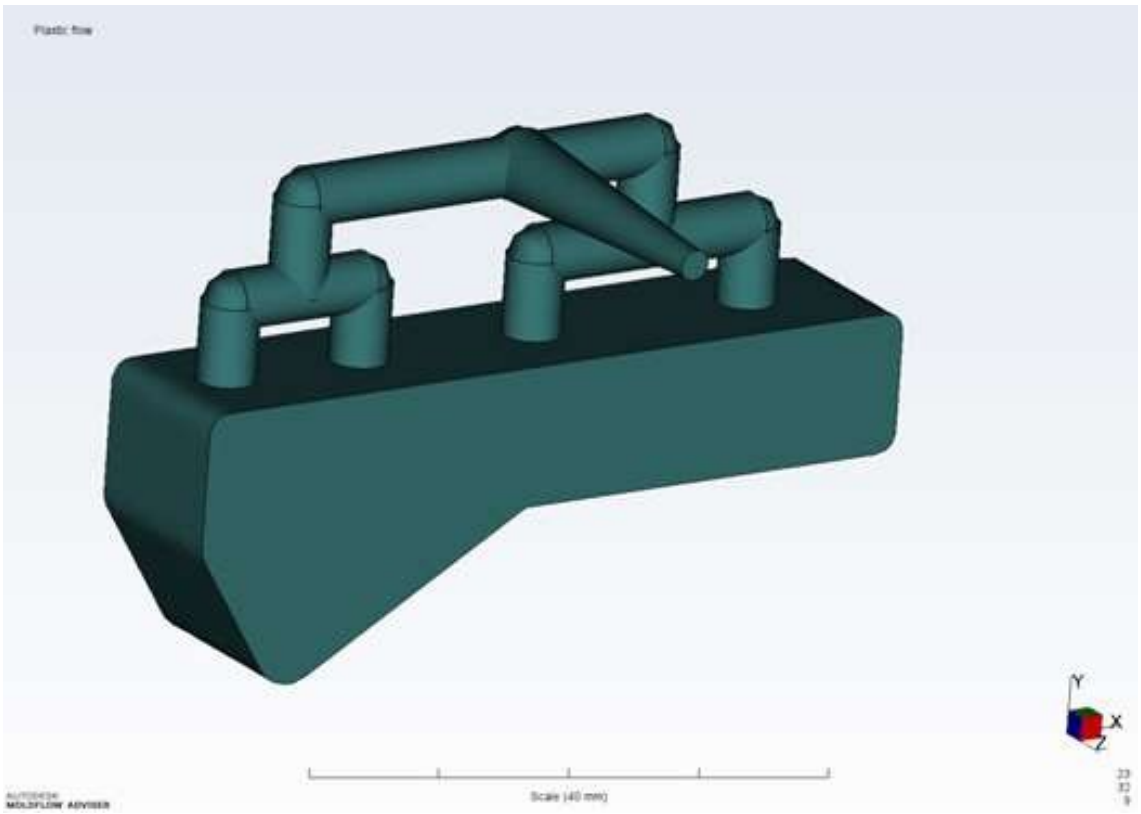

Figure 23: Mold plastic flow simulation results showing, final design [11]

CHAPTER IV

METHODOLOGY AND EXPIREMENTAL SETUP

This chapter outlines the various equipment and procedures used to manufacture the injection-molded Thermoplastic Polyurethane-Carbon Nanofiber (TPU-CNF) composite inserts using the new mold design. The chapter also details the equipment used to test the electrical resistivity of the new composite inserts. The first tester, the Materials Test System 810, was used for initial validation of the electrical conductivity of the composite inserts. Then the four-Bearing Chamber Tester (4BCT), which is housed in a temperature controllable chamber designed by the University Transportation Center for Railway Safety (UTCRS) team, was utilized to test the pads with the conductive inserts in environments that closely mimicked the operating conditions in freight railcar service. Finally, the processes used to develop images of the sample inserts using a Scanning Electron Microscope (SEM) are also detailed herein.

4.1 Mold Manufacturing

The stereolithographic model of the new mold design was first created using SOLIDWORKS®, a computer-aided drafting software, and then transferred into MasterCAM®, which is a software used to generate tool paths for computer numerical control (CNC) machines. These CNC machines are used to manufacture parts out of raw materials. Hence, utilizing this technology, several tool paths were generated for this newly redesigned mold cavity to be machined out of a billet of aluminum. The mold block was machined to accept both the aluminum insert and the nozzle gun bushing, as shown in Figure 24.

Figure 24: (left to right) Mold block A (male) with machined cavity and nozzle gun bushing [13]

Mold block B (female), pictured in Figure 25, had a series of water channels drilled into it forming a pathway as indicated by the blue arrows. The drilled channels allowed hot water, generated by a water heater, to circulate through the mold block to ensure the mold was maintained at a constant 40°C (104°F). Upon completing the machining process of the mold blocks and the aluminum mold cavity, the mold was installed on a BOY 22A injection molding machine. This allowed for injection-molding of individual pad inserts for testing purposes.

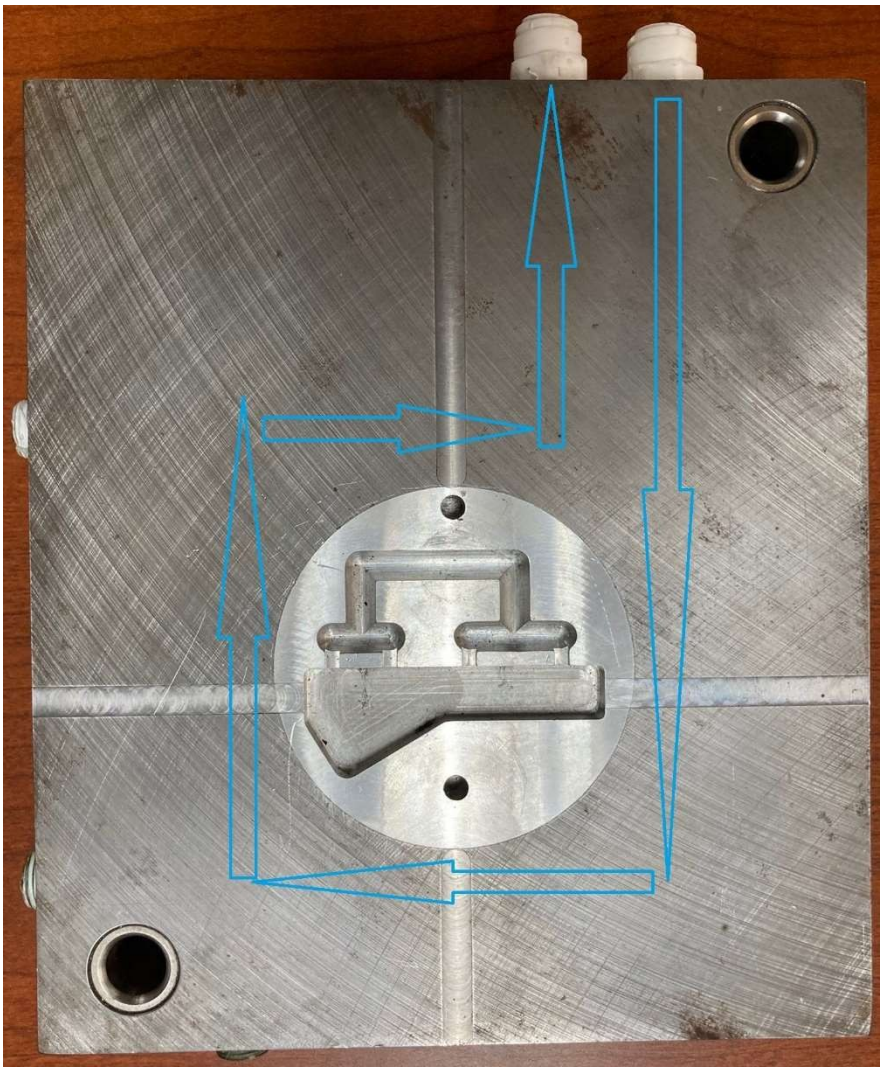
Figure 25: Mold block B (female) with machined insert cavity and water channel path

4.2 BOY 22A Injection Molding Machine

The polymer used to create these inserts is 85 wt% Elastollan® 1195a and 15 wt% carbon nanofibers which were procured by the UTCRS in a pelletized form. These pellets must first be placed in an industrial oven for two hours at a temperature of 110°C (230°F), to allow for any moisture to evaporate and reduce the probability of imperfections forming during the injection molding process. After curing, pellets can be fed into the hopper of the BOY 22A, shown in Figure 26 for composite insert manufacturing. The temperature and injection molding parameters

are summarized in Table 1 and follow the processing recommendations technical data sheet provided by BASF for Elastollan® 1195a [4].

Figure 26: BOY 22A injection molding machine [14]

Table 1: Temperature and injection molding parameters [10]

Temperature Parameters			**Injection Molding Parameters**	
Mold Temperature [°C]	49		Shot Size [mm]	38.5
Nozzle Temperature [°C]	227		Shot Hold [s]	10
Barrel 1 Temperature [°C]	204		Mold Hold [s]	90
Barrel 2 Temperature [°C]	204		Total Cycle Time [s]	100
Barrel 3 Temperature [°C]	204		Injection Speed [mm/s]	55
Barrel 4 Temperature [°C]	204		Mold Clamping Force [N]	890
			Injection Pressure [kPa]	13.8

In total, 21 individual composite inserts were produced. The first five were discarded to reduce the risk of potential impurities and internal contamination of the insert by other plastics that can remain in the barrel of the 22A due to prior usage. This allowed for 16 usable inserts.

The samples were left to air cool for approximately seventy-two hours to allow the polymer microstructure to stabilize and settle into a final arrangement before being tested. Six inserts were fused using a two-part urethane adhesive (JB Plastic Bonder) and a compressive clamp shown in Figure 27*Figure 27*: One individual insert and one insert set fused . This process was performed twice to produce two amalgamated test samples, each composed of six fused inserts. The selection criteria of these inserts prioritized those with a reduced number of visible defects. These defects included burn marks, jetting, surface delamination, and cloudiness [10].

Figure 27: One individual insert and one insert set fused [10]

The two urethane-bonded composite insert sets were allowed to cure for 24 hours before being installed into a modified adapter pad. Any excess bonding material could negatively impact conductivity or cause signal interruption to the onboard systems and was therefore carefully removed.

A portion the interlock section of the adapter pad was cut away to accept one of the newly fused composite insert sets, a ‘half-pad’, as only half of the adapter pad has had the interlock portion replaced, is shown in Figure 28. This composite set was installed and kept in place using the same two-part urethane adhesive and a large compressive clamp. The composite insert set was kept flush with the top surface of the adapter pad to maintain a flat surface

alignment. This was done to ensure that the modified adapter pad and composite inserts made even contact with the load applied by the testers. This also maintains the structural integrity of the pad when being handled or tested. As before, excess bonding material was removed to prevent conductivity issues. The results are discussed at length in Chapter 5. The final thickness of each injection-molded composite insert was 1.23 cm (0.49 in) and the top in-contact surface area of was 49.88 cm^2 (7.73 in^2).

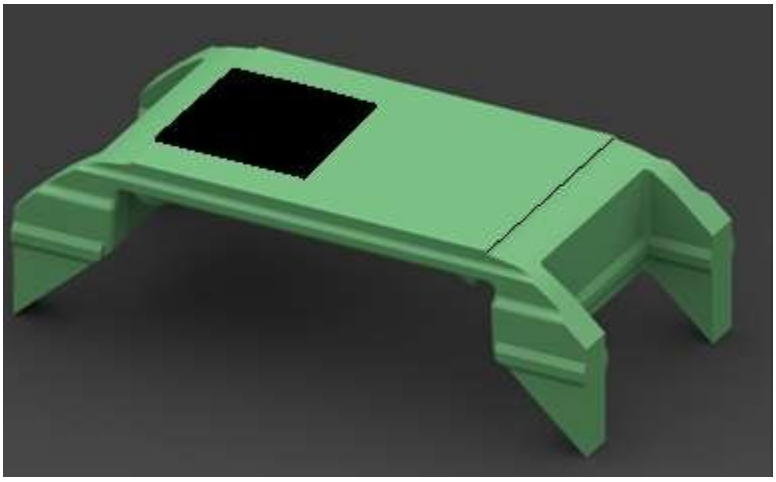

Figure 28: Modified adapter pad with a single composite insert set installed. This configuration is referred to as 'half-pad' insert [10]

4.3 MTS 810 Materials Test Systems

The Materials Test System 810 (MTS 810) is a servo-hydraulic materials tester, pictured in Figure 29: Polymer pad testing on the MTS 810 The MTS 810 was used to perform static and dynamic testing and validate the electrical resistivity of the modified adapter pad with the prototype TPU-CNF inserts. All MTS 810 testing was performed at an ambient temperature of 22 ± 2°C (72 ± 3.5°F), and under free convection conditions. A load of 26 kN (5.85 kips) was applied to mimic an empty, unloaded railcar. The electrical setup used to conduct resistivity testing is discussed in 4.5 Electronic Setup.

Figure 29: Polymer pad testing on the MTS 810

To accurately simulate the modified adapter pad on a railcar, a bearing substitute was created by cutting the outer ring (cup) of a class F bearing in half and welding a 6.35 mm (0.25") plate to the bottom half of the bearing. A thin piece of sheet metal is placed on the top surface of the modified adapter pad to distribute voltage across the system evenly.

This bearing assembly mockup includes the modified adapter pad, an adapter, the half-bearing, and two pieces of 12.7 mm (0.5") thick acrylic sheets placed between the platens of the MTS 810 to ensure that it was electrically isolated from the test stack, as depicted in the schematic diagram of Figure 30. Lastly, an I-beam was placed on top of the acrylic sheet to

allow uniform distribution of the load applied from the MTS 810 to the modified adapter pad and composite inserts [10].

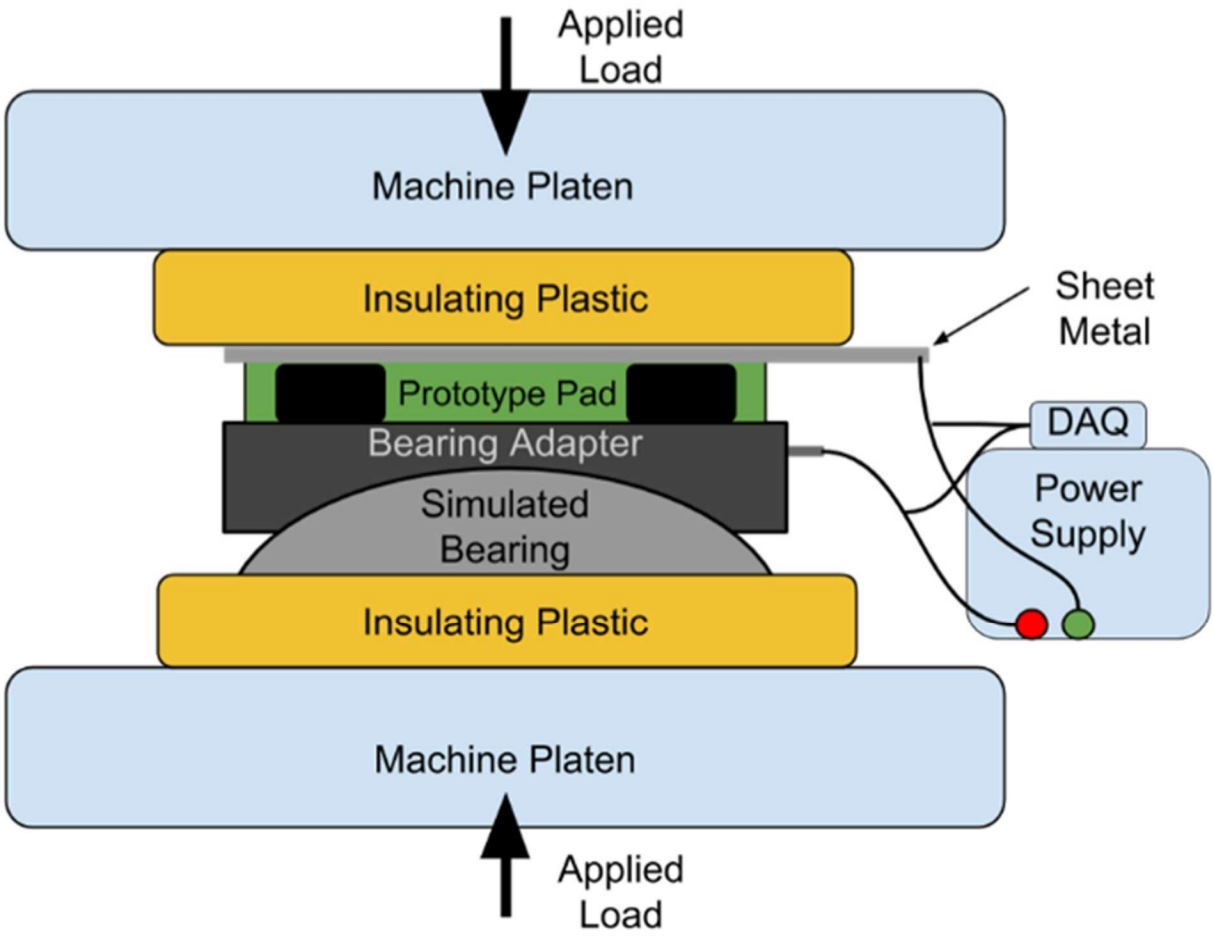

Figure 30: MTS 810 test stack schematic diagram [10]

4.4 Four-Bearing Chamber Test Rig

The Four-Bearing Chamber Tester (4BCT) designed by the UTRCS team, pictured in Figure 31, is used to simulate the various operating conditions experienced in freight railcar service. This tester was used to evaluate the electrical resistivity of the modified adapter pad in a simulated dynamic environment. Testing the electrical resistivity was conducted utilizing the same experimental setup used during the MTS 810 testing.

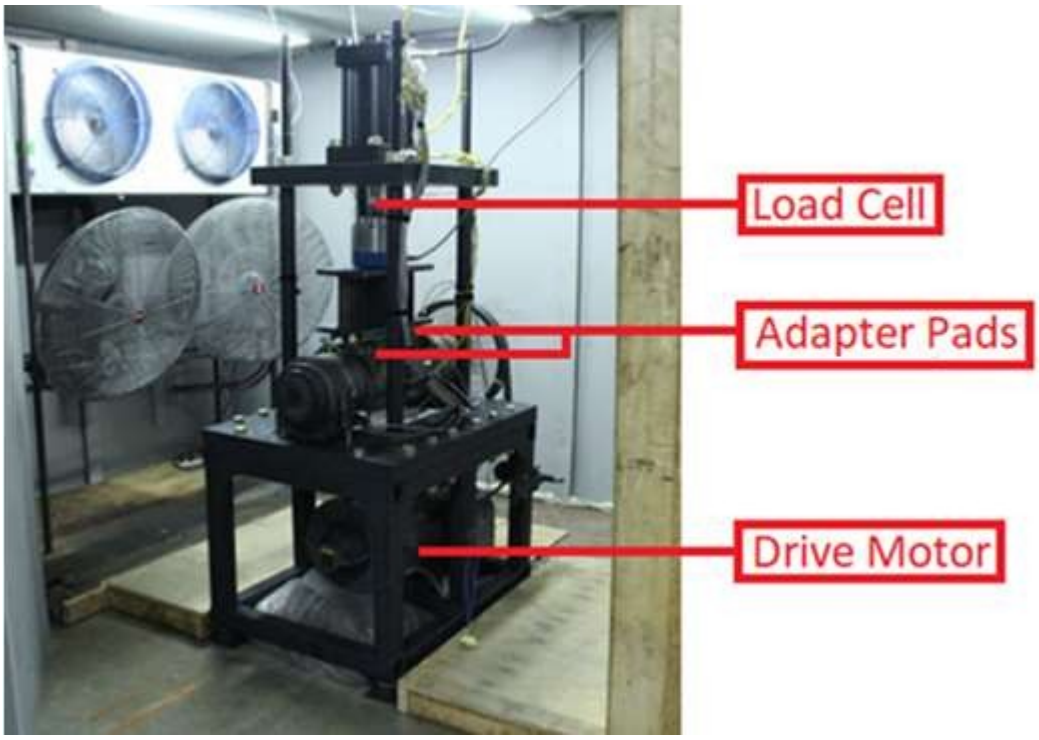

Figure 31: Four-bearing dynamic tester housed in an environmental chamber [10]

However, this dynamic test rig is housed in an environmental chamber equipped with an industrial-size refrigeration unit that controls ambient temperatures. Controlled ambient temperatures can range from a low of -40°C (-40°F) to a high of 65°C (150°F). When conducting tests in the chamber test rig, loads of 26 kN and 153 kN (5.85 and 34.4 kips) are typically applied to the adapter pad, to simulate the force of an unloaded (empty) railcar and a fully loaded railcar, respectively. Testing on the 4BCT was performed at typical railcar operating speeds of 40 km/h to 97 km/h (25 mph to 60 mph) and a maximum tester speed of 137 km/h (85 mph) for test cases requiring excessive heat generation within the bearings.

4.5 Electronic Setup

Electrical resistivity is a material property that describes the tendency of a material to interrupt electrical current. Resistivity is also a key property of the TPU-CNF composite inserts as electrical resistivity will be measured during all experiments. This is done to determine whether the composite insert can be considered a viable replacement for the two-copper stud

design. Resistivity values below a certain threshold will mark the composite insert design as a viable replacement, with low resistivity suggesting high conductivity. The equation used to calculate resistivity is,

$$\rho = R\frac{A}{L}$$

Equation 1: Equation to solve resistivity [10]

with R is defined as the electrical resistance of a uniform specimen of the material, L is the length of the path of conductivity, A is the cross-sectional area of the conductor, and ρ is the resistivity of the material [10].

During resistivity testing, a solenoid-driven air valve was added in series to the electrical test circuit and a current was applied. Current passes through the modified composite insert pad and allows the solenoid valve to successfully actuate. This must be demonstrated under each condition rather than just inferred from the measurement of resistivity. Voltage was applied and slowly increased until the valve opened.

For valve actuation tests, a driving voltage of 24 volts was provided by a power supply. National Instruments (NI) LabVIEW®, a data acquisition software, and an NI breadboard were used to continuously record the voltage across the pad. The resulting pad resistivity was plotted in MATLAB® [10]. Electrical resistivity is also continuously measured and calculated by the data acquisition (DAQ) software during testing. A schematic of the DAQ circuit is provided in Figure 32.

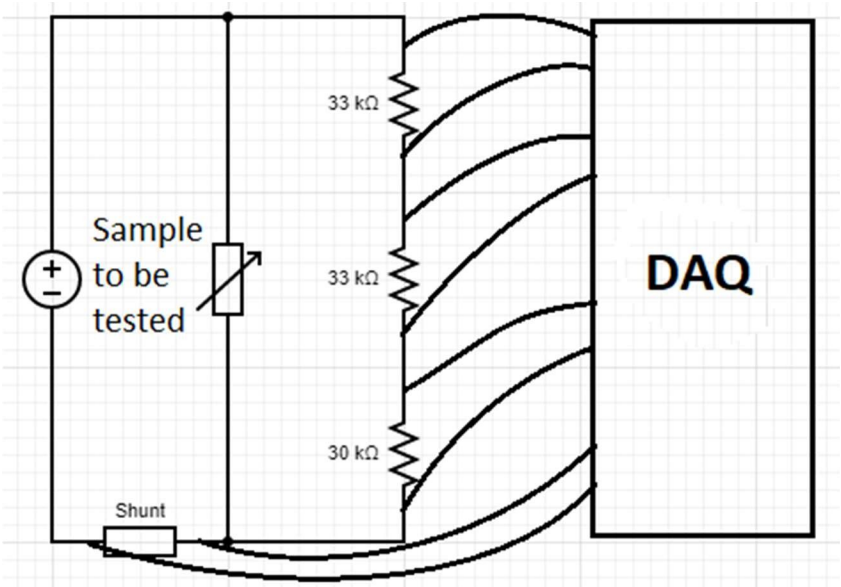

Figure 32: Data acquisition circuit [10]

For long-term measurement of pad resistivity, the solenoid is removed from the electrical test circuit and the modified adapter pad is subjected to a driving voltage which was varied between 5 to 10 volts. This voltage represents the net voltage available to drive current through the pad in service applications after losses due to impedance of the solenoid air valve.

Voltage was again applied and slowly increased until the valve opened. Since 16 volts are required to actuate the valve and 24 volts are the typical power applied to the system, 8 volts are the potential difference available to the modified adapter pad. The electrical setup is pictured in Figure 33. Not pictured in Figure 33 is a secondary DAQ, the NI TC-01 which takes samples of the internal temperature of the TPU-CNF composite insert during testing. The temperature samples (like current and voltage) are taken every three seconds. The results of these tests are discussed in detail in Chapter 5.

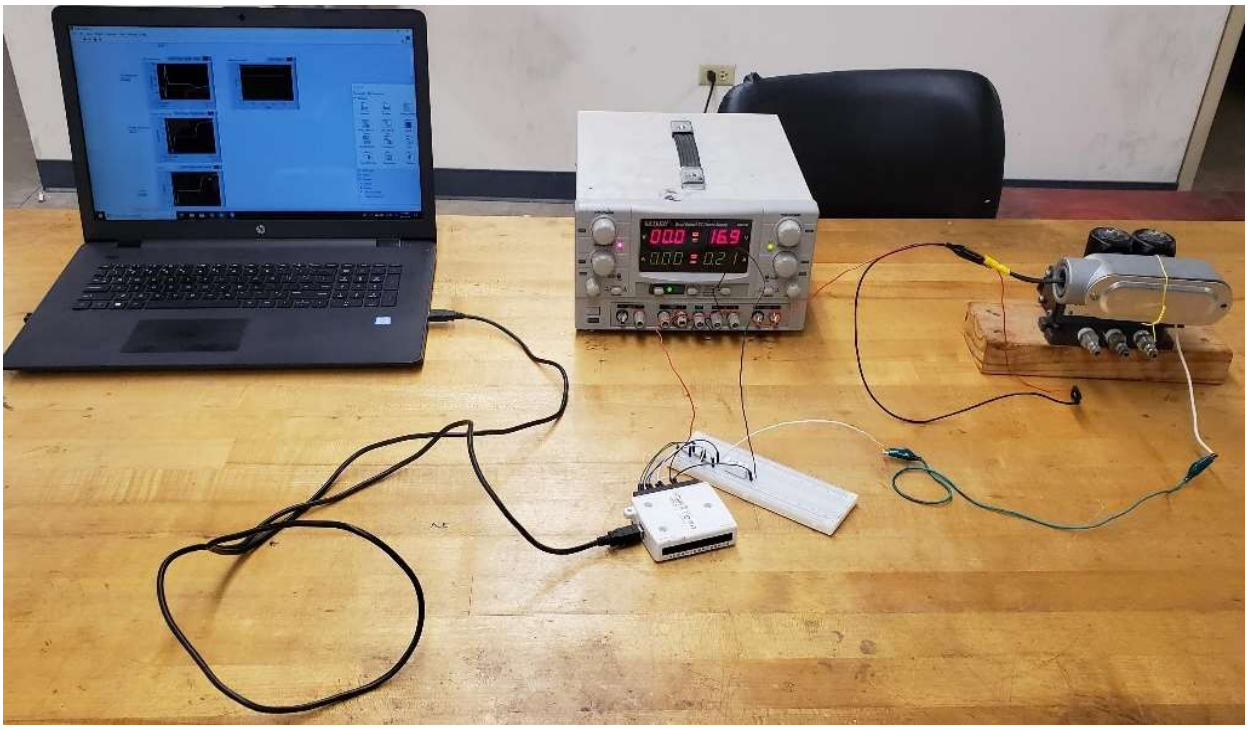
Figure 33: Solenoid valve experimental setup [10]

4.6 Scanning Electron Microscope (SEM)

The SEM is used to generate detailed images of the surface of an object at the microscopic level. The resolution range of an SEM ranges from 0.4-20 nm. The level of magnification of an SEM is an order of six magnitudes, 2.0 to 3×10^6 [15].

The SEM functions by focusing an electron beam on the surface of the sample object. This beam is produced by an electron gun, located at the top of the SEM. While in a vacuum, the beam of electrons travels through a lens and a power magnetic field before colliding with the sample, causing the electrons and x-rays to be emitted from the sample surface. The resulting signals are used to obtain the microscopic composition and surface topography of the sample. A design layout of an SEM can be seen in Figure 34. There is a secondary electron detector which collects the emitted electrons, and a signal processor converts the emissions into a final image [15].

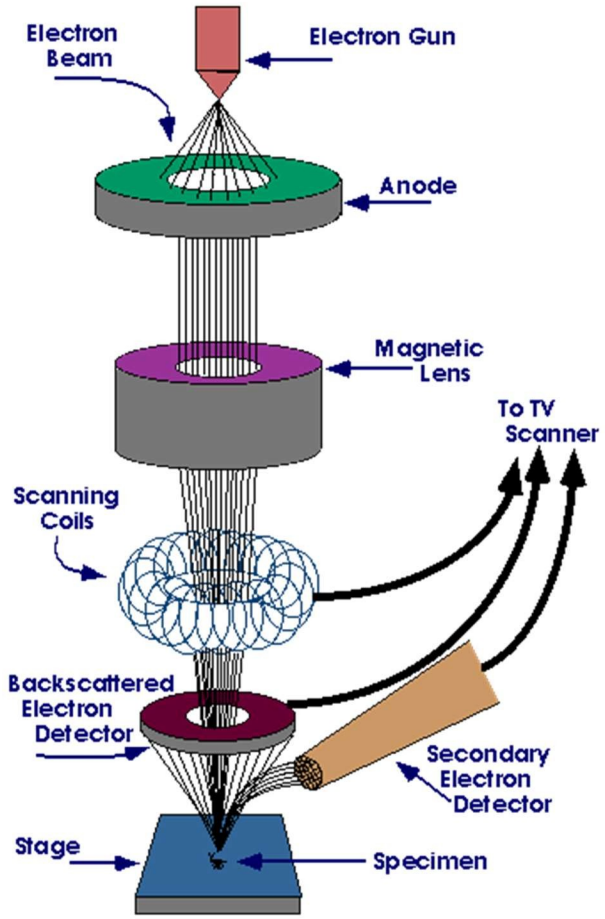

Figure 34: Diagram of a scanning electron microscope [15]

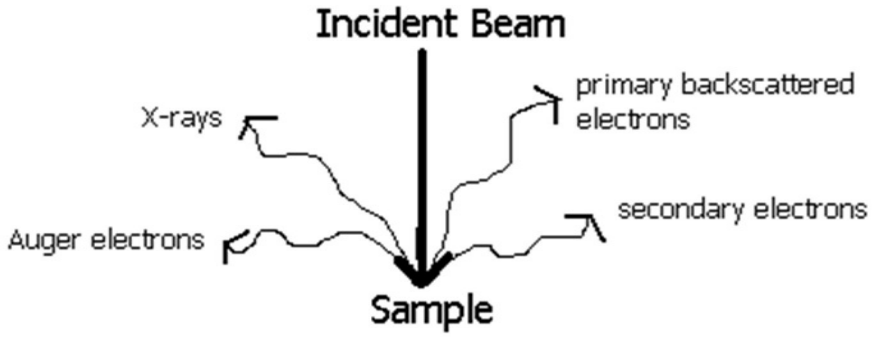

Figure 35: Electron beam interaction with test specimen [15]

Before imaging can begin, a sample must first be sputter coated. This process involves applying a thin coat of gold which allows any non-metallic object to be electrically conductive, seen in Figure 36. The Denton Vacuum, Desk II sputter machine was used for the coating

process. The current applied was 45 mA for a duration of 15 seconds. The thickness of gold sputter coat was 38.1×10^{-3}mm (1.5×10^{-3} inches) [16].

Figure 36: Sputter process [17]

Before the SEM imaging of the TPU-CNF composite inserts can begin, a single composite insert sample was first notched on the largest surface to aid in breaking the individual insert into smaller samples for imaging. The surface was cleaned to remove debris and cleaned again with isopropyl alcohol to remove any grease or other contaminants. The samples were placed in a small container of liquid nitrogen for approximately two minutes. The samples were then removed from the small container and struck with a chisel on the notch to fracture the sample at that location. Each section was placed in a small, numbered plastic bag to minimize the introduction of dirt and debris to the exposed surface that would be studied. The samples were

sent to the SEM laboratory to complete the imaging process. The analysis of the SEM images focused on fiber orientation, fiber dispersion, fiber length, and how well the carbon nanofibers blended with the thermoplastic. The results of these images are discussed in 5.4 Scanning Electron Microscopy Results.

CHAPTER V

RESULTS

This chapter outlines the results of the tests conducted on the composite adapter pad inserts, the parameters that define a successful test, and whether the outcome justifies using Thermoplastic Polyurethane-Carbon Nanofiber (TPU-CNF) composite inserts to replace the current two-copper stud design used in freight railcar service.

To reiterate, one composite insert set is comprised of six individual injection-molded TPU-CNF inserts (Figure 37 depicts one insert) fused to create the interlock portion of the adapter pad. There are two of these insert sets, one on each side of the adapter pad, in the interlock sections, as pictured in Figure 38.

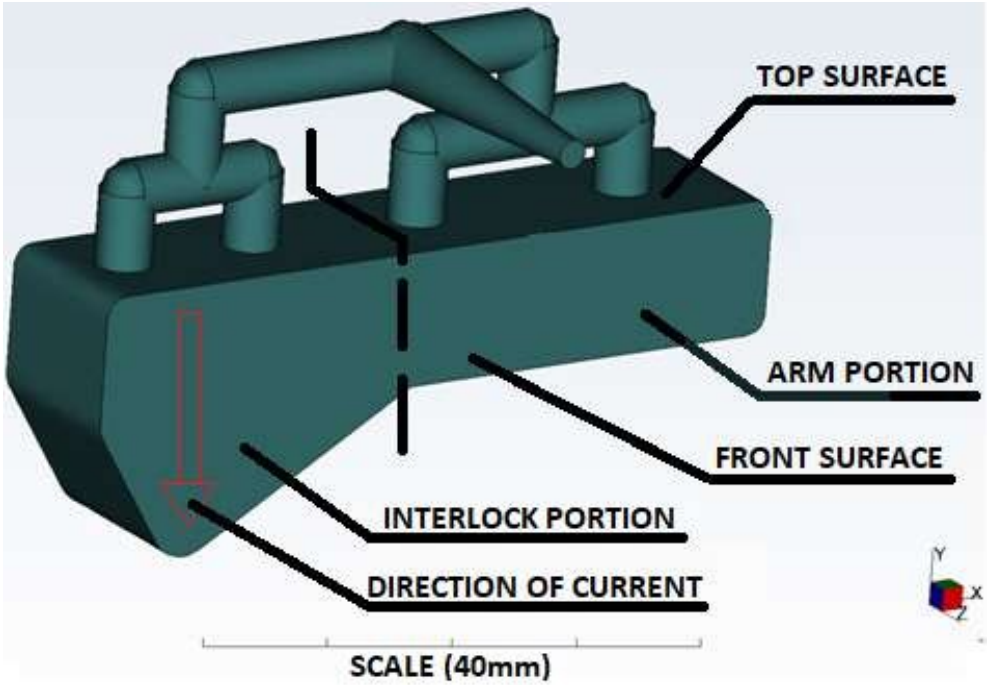

Figure 37: Composite insert anatomy

When one of these composite insert sets is installed, the configuration is referred to as a "half-pad" insert, as only half of the adapter pad has had the interlock portion replaced. When both composite insert sets are installed, the pad is referred to as a "full-pad" insert, shown in Figure 38. The combined top-surface area of the insert sets is 99.76 cm^2 (15.46 in^2) with an average insert thickness of 1.23 cm (0.49 in).

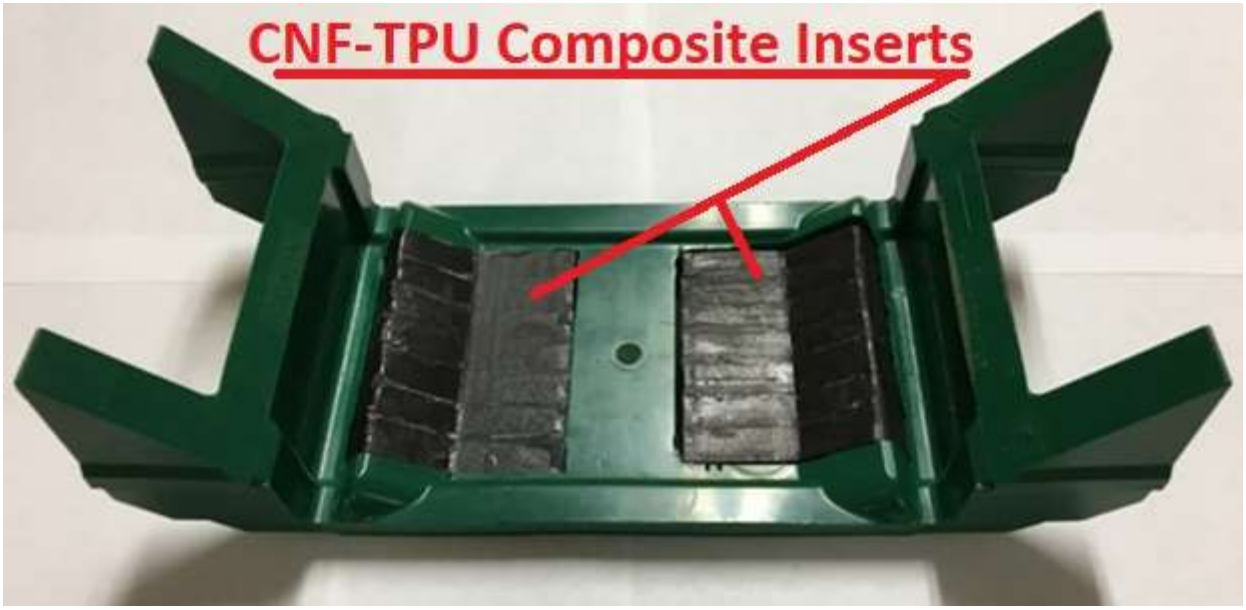

Figure 38: Modified composite adapter pad with the two interlock sections replaced with two insert sets. This configuration is referred to as 'full-pad' insert.

5.1 MTS 810 Materials Test Systems Results

The Materials Test System 810 (MTS 810) tester was used to validate whether the TPU-CNF composite adapter pad insert possessed the required conductivity to actuate a solenoid valve while under a load of 26 kN (5.85 kips), the approximate force applied to each adapter pad by an empty freight railcar. The laboratory solenoid valve setup operates comparably to the valves used in railcar service.

For initial testing, a single "half-pad" was made. Test data was collected using National Instruments™ LabVIEW®, a data acquisition (DAQ) software, and plotted using MATLAB®. Resistivity was calculated using the DAQ by inputting the recorded current, the top surface area

of the composite pad insert set, and thickness values into Equation 1, found in 4.5 Electronic Setup.

5.1.1 Half-Pad Results

Figure 39 displays the results of the first six tests conducted on the MTS 810 tester. All tests were conducted at a simulated empty railcar load of 26 kN and an electric potential between 5 and 10 volts. The 'maximum for valve operation' line is plotted to indicate the maximum permissible resistivity that will still allow the solenoid valve to function. Any value above this blue line implies that the TPU-CNF composite adapter pad inserts lack the conductivity to effectively transmit electrical current, which prevents actuating (opening) the solenoid valve placed in series with the electrical test circuit, thus resulting in a failed test.

Any value between the blue and orange lines indicates the successful operation of the solenoid valve, but only by a slim margin. A factor of safety is used preventively with the knowledge that solenoids age or suffer from performance decay. Hence, a 'target resistivity' of 600 Ω·cm, represented by the orange dashed line, was used to gauge the required pad conductivity. So, a value below the orange 'target resistivity' line is considered ideal and is the metric for a successful test. It is important to note that low resistivity equates to high conductivity as they are inversely related.

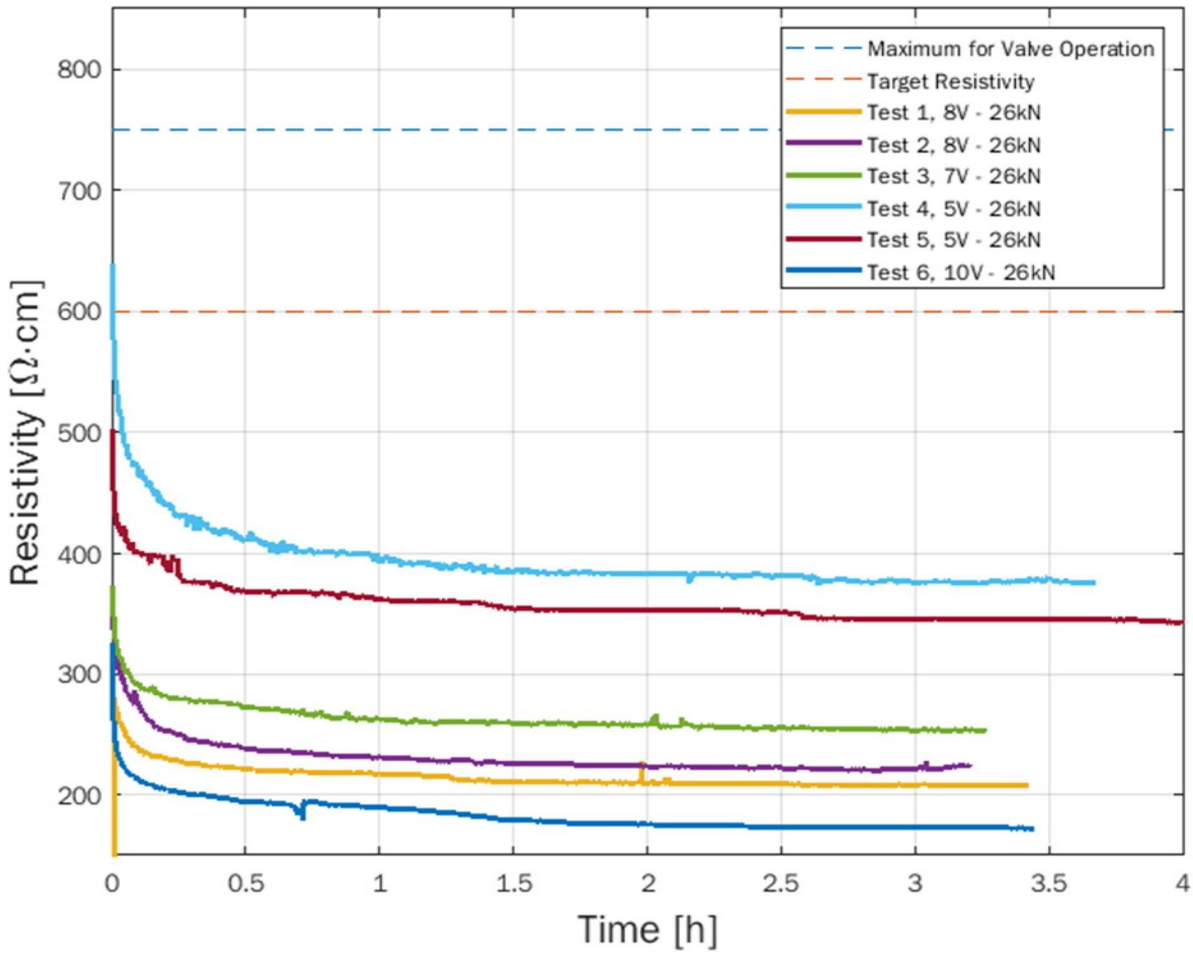

Figure 39: Resistivity of one conductive interlock insert with an empty railcar load MTS 810

The resistivity of all tests began near or below the target resistivity line, indicated by the orange dashed line. All six tests successfully fell below the target resistivity of 600 Ω·cm required to actuate the pneumatic valve after four hours of testing. The rapid drop in resistivity at the beginning of each test is due to a reduction in the contact resistance between the metal components and the polymer pad. There is a notable correlation between the voltages applied and the resistivity of the modified adapter pad with one TPU-CNF composite insert set. As the voltage increases, the steady-state resistivity occurs at lower values. This is consistent with the mechanism of conduction where the conductive filler is not continuous. Higher voltages allow

current to be carried over larger gaps between conductive fibers, thus opening new paths for current and reducing the overall resistivity.

The fact that acceptable resistivities were obtained with as little as five volts applied to the half-pad indicates a robust conductivity which should permit valve function even when system voltages drop below normal. Valve actuation tests were conducted at random periods during testing. In all test cases, a solenoid valve installed in the circuit functioned when the test voltage of 24 volts was applied to the full test circuit.

The other immediate observations are the initial responses and the behavior of resistivity. All the tests began at much higher resistivities, and over a period of thirty minutes to two hours reached steady-state below the level of 'target resistivity' with two-thirds of tests achieving a steady-state resistivity that is half of the required resistivity needed to actuate the solenoid valve.

As the polymer in the pad conforms to the metal surfaces due to creep under the applied load, the improved contact causes a rapid reduction in contact resistance. The continued slow decline in resistivity is probably due to low levels of creep by the polymer matrix of the pad which will reduce the gaps between conductive fibers. This ability to conform to less-than-ideal surfaces suggests the system will adapt to some level of surface roughness in the side-frame which will rest on the pad as well as the surface of the adapter between the pad and the bearing.

5.1.2 Full-Pad Results

The results obtained from the adapter pad with a single conductive insert at an unloaded railcar load provided the impetus to mold additional oriented fiber TPU-CNF composite inserts and construct a modified adapter pad with both interlock elements replaced with the composite inserts. The 'full-pad' was subjected to the same conditions as the 'half-pad', but a voltage potential of 8 volts was utilized instead of the 5 to 10 volts range used previously. These results

are shown in Figure 40.All further testing conducted in this thesis was performed using the 'full-pad' configuration. Moreover, most of the testing was carried out utilizing the empty railcar load (i.e., 26 kN per bearing) because achieving consistent and reliable pad electrical conductivity at this low load guarantees a conductive pad at the fully loaded railcar condition (i.e., 153 kN or 34.4 kips).

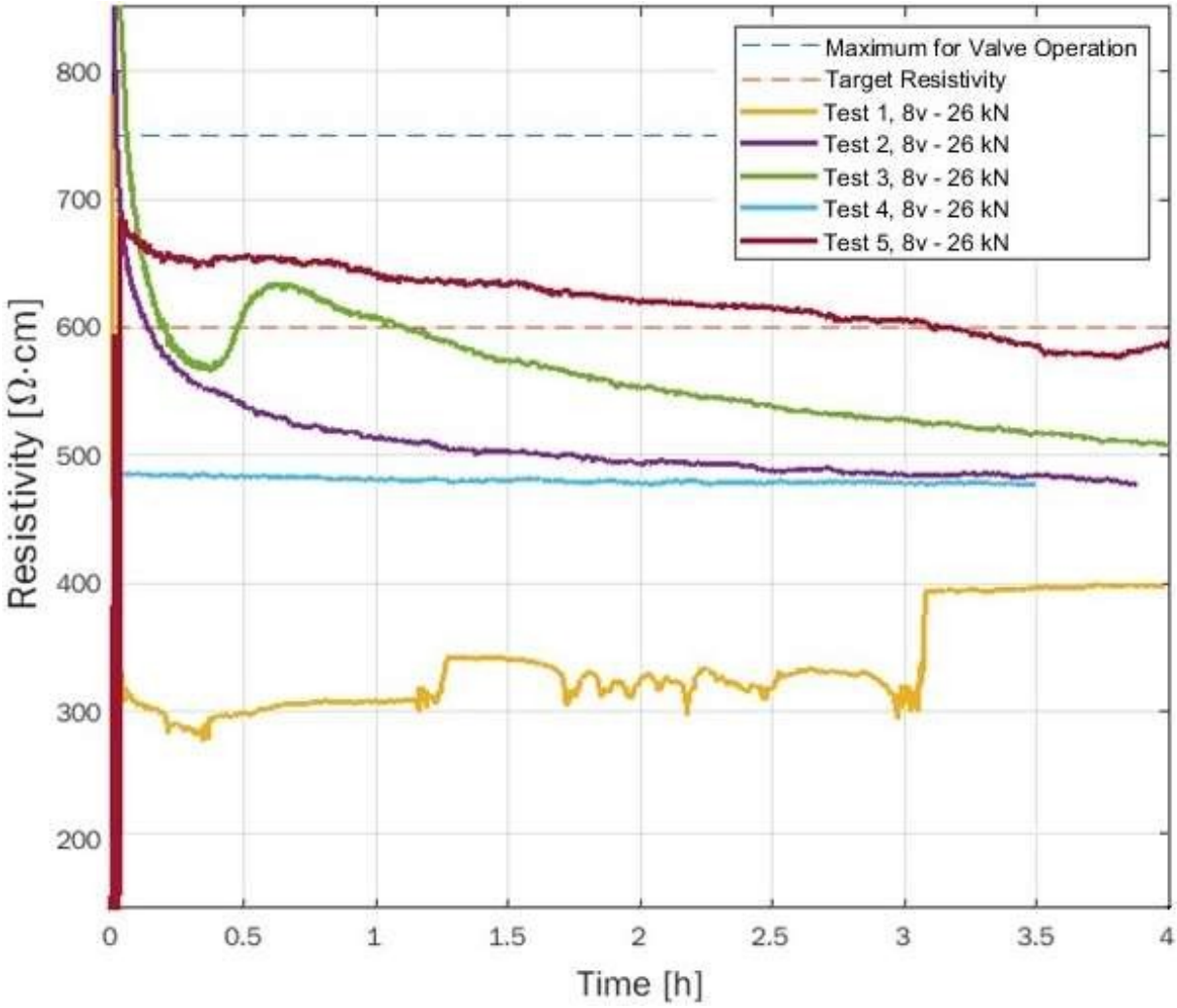

Figure 40: Resistivity under static empty freight car with two conductive interlock inserts.

Like the half-pad test results of the previous section, tests 1, 2, 3, and 5 began above the target resistivity line but after a short period, between 30 minutes and two hours, all tests reached an electrical steady state resistivity. Test 4 reached steady state almost immediately. All five tests

ended under the minimum target resistivity of 600 Ω·cm, which is the ideal value required to actuate the solenoid valve. There is no immediate correlation between the voltage applied and the final resistivity value after four hours as all tests were performed at the same voltage.

As before, the drop in resistivity seen in tests 1, 2, 3, and 5 was due to a reduction in the contact resistance between the metal components and the polymer pad. The behavior of test 1 was unlike the previously conducted half-pad tests, and after three hours, the resistivity value jumped by about 80 Ω·cm and settled at 400 Ω·cm. The plotted resistivity may result from an electrical issue caused during tear down and set up of instrumentation between tests of the half-pad and the full-pad.

Test 3 exhibited a noticeably irregular jump before settling near 300 Ω·cm. These plotted resistivity anomalies may result from load shifting between the pad inserts and the pad itself as the load is applied. It is also possible that there was a brief mechanical issue with the MTS 810 and the force applied changed. Regardless of unforeseen issues, both test 1 and test 3 began as a normal test with a normal ramp-up in resistivity and a gradual decline towards a steady-state resistivity. If test 3 were to continue as normal, without the jump seen after thirty minutes, it would have settled in the same range as tests 2 and 4. Despite the jump, the test was successful as it settled within the target resistivity. Solenoid actuation was tested multiple times at random intervals during all tests with the valve actuating properly during these tests.

After these five tests were concluded, additional testing was performed to determine the minimum amount of force required to allow the solenoid valve to actuate at 24 volts. A minimum force of 10 kN (2.25 kips) was necessary for successful actuation and is approximately one-third of the minimum force the axle-bearing and adapter pad will ever experience in freight

service. These positive test results led to the decision to continue testing on the four-bearing chamber tester.

5.2 Four-Bearing Chamber Tester Results

The full pad was subjected to long-term testing on the 4-Bearing Chamber Tester (4BCT) which now allowed the modified adapter pad to be tested at different ambient temperatures, axle speeds, and applied loads. The ambient temperature of the 4BCT was regulated between 4°C and 29°C (40°F and 85°F); the simulated train speeds ranged between 72 and 137 km/h (45 and 85 mph); and test loads used included 26 kN, which represented an empty railcar load, and 153 kN, which corresponded to a full railcar load.

5.2.1 Unloaded Results

The seven tests plotted in Figure 41 were performed at 26 kN to simulate the force applied by an empty railcar. Ambient temperatures ranged from -17°C to 8°C (1°F to 46°F). These seven tests were considered the "worst-case scenario" because the modified adapter pad was under the least amount of compressive force and experienced the low temperatures at average railcar speeds.

It is hypothesized that the lower the temperature, the higher the resistivity due to the nature of the material. Previous work by Villarreal [10] proved that the greater the force applied to the modified adapter pad inserts, the lower the resistivity. Table 2 gives the test axle revolutions per minute (RPM) and the corresponding train speeds in km/h and mph.

Table 2: Simulated axle speeds and axle RPM

Revolutions Per Minute [RPM]	Velocity [km/h]	Velocity [mph]
234	40	25
280	48	30

327	56	35
374	64	40
420	72	45
467	80	50
498	85	53
514	89	55
560	97	60
618	106	66
700	121	75
796	137	85

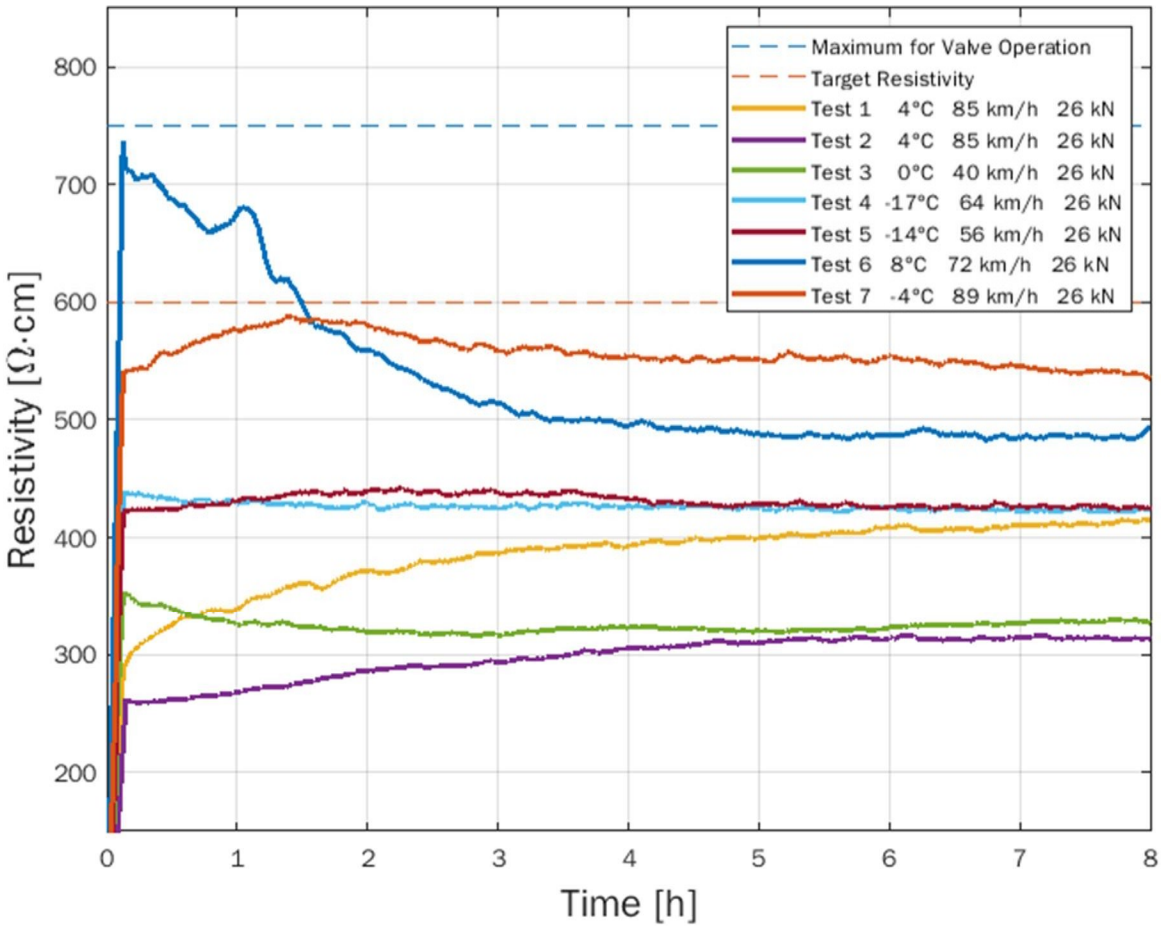

Figure 41: Resistivity of full pad insert four-bearing tester under simulated service conditions.

As in the earlier static tests on the MTS 810, all tests produced a jump in resistivity at the beginning of each test. Tests 3 and 6 had a decline in resistivity which largely levels after three hours of testing. Tests 1, 2, and 7 slowly increased to their steady-state resistivity, while tests 4 and 5 immediately reached their stead-state resistivity values. All tests started below the target resistivity line except for test 6, which started below the 'maximum for valve operation' dashed line and reached steady-state resistivity value of about 500 Ω.cm after three hours of testing. All tests settled between resistivity values of 310 and 540 Ω·cm.

Throughout testing, the solenoid valve was connected in series with the electric circuit, and like previous tests, the solenoid valve never failed to actuate during these random inspections, regardless of the ambient temperature, axle speed, or load applied.

While in service operation, the bearings and polymer adapter pads are always under an applied load, regardless of whether the railcar is empty or fully loaded, therefore, the transient start-up response is not an operational concern. Baseline resistivity at all temperatures were well below the target value and appeared to be mostly independent of temperature over the range tested, meaning that the worst-case scenario is something that will not be a concern when the TPU-CNF composite inserts are used in service.

5.2.2 Loaded Results

These ten tests on the 4BCT were conducted at a load of 153 kN to simulate a fully loaded freight railcar. Ambient temperatures varied from 3°C to 25°C (37°F to 77°F), and the simulated train speeds ranged from 40 to 90 km/h (with an outlying study conducted at the extreme velocity of 120 km/h). Figure 42 summarizes the results and gives the resistivities measured for the two-element pad (full pad) during the ten tests performed at a full railcar load.

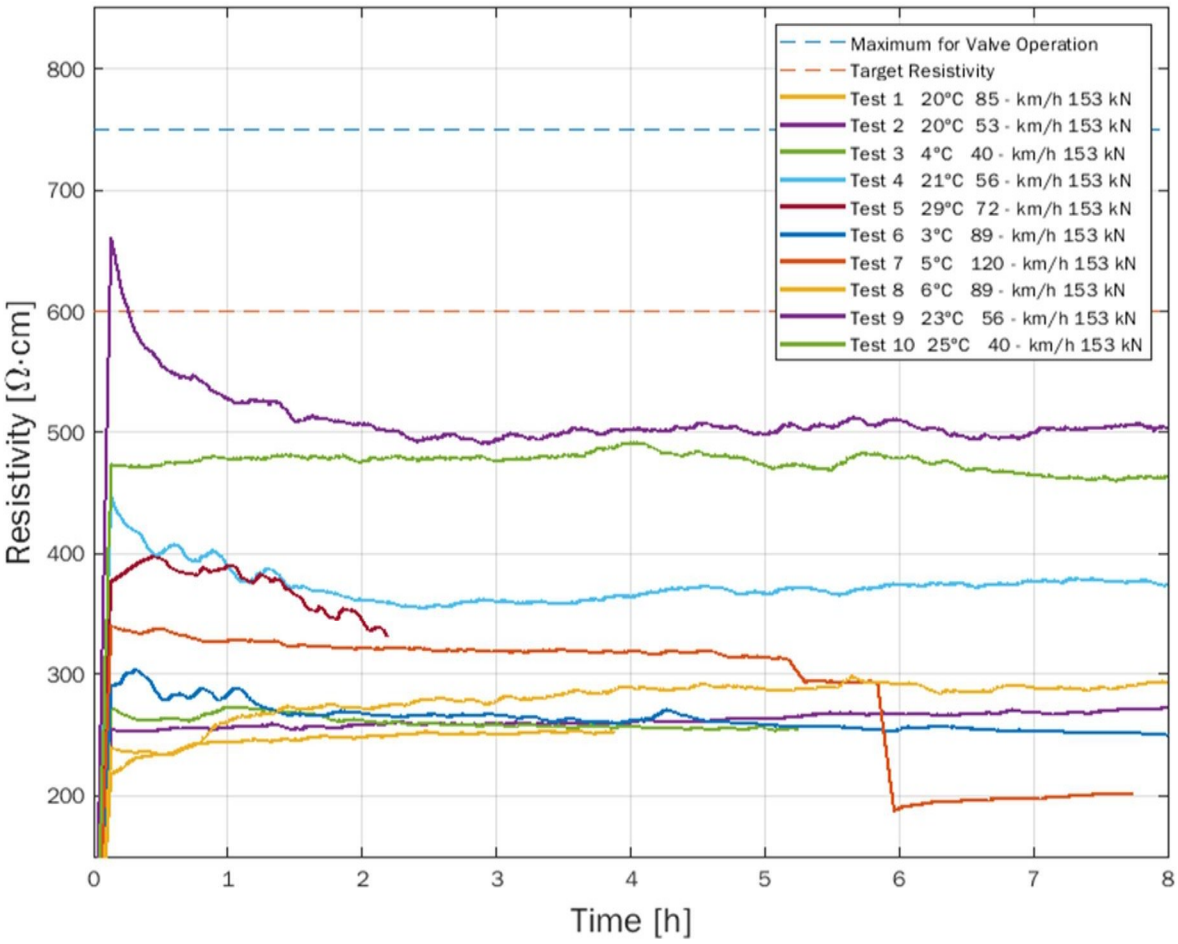

Figure 42: Resistivity of full pad insert tested on four-bearing tester under simulated service conditions.

Like the unloaded tests conducted on the 4BCT, the resistivity quickly rises and begins to settle with all tests reaching steady state resistivity values within two hours of testing under full load, except for test 5, which was cut short due to computer issues. All tests carried out at the full railcar load had steady state resistivity values that fell in the range of 200 to 500 Ω·cm, which is well below the 'target resistivity'. The solenoid valve was randomly actuated multiple times during these ten tests and never failed to actuate, regardless of the ambient temperature or axle speed.

The 120 Ω·cm drop in resistivity in less than one hour produced in Test 7 is likely the result of not pausing the DAQ software during the random testing of the solenoid valve. This

jump is consistent with applying additional power (24 volts) to the system versus the 8 volts the pad normally experiences during routine resistivity testing (as opposed to solenoid valve actuation testing). This behavior is caused by the quantum tunneling phenomenon. As the voltage increased, the jumps the current is required to make between fibers are shorter which aids in lowering the resistivity of the composite adapter pad.

These tests proved that the modified adapter pad with the TPU-CNF composite inserts was successful in actuating the solenoid valve regardless of the ambient temperature, axle speed, or load applied.

5.3 Hysteresis Results

To ensure that the heat generated from cyclic mechanical loading would not negatively impact the performance of TPU-CNF composite pad inserts, hysteretic testing was conducted comparing an unmodified adapter pad to the modified pad with composite inserts. Figure 43 is the plotted temperature data derived from the investigation of the thermal hysteresis of the composite pad inserts. These pads were subjected to dynamic loading as described in Table 3. The results from the cyclic testing show that the unmodified control pad achieves a thermal steady state slightly faster than the full pad. Results also show the full pad reaches a slightly higher temperature while testing, with temperatures ranging from 24.8°C to 26.3°C (76.6°F to 79.3°F), compared to the unmodified control pad temperatures which ranged from 22.6°C to 23.8°C (72.7°F to 74.8°F). Ultimately, the cyclic testing did not have a negative effect on the resistivity of the full pad, meaning that oscillating loads that might be experienced in rail service are unlikely to hinder the performance of the pad with conductive composite inserts.

Table 3: Hysteresis testing parameters

Test	Force [kN]	Amplitude [kN]	Force [kips]	Amplitude [kips]	Frequency [Hz]
1	26.0	4.45	5.85	1	3
2	26.0	8.9	5.85	2	3

3	26.0	17.8	5.85	4	3
4	53.4	26.7	12.7	6	6

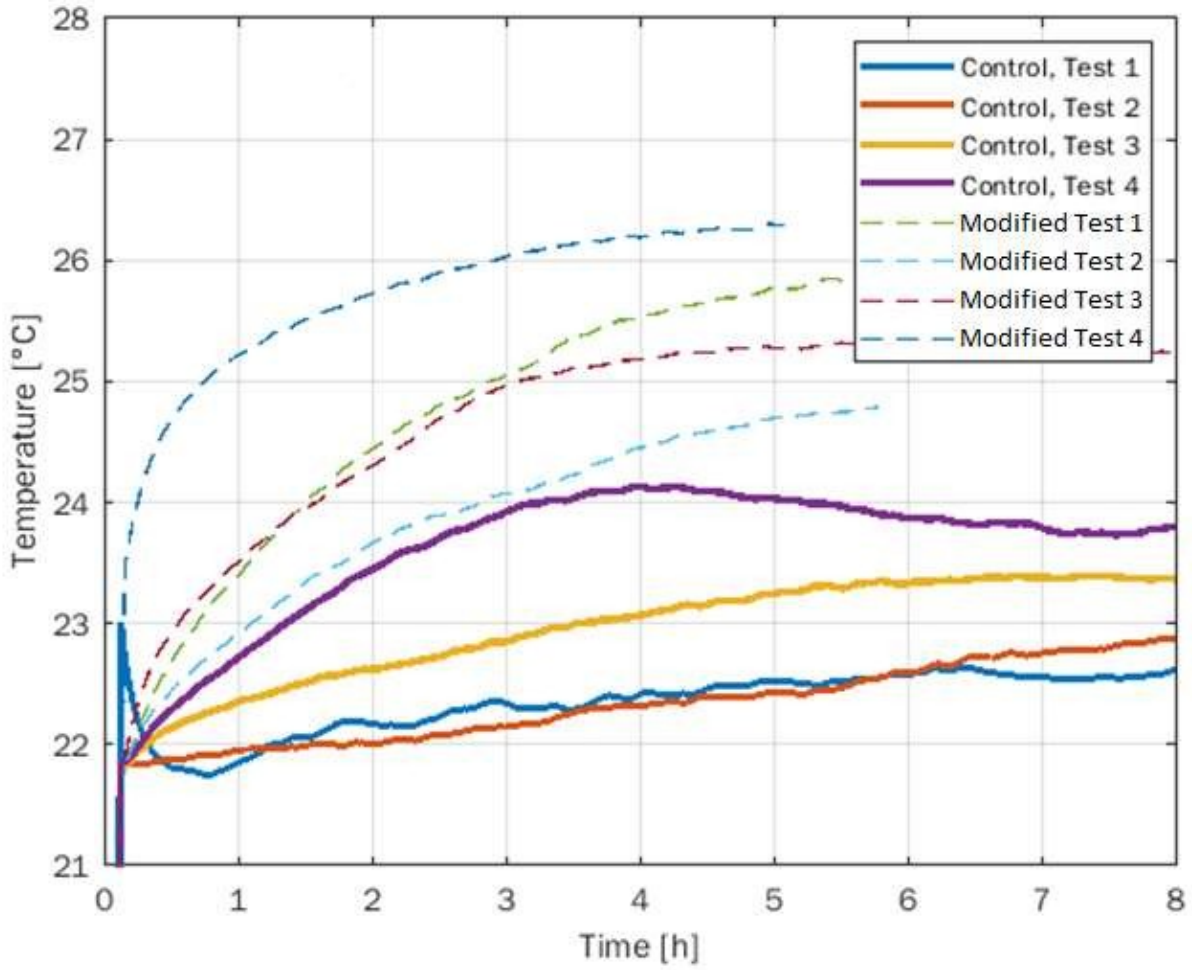

Figure 43: Hysteresis results

5.4 Scanning Electron Microscopy Results

The other major objective of the work performed in this thesis was to determine whether commercial mold flow software could guide mold and gate design. For commercial deployment of this technology, a larger, probably multi-cavity, mold would likely be required. Prediction of fiber alignment during mold filling using standard mold flow software would greatly facilitate the design process. Commercial software generally does not include flow data for nanofiber systems so modeling and mold design was done using data for standard short fibers.

The models which guided the mold redesign provided an overall map of fiber alignment and predicted high levels of alignment in certain regions. Scanning electron microscopy of these key sections indicates that the alignment obtained is consistent with the model predictions. Two examples of the Mold Flow fiber alignment predictions being validated through SEM images are provided hereafter. Figure 44 and the location and section view of the sample areas 1 and 2 for which SEM images are shown.

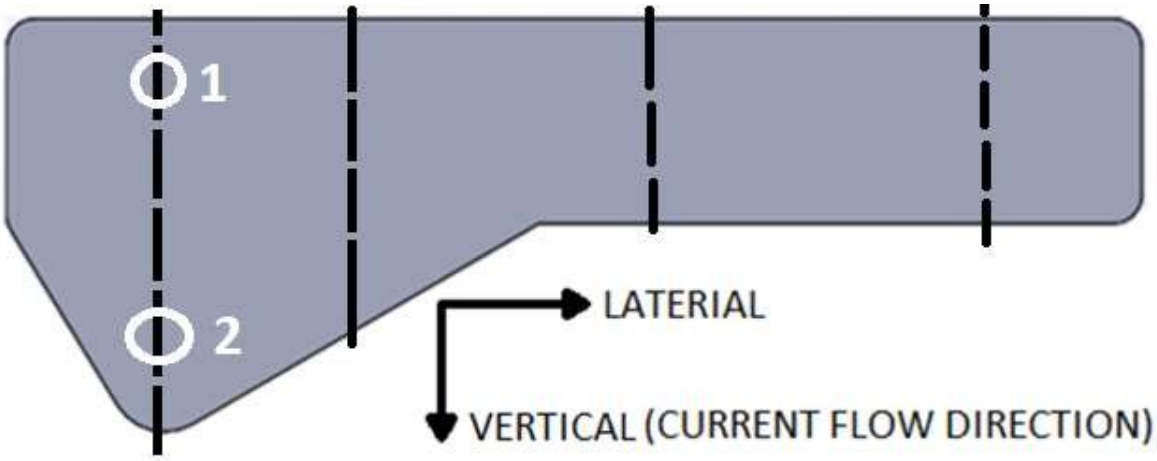

Figure 44: Location of notches and section cuts for SEM imaging

Sample SEM images showing the high levels of fiber alignment certainty in sample area 2 are provided in Figure 46 and Figure 47 at 2000 and 5000 magnification, respectively. Similarly, the SEM images for sample area 1 are provided in Figure 48 and Figure 49 at 2000 and 5000 magnification, respectively. The uniformity of the long and unbroken carbon nanofibers can be seen in both images with no apparent clumping or entanglement of the fibers.

The orientation of the fibers is in a generalized, single direction which aids in validating the Moldflow simulation design created at the start of this work. More importantly, it proves that fiber alignment in the vertical direction does create the conductive adapter pad, originally hypothesized at the start of this work. Additional SEM photos can be found in APPENDIX A .

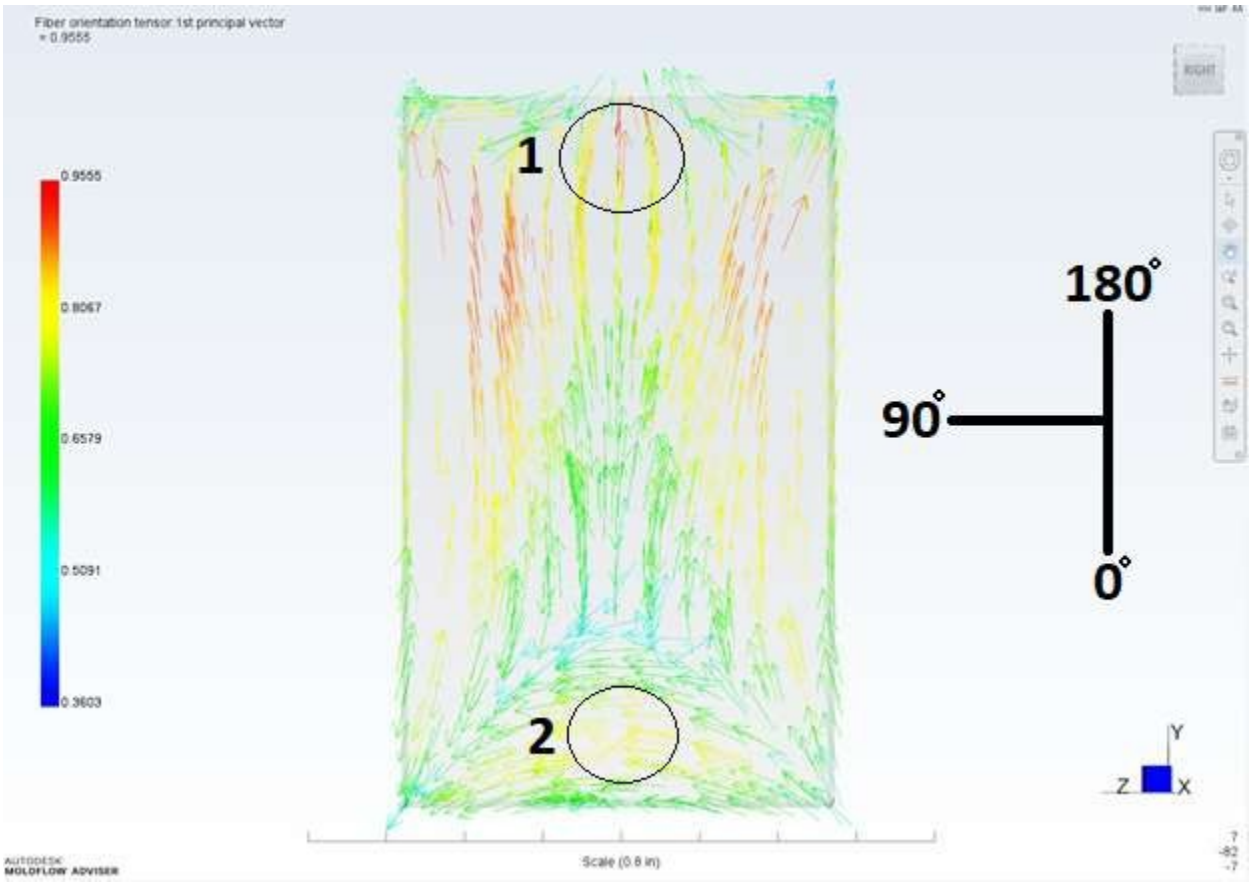

Figure 45: Section-view of sample area 1 and 2

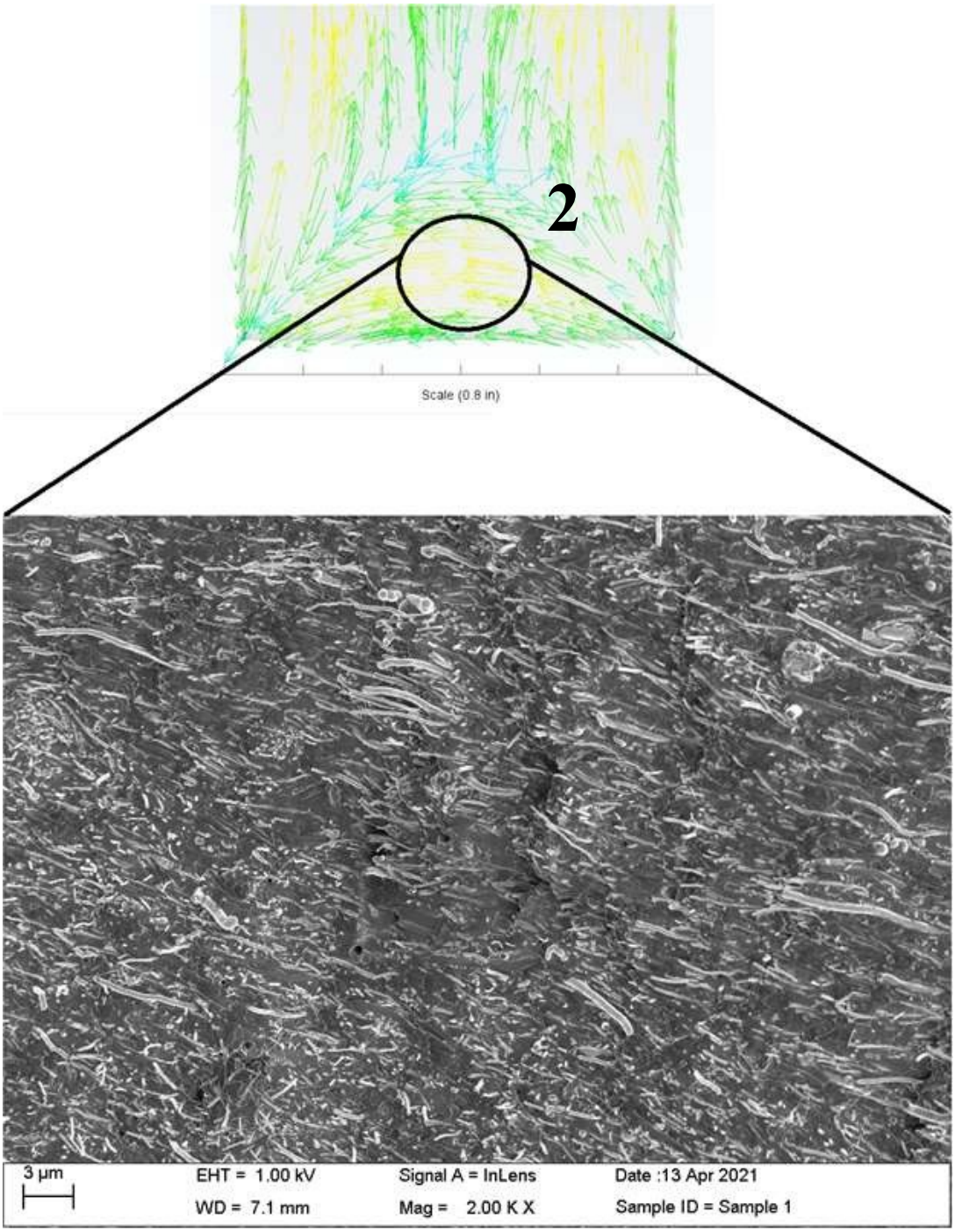

Figure 46: Sample 1, section 2, micrograph results 2000x at magnification

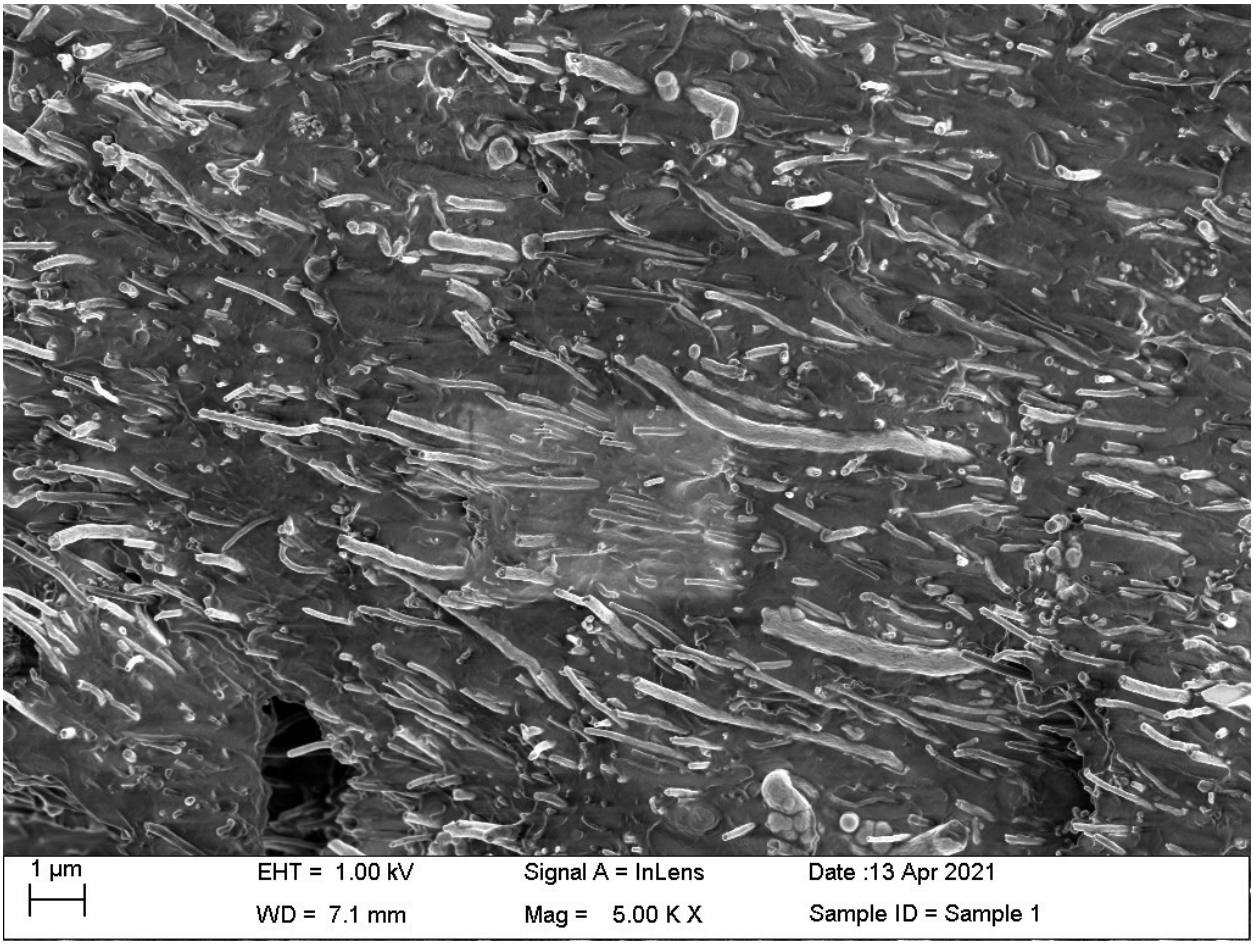

Figure 47: Sample 1, section 2, micrograph results 5000x at magnification

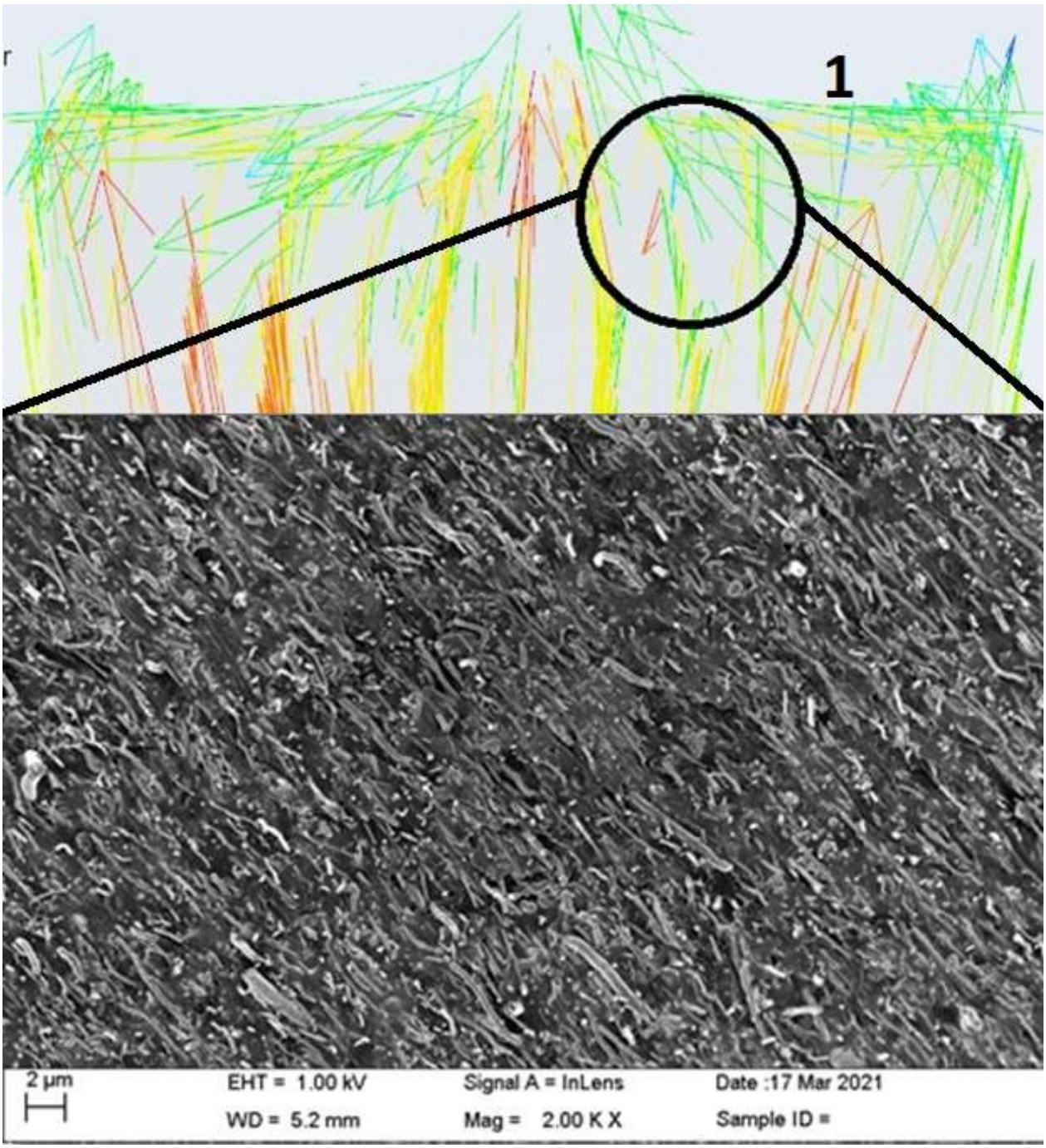

Figure 48: Location of SEM sample area to validate alignment, near top section cut of sample and sample 1, section 2, micrograph results at 2000x magnification

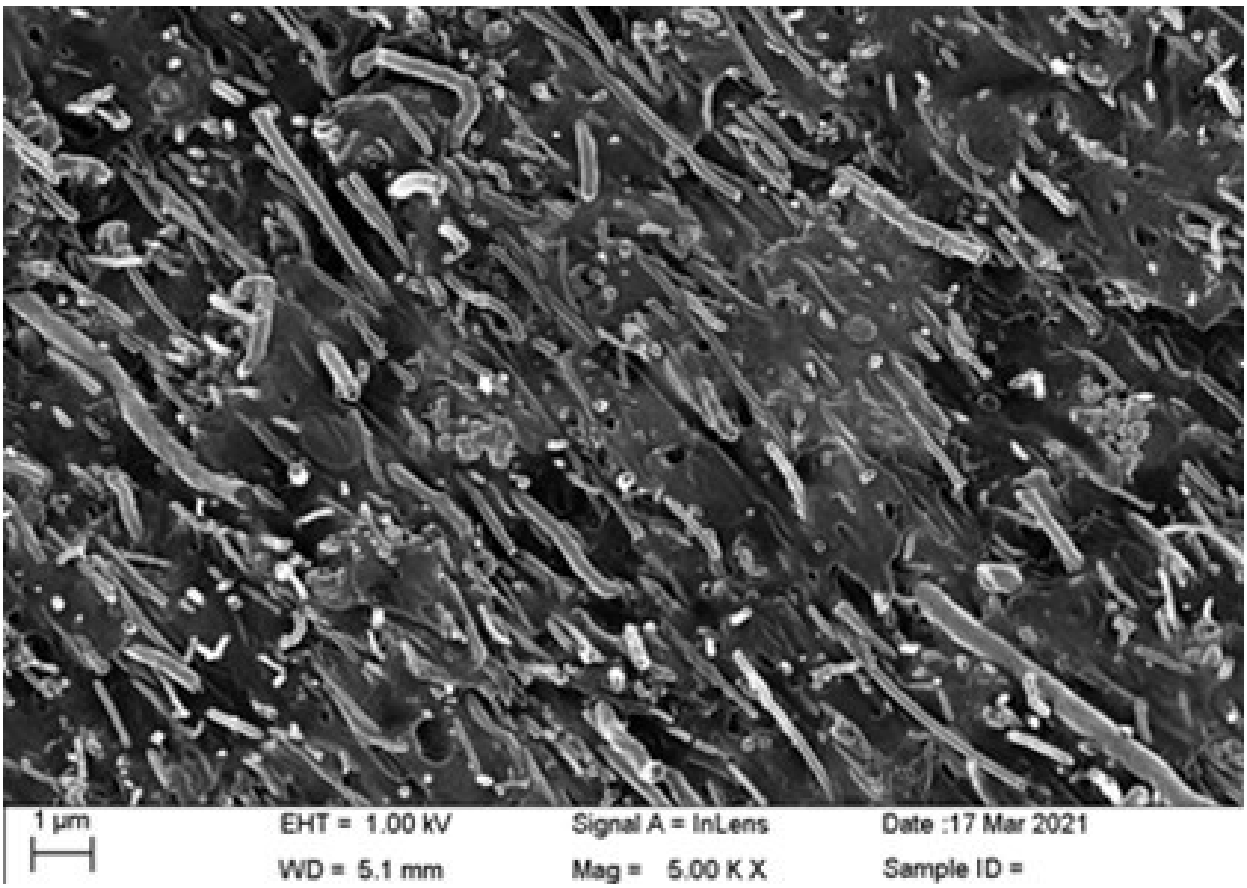

Figure 49: Sample 1, section 2, micrograph results at 5000x magnification

Image-Pro Plus®, a photo imaging analysis software, was used to analyze the SEM images of the TPU-CNF insert sample. Figure 50 shows the plotted angles of carbon nanofibers. Simulations of the composite mold insert flow showed that these areas had a higher level of fiber alignment certainty. At this location of imaging, the plot shows that nanofibers oriented in a general direction of, 114 degrees with a deviation of ±32°.

It is important to note that the software used, Image-Pro Plus® considers the six o'clock position to be 0°, the nine o'clock position to be 90°, and the 12 o'clock position to be 180°.

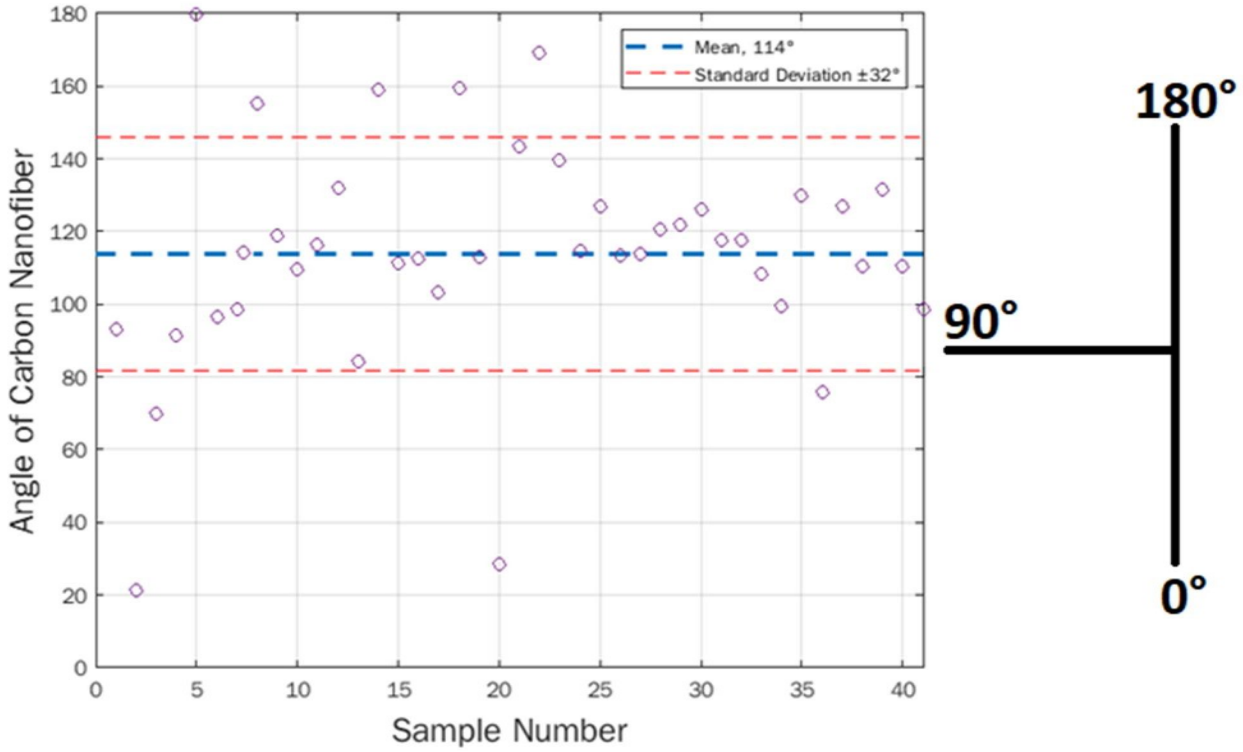

Figure 50: Angle of fiber alignment of sample 1 composite insert, section 1, area 2

5.5 Extended Testing Results

Additional extended duration tests were performed on the MTS 810 and the 4BCT to ensure that the full pad would remain conductive after eight hours and that the resistivity values would not begin to trend upwards towards the target resistivity or higher. To investigate this matter, tests on the TPU-CNF composite inserts were performed utilizing an empty railcar load and low ambient temperatures, which are concerned to be unfavorable operating conditions.

Tests conducted on both testers followed similar trends and patterns. On the MTS 810, the modified adapter pad maintained a consistent resistivity under the target resistivity after 300 hours of continuous uninterrupted testing. Tests conducted on the 4BCT also maintained a consistent resistivity well below the target resistivity value at an ambient temperature of 1°C (34°F) and 26 kN of applied force (i.e., empty railcar load) after 100 hours of continuous testing.

The sudden jumps in resistivity exhibited in test 1 on the 4BCT are caused by sudden changes to the simulated train speed during testing. Changes to train speed affect the bearing operating temperature, which in turn, affects the pad operating temperature. Nevertheless, despite these sudden changes to the operating conditions of the test, the resistivity stayed well within the target resistivity value of 600 Ω.cm. The latter validates the effectiveness and reliability of the modified pad with composite inserts in providing an electrically conductive solution that is not affected by changes in the operating conditions of freight railcars in service.

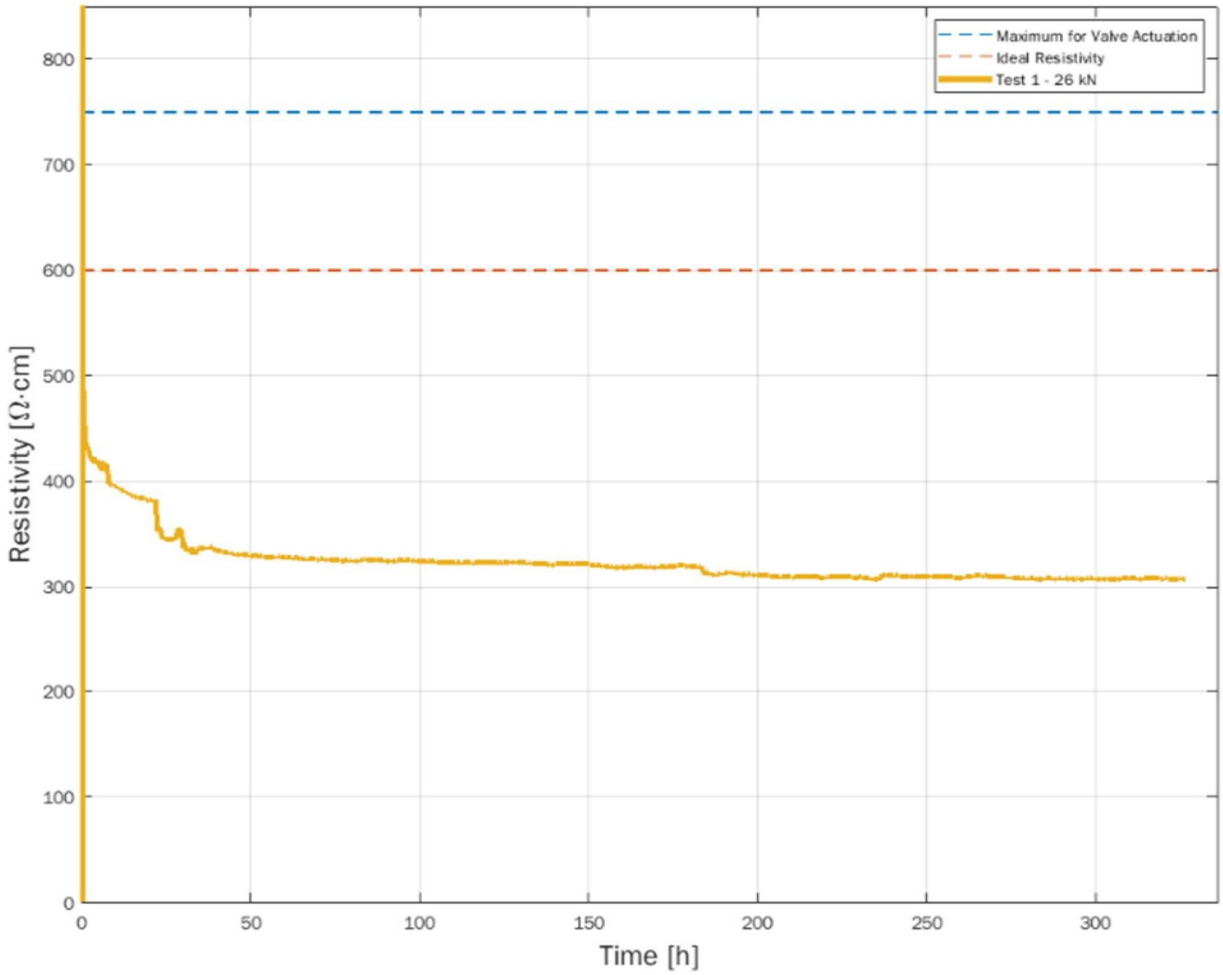

Figure 51: Angle of fiber alignment of sample composite insert

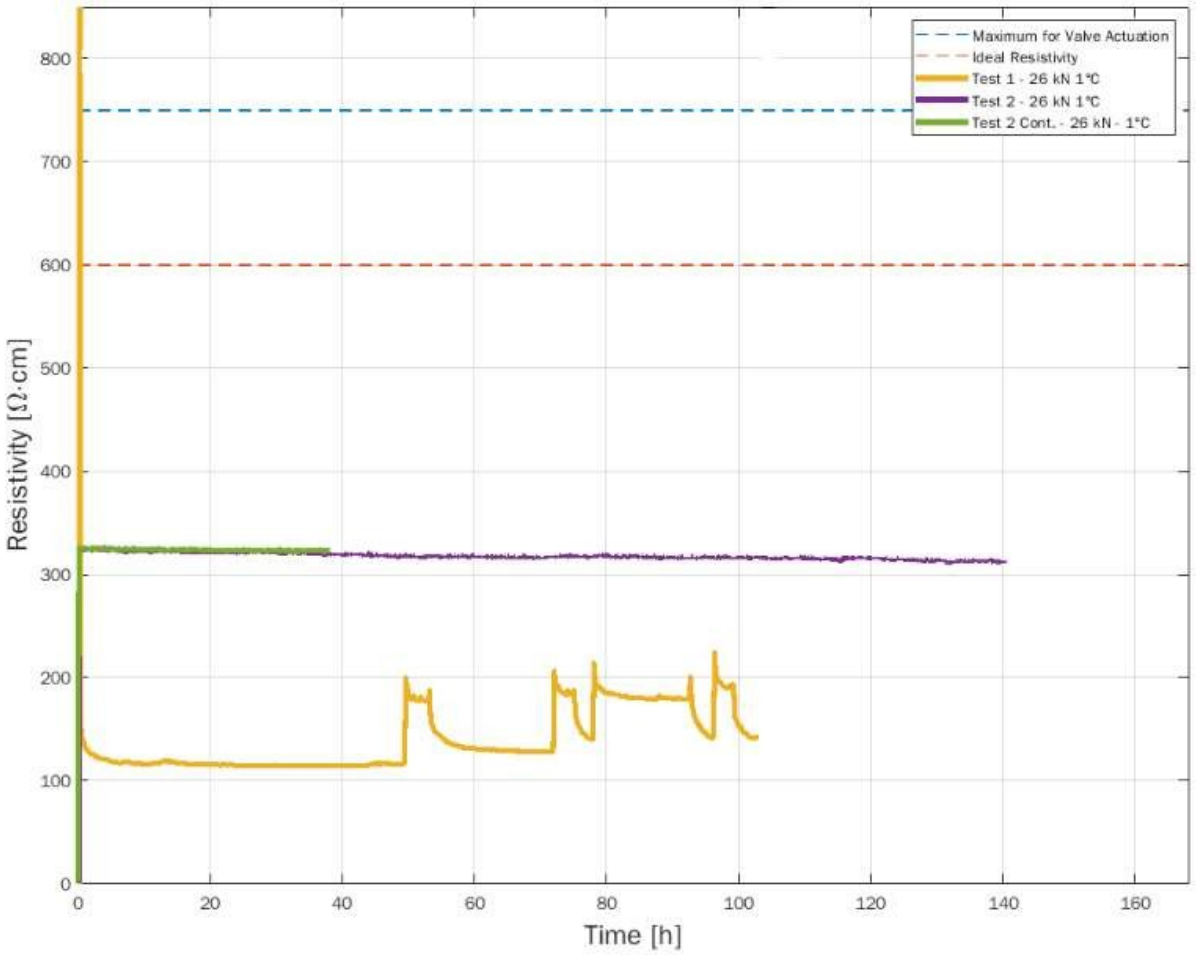

Figure 52: Angle of fiber alignment of sample composite insert

5.6 Optimization

With a successful composite insert design in hand, there is a motivation to reduce the overall footprint of the composite adapter pad inserts and confine them to the interlock "triangle" section of the pad only. This goal was achieved by removing the leg portion of the composite insert, resulting in an "interlock-only" composite insert. This opportunity to optimize and reduce the size of the insert led to a reduction of 53% of the volume of each insert and would significantly reduce the amount of CNF material used as this material is pricey.

These optimized inserts were tested in 3 configurations: 3×3, 4×4, and 5×5. The 3×3 configuration means that 3 interlock-only composite inserts were installed in both sides of the

modified adapter pad, meaning 6 interlock-only composite inserts installed per adapter pad. The 4×4 configuration has 4 interlock-only composite inserts installed, totaling 8 inserts for the full pad, and the 5×5 configuration (pictured in Figure 53) has a total of 10 interlock-only composite inserts installed per full pad. All configurations were subjected to extended testing and periodic solenoid valve actuation testing.

Figure 53: 5x5 interlock-only composite inserts on the MTS 810

Figure 54 shows the results of the 3×3, 4×4, and 5×5 configuration testing. Similar to the half pad testing at different voltages on the MTS 810, the resistivity settled at different levels based on the number of interlock-only composite inserts installed when a constant potential of 8 volts was supplied. As the number of inserts increased from 6 to 10, the settling range of resistivity also increased. All random valve actuation tests conducted on the MTS 810 were

successful. As the number of inserts decreased, the resistivity also decreased, but the amount of voltage required to actuate the solenoid valve increased.

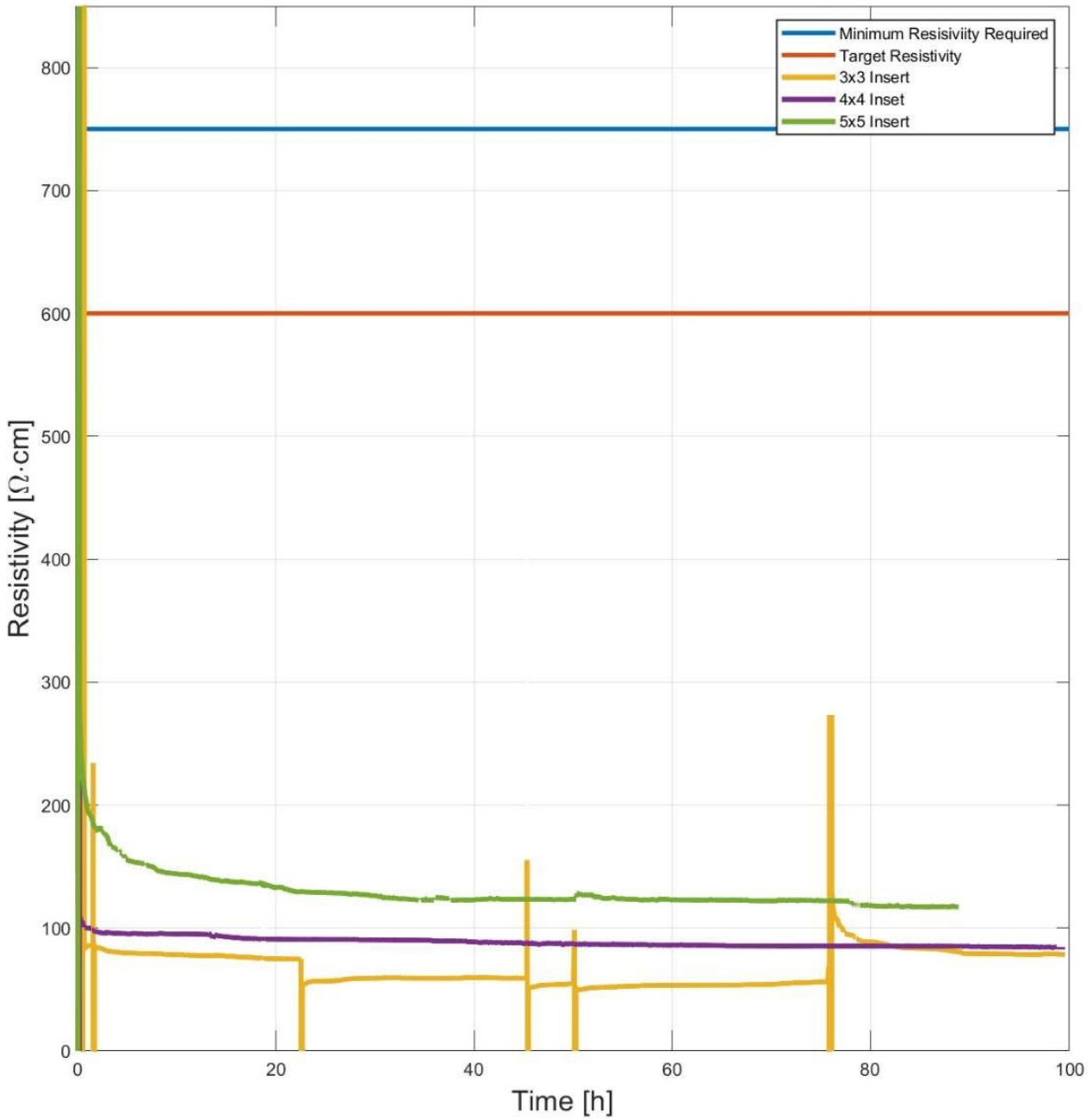

Figure 54: Resistivity results of the 3×3, 4×4, and 5×5 insert configurations after 100 hours of laboratory testing.

The random jumps in resistivity during the 3×3 configuration test were a result of neglecting to pause the DAQ while voltage was paused and increased during random solenoid valve testing. Like previous extended tests, the resistivity of the interlock-only inserts did not

climb toward the target resistivity even after 195 hours of continuous testing, as illustrated in Figure 55. However, these results indicate that a 3×3 interlock-only composite insert configuration has the required resistivity needed to actuate the solenoid valve while significantly reducing the footprint of the TPU-CNF insert set and the amount of CNF used. Hence, these results shared here demonstrate that the composite insert design can be greatly optimized for performance and cost.

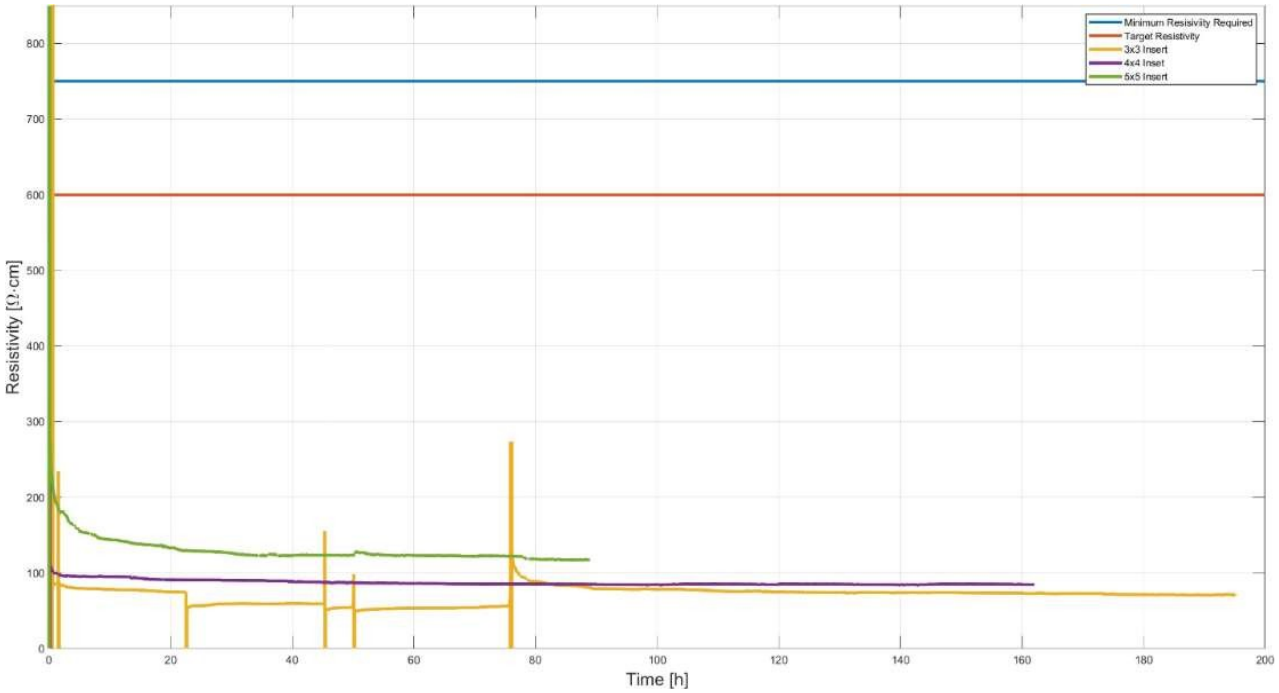

Figure 55: Resistivity results of the 3×3, 4×4, and 5×5 insert configurations after 180 hours of laboratory testing.

CHAPTER VI

CONCLUSIONS AND FUTURE WORK

This work is a succession to the previous efforts of the University Transportation Center for Railway Safety (UTCRS). The goal was produce an inherently conductive composite polymer pad using an insert composed of Thermoplastic Polyurethane-Carbon Nanofiber (TPU-CNF). This modified adapter pad would replace the traditional two-copper stud design currently used in service. The required injection-molding process was refined using Autodesk® Moldflow simulation software which allowed for finer control over the direction of polymer flow and in turn yielded a fiber alignment with a strong potential for electrical conductivity. The material used to create these composite inserts, by weight, is 85 wt% Elastollan® 1195a TPU and 15 wt% carbon nanofibers. The polymer exhibited a range of characteristics including high toughness, and a resistance to abrasion and tear propagation. These properties made this material ideal for the dynamic and cyclic loading conditions typically experienced in railcar service. The conductive inserts replace the interlock-portion of the suspension adapter pad. The 810 Materials Test Systems (MTS 810) and the UTCRS-designed Four-Bearing Chamber Tester (4BCT) were used to evaluate the modified adapter pad under varying conditions. These conditions included dynamic and cyclic loading with forces ranging between 26 kN and 153 kN (5.85 kips to 34.5 kips), ambient temperatures ranging from -17°C to 65°C (1°F to 150°F), and simulated axle speeds ranging from 40 km/h to 105 km/h (25 mph to 65 mph).

6.1 MTS 810 Test

The tests involving the half-pad-yielded resistivity values between 175-and 580 Ω·cm with an applied load of 26 kN (5.85 kips), which is representative of an unloaded railcar. Loading tests proved that 10 kN (2.25 kips) was the minimum required load to enable the valve to actuate-that 26 kN loads will always be sufficient for valve actuation. An ambient temperature of 22 ± 2°C (72° ± 3.5°F) was sustained, along with free convection conditions. The tests involving the full-pad resulted in resistivity values between 400 and 580 Ω·cm having experienced the same applied load, ambient temperature, and free convection conditions as the half-pad.

These results are well below the 750 Ω·cm threshold needed to actuate the solenoid valve. The half-pad successfully actuated the 24-volt solenoid valve under every experimental condition, which is the primary benchmark for a successful TPU-CNF composite adapter pad insert. These actuation tests were conducted concurrently throughout all 11 resistivity tests at regular intervals during testing. This confirms the fiber alignment hypothesis first proposed by Villareal [10] who stated that overall fiber direction was a necessary feature in creating a conductive polymer insert to replace the shear-prone two-copper stud design.

The correlation that quantum tunneling is directly responsible for low resistivity is seen in tests with higher voltages applied to the circuit and the half-pad. As the voltage increased, the resistivity values decreased. The voltage applied to the inserts is enabling the current in bridging larger gaps between nanofibers that are not in direct contact, as discussed in the literature review. All half-pad and full pad tests successfully actuated the solenoid valve, allowing the TPU-CNF composite inserts to undergo further validation on the robust 4-Bearing Chamber Tester where the harsh conditions of railway service can be simulated.

6.2 4-Bearing Test, Unloaded

The goal of these tests was to expose the modified adapter to a "worst-case scenario" defined by low ambient temperatures and unloaded railcar forces. The full-pad tests yielded resistivity values between 310 and 540 Ω·cm. Simulated axle speeds ranged from 40 to 89 km/h (mph) and a force of 26 kN (5.85 kips). The ambient temperature for these tests ranged between -17°C and 8°C (1.4°F and 46.4°F). The results were below the 750 Ω·cm threshold required to actuate the solenoid valve.

Regardless of temperature and applied load, the resistivity of the composite adapter pad fell below the target resistivity which is ideal for solenoid valve actuation. The resulting heat produced by bearing friction serves to reduce resistivity. Lower polymer resistivity is achieved at higher temperatures because it is easier for the nanofibers to realign and for electrons to tunnel through the polymer. This heat also results in better surface contact between the modified composite adapter pad and the simulated railcar due to increased polymer creep.

6.3 4-Bearing Testing, Loaded

The modified adapter pad was subjected to simulated speeds ranging from 40 to 120 km/h (25 to 75 mph) and 153 kN of applied load, representative of a fully loaded railcar, and yielded resistivity values between 200 and 500 Ω·cm, which was well below the desired resistivity threshold. The solenoid valve was successfully actuated without fail throughout every experimental condition performed on the 4BCT.

As proven in previous experiments, subjecting the adapter pad to higher loads (153 kN), causes the insert set to level out at a minimum resistivity value faster than when subjected to lighter 26 kN loading conditions. The rate at which the pads reach this baseline resistivity indicates that the relaxation mechanisms involved are slow to respond. Hence, the short-term excursions that result in a loss of contact between the railcar and the adapter pads (impact forces

like those caused by track defects or flat spots on wheels) will not affect resistivity levels because the material response to the force impulse will be too slow to surrender the established state of fiber compression and surface morphology. The low resistivity equilibrium is reached within a few hours which is ample time for a newly installed pad to achieve this state before serving its intended purpose as a conductor.

6.4 Extended Testing, MTS 810 and 4BCT

The endurance tests are conducted under 'worst-case scenario' conditions that include lighter loads and lower temperatures. The tested inserts remained under the target resistivity with no extreme fluctuations throughout 168 hours, having mostly leveled off to a steady-state resistivity within a few hours. The static-load temperature tests were evaluated at 1ºC while the axle was stationary so that no additional heat was being generated from the bearing to contribute in lowering resistivity. The results suggest the adapter pad inserts will maintain the resistivity required to successfully actuate the solenoid valve regardless of railcar motion and independent of bearing heat generation. These tests imply that the TPU-CNF inserts may be a viable replacement for the two-copper stud design in terms of long-term reliability.

6.5 Hysteresis Testing

Hysteretic cyclic loading tests revealed a small increase in temperature in the modified adapter pads as compared to the unmodified controls. This indicates that the addition of composite inserts did not have a significant impact on the hysteretic properties of the modified adapter pad. The resulting slightly higher operating temperature of the modified adapter pad may be beneficial by effecting lower resistivity values and improving surface contact between the metal railcar components and the adapter pad.

6.6 SEM

The fiber alignment of the TPU-CNF composite insert is directly responsible for conductivity in the TPU-CNF composite insert. In the previous works by Suarez [3], Basaldua [9], and Villareal [10], the fiber orientation was not scrutinized which proved to be the reason behind the insufficient conductivity for previous iterations of adapter pad inserts.

Scanning Electron Microscope (SEM) microscopy produced detailed images of the TPU-CNF composite inserts revealing considerable amounts of fiber alignment. The observed alignment follows the predictions generated by the adapted mold flow software giving credence to the software as a viable tool in simulating the orientation of the nanofibers.

6.7 Optimized

Optimization efforts revealed that 76% of the top surface area of the polymer adapter pad inserts was being used redundantly, as only 24% of the surface area was required to reliably actuate the solenoid. Limiting inserts to the interlock area yielded resistivity values near those of the half-pad test on the MTS810. This is consistent with the Moldflow® models which generated regions of high fiber alignment in the interlock section as compared to the moderate alignment present in the arm section. The size-reduced, interlock-only inserts provide a cost-efficient direction for the next iteration of the conductive insert design.

6.8 Summary

Given the results of all the tests conducted on the modified composite adapter pad inserts on both the MTS810 and the 4BCT, it can be concluded that the composite adapter inserts will be a suitable replacement for the two-copper stud design currently in service today.

The composite adapter pad inserts were conductive throughout all loading conditions. Specifically, with the unloaded railcar conditions, the minimum load the adapter pad will

experience in service is enough compressive force to reach the resistivity that allows the solenoid valve to actuate. There is no loading condition, in reference to expected railcar service loads, that prevents the modified adapter pads from reaching the desired resistivity, with any further increase in load yielding an increasing benefit to conductivity.

This is further proved at colder temperatures, where minimum loading conditions will produce the electrical resistivity required to actuate the solenoid valve, regardless of bearing heat generation, i.e., railcar motion. As the bearing generates heat, the adapter pad increases in temperature, causing resistivity to decline as heat generally benefits fiber alignment. The electronic freight valve actuated without fail when exposed to all temperature, simulated axle speed, and load conditions in the laboratory setting.

Lastly, the micrograph imaging results present high levels of certainty regarding fiber alignment in the interlock portion of the adapter pad insert. The images from those select areas match the short fiber alignment predicted in the mold design and validate the hypothesis of fiber alignment proposed by Villareal [10] who stated that vertical fiber alignment was a critical property in allowing the composite insert to reach the conductivity necessary for solenoid valve actuation. These results suggest that the TPU-CNF composite adapter insert is a practical replacement for the two-copper stud design, which can be corroborated by a later field study.

6.9 Future Work

The progression of this work could begin where the optimization study left off, with the development of a smaller, more efficient composite insert and accompanying reduced-waste mold design. The next iteration of this design should feature a smaller footprint while producing an equal or better level of conductivity. A reduction in area will be more cost effective as the CNF needed to manufacture composite adapter pad inserts has a high price to volume ratio.

Given its success in laboratory conditions, the next phase of testing must be to implement this technology in the field for at least six months and investigate whether the TPU-CNF composite inserts can handle the harsh conditions of freight service. Moreover, further optimization can be performed by utilizing recycled TPU in composite inserts. This additional research would require balancing effective conductivity with the amount of recycled material necessary to create a polymer insert while reducing waste composite material.

REFERENCES

[1] Tarawneh, Constantine, M. Fuentes, Arturo A. Kypuros, Javier A. "A Vibration Energy Approach Used to Identify Temperature Trending in Railroad Trending in Railroad Tapered-Roller Bearings." International Journal of Acoustics and Vibration, Volume 20, No.2, March 2014.

[2] Amsted Rail. http://www.imajteknik.net/uploads/adapter-plus-steering-pad-system.pdf

[3] Suarez, R., "Design and Optimization of a Railroad Conductive Suspension Element Pad Composed of Thermoplastic Polyurethane and Carbon Black," Master's Thesis, University of Texas Pan-American, August 2013.

[4] BASF. Elastollan® 1195a TPU Technical Data Sheet

[5] Holden, G. Thermoplastic Elastomers. Third Edition. Munich: Hanser Publishers, 2004. Print.

[6] Drobny, J. G. Handbook of Thermoplastic Elastomers. Norwich, NY: PDL Plastics Design Library/William Andrew Pub., 2007. Print.

[7] "A Comparison of Carbon Nanotubes and Carbon Nanofibers." Pyrograf® Products Inc. Applied Sciences, n.d. Web. 13 Nov. 2014

[8] Al-Saleh, Mohammed H., and Sundaraj, Uttandaraman. "A Review of Vapor Grown Carbon Nanofiber/polymer Conductive Composites." Carbon 47.1 (2009). 2-22. Web.

[9] Basaldua, D. T., "Effects of Vapor Grown Carbon Nanofibers on Electrical and Mechanical Properties of a Thermoplastic Elastomer," Master's Thesis, University of Texas Pan-American, December 2014.

[10] Villarreal, A. "Microstructural Influences on the Mechanical and Electrical Properties of Carbon Nanofiber Thermoplastic Polyurethane Composites." Master's Thesis, The University of Texas Rio Grande Valley. August 2019.

[11] Siegel, Harry. "The Effects of Residual Crystallization on the Resistivity of TPU-CNF Blend" Dwight D. Eisenhower Transportation Fellowship Program Final Report. 2019

.

[12] Autodesk® Moldflow Advisor, Support and Learning. https://autode.sk/37FHbz6

[13] https://store.dme.net/mud-sprue-bushings

[14] https://www.dr-boy.de/en/products/boy-injection-moulding-machines/boy-22-a-pro/

[15] purdue.edu/ehps/rem/laboratory/equipment%20safety/Research%20Equipment/sem.html

[16] https://www.mdp.edu.ar/microscopia/documentos/DentonVacuum_manual.pdf
Desk II Cold Sputter/Etch Unit Operation Manual.

[17] Alex E. Salinas. “Sputter Process.” Photograph used with permission. 2021.

APPENDIX A

APPENDIX A

SEM MICROGRAPHS

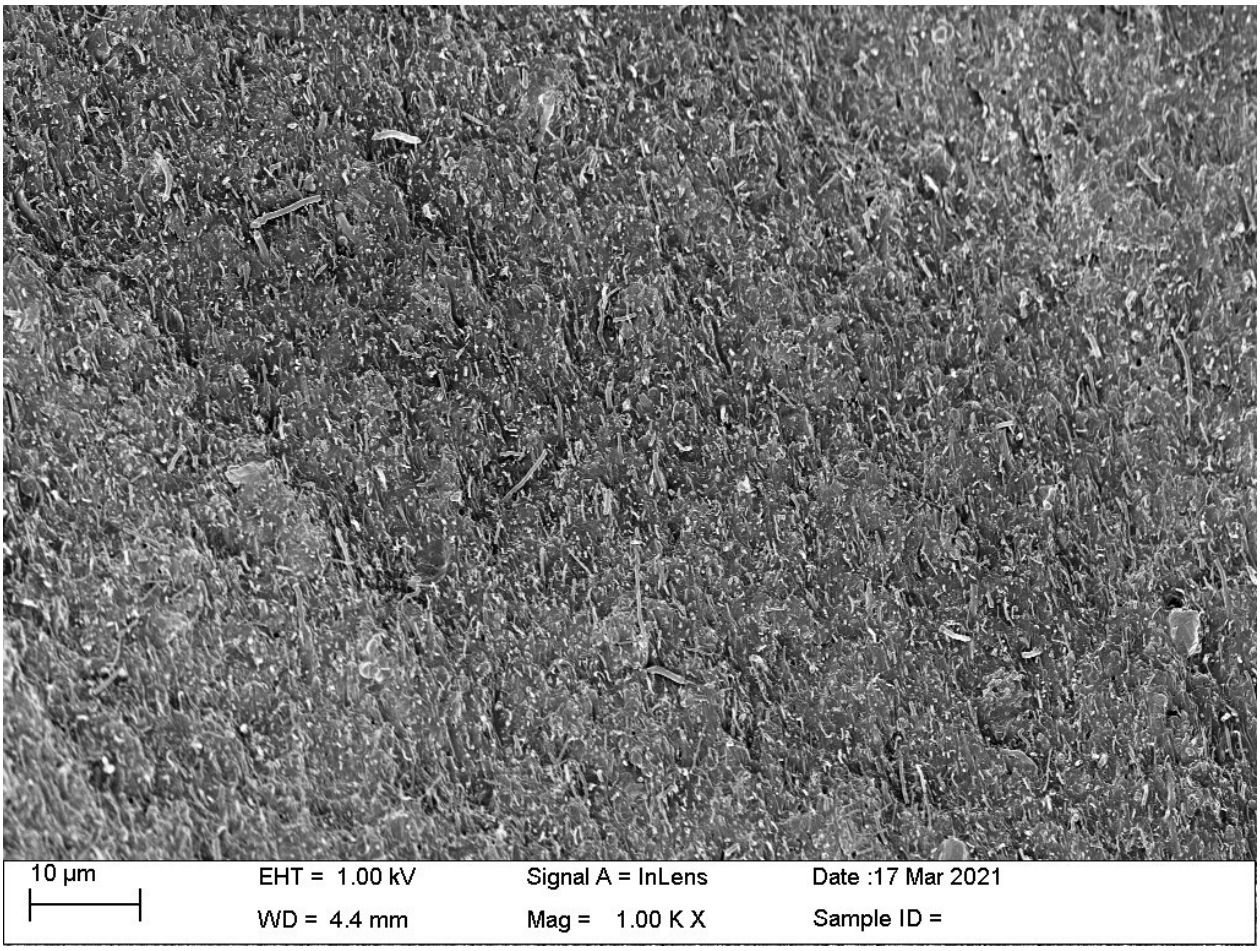

Figure 56: Sample 2, 1K magnification

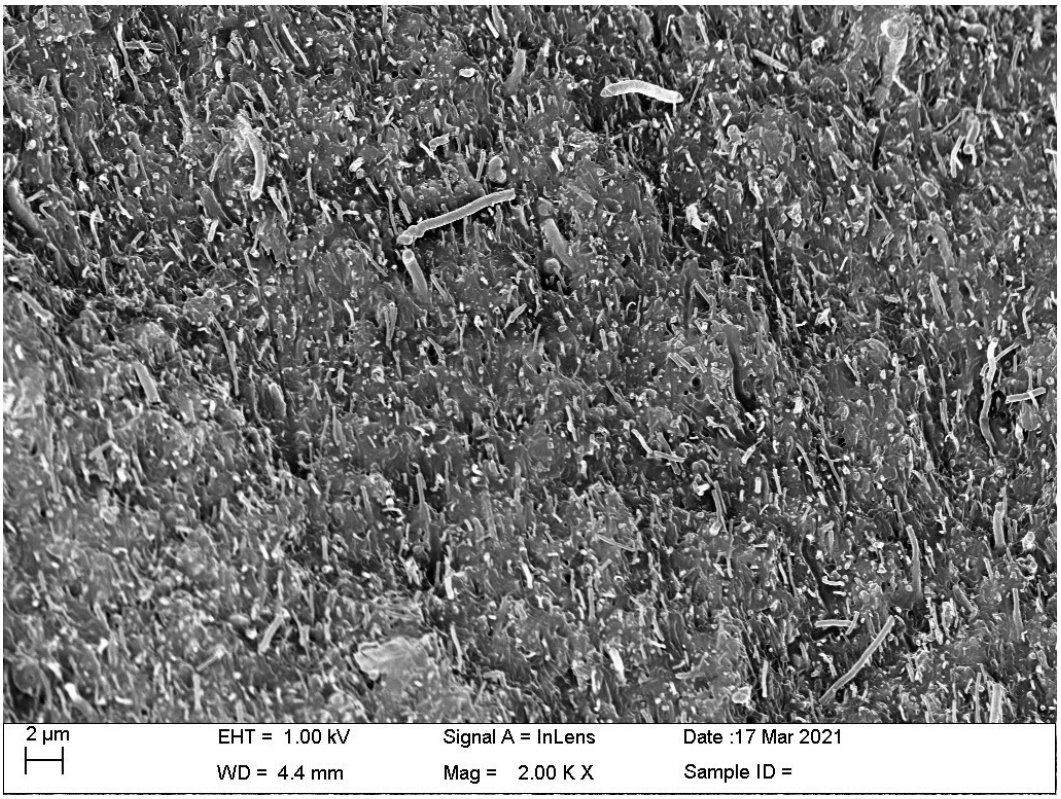

Figure 57:Sample 2, 2K magnification

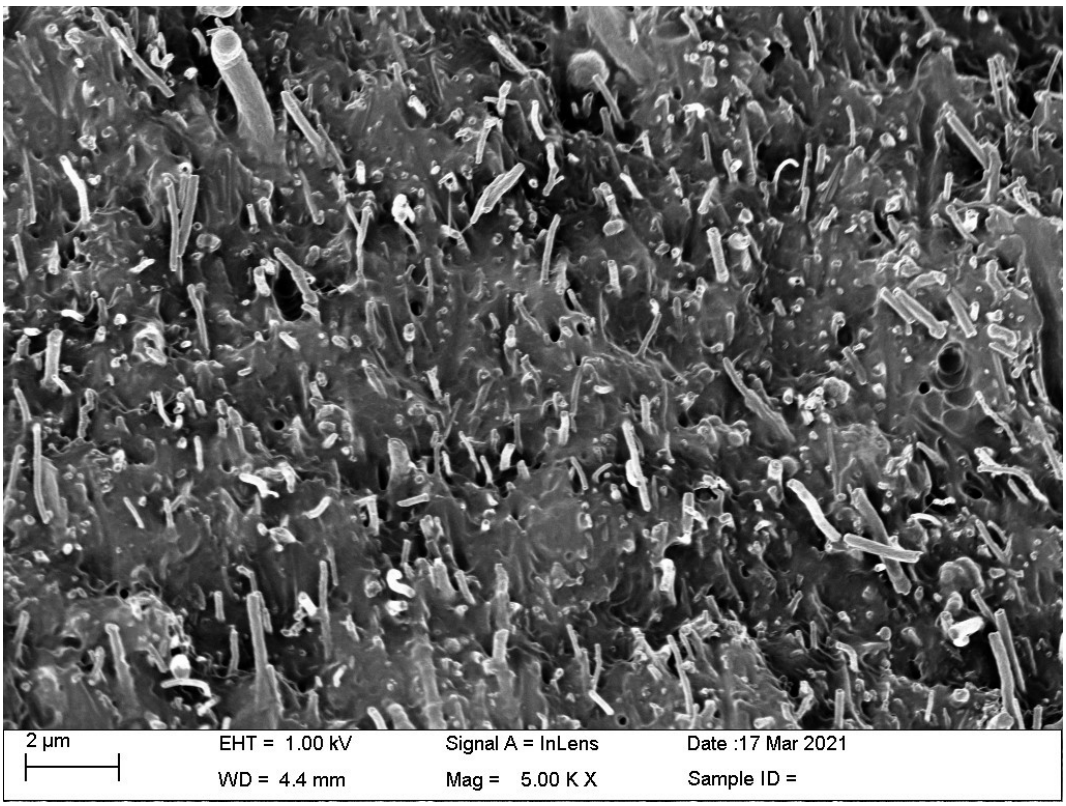

Figure 58: Sample 2, 5K magnification

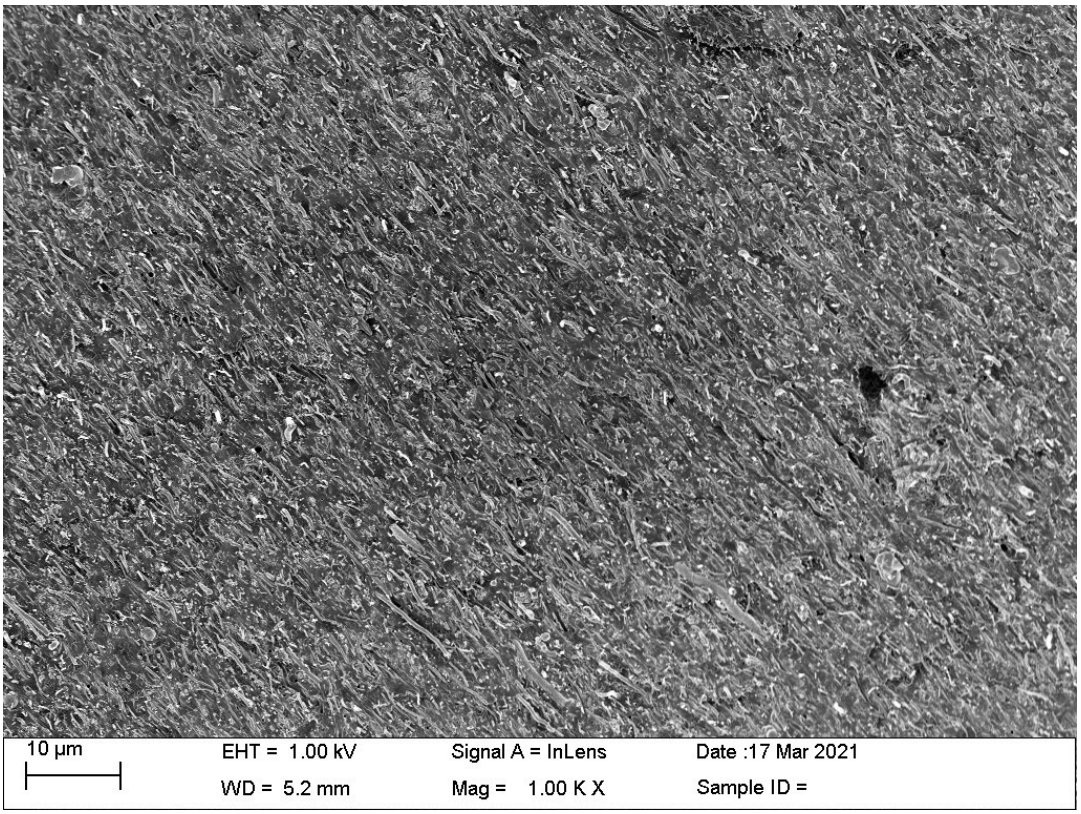

Figure 59: Sample 2, area 2, 1K magnification

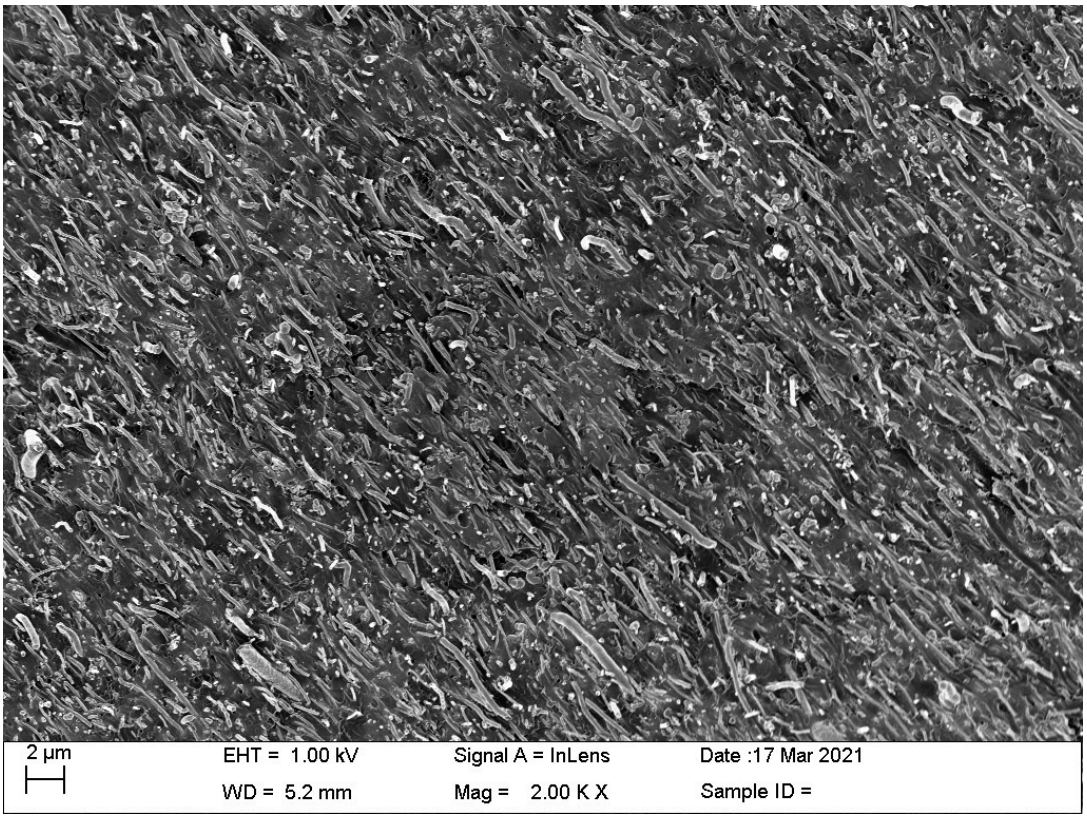

Figure 60: Sample 2, area 2, 2K magnification

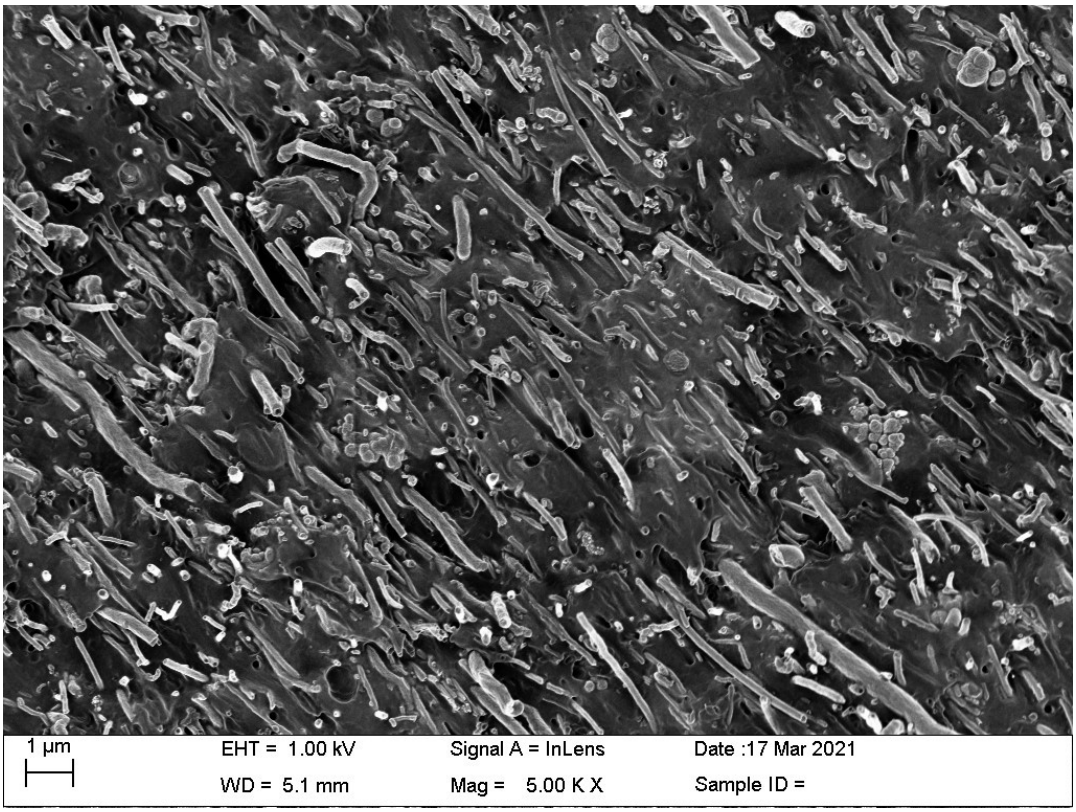

Figure 61: Sample 2, area 2, 5K magnification

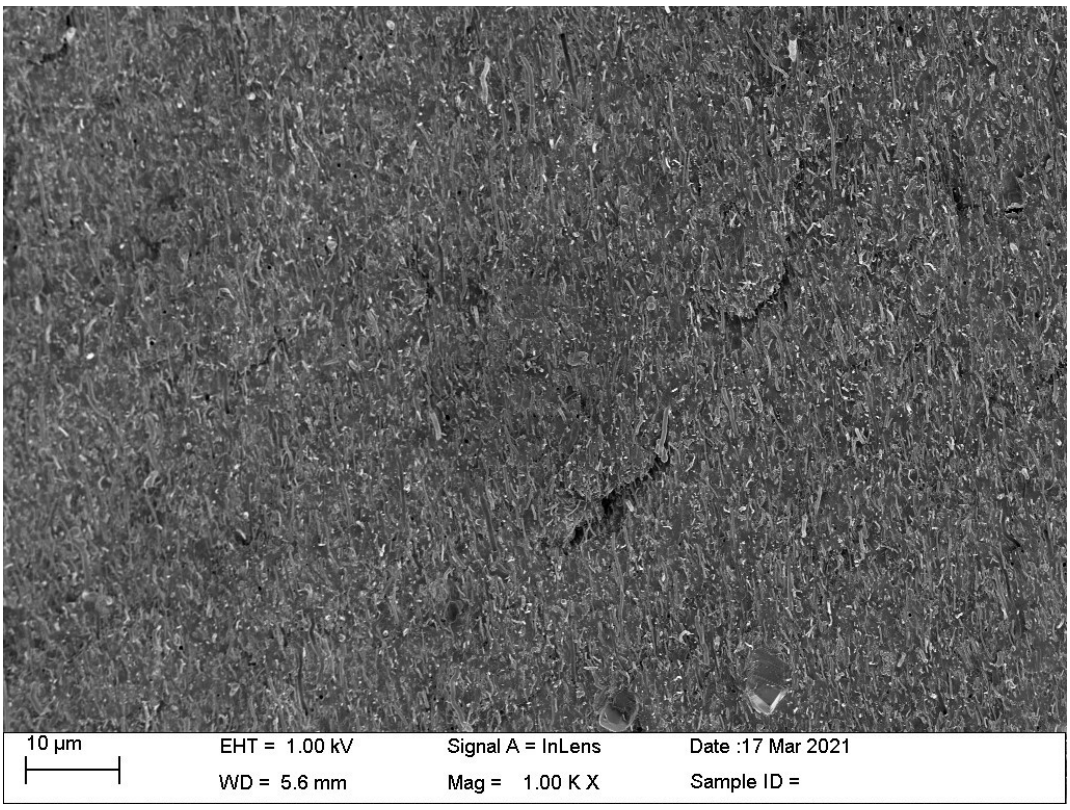

Figure 62: Sample 2, area 3, 1K magnification

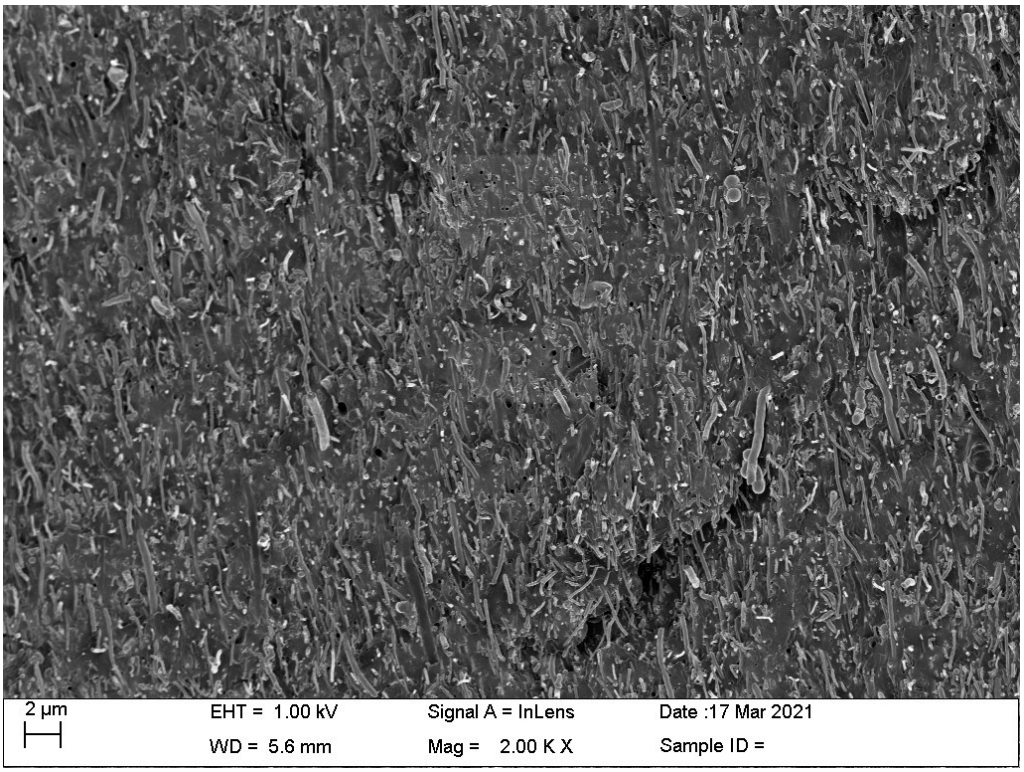

Figure 63: Section 2, area 3, 2K magnification

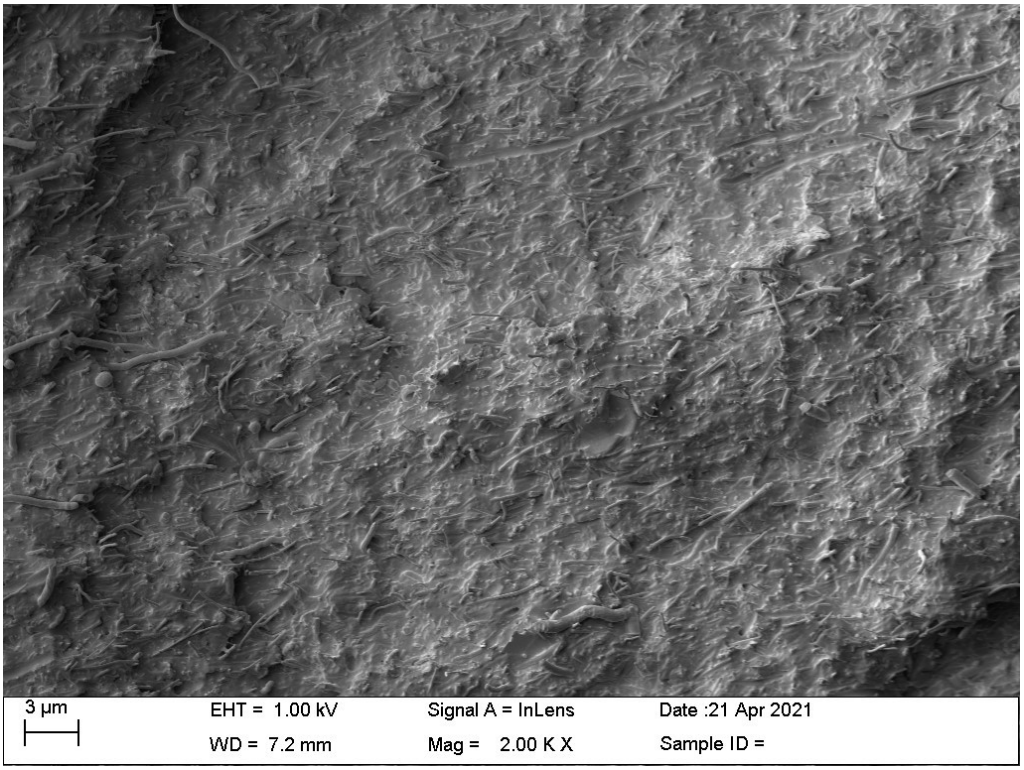

Figure 64: Sample 3, area 1, 2K magnification

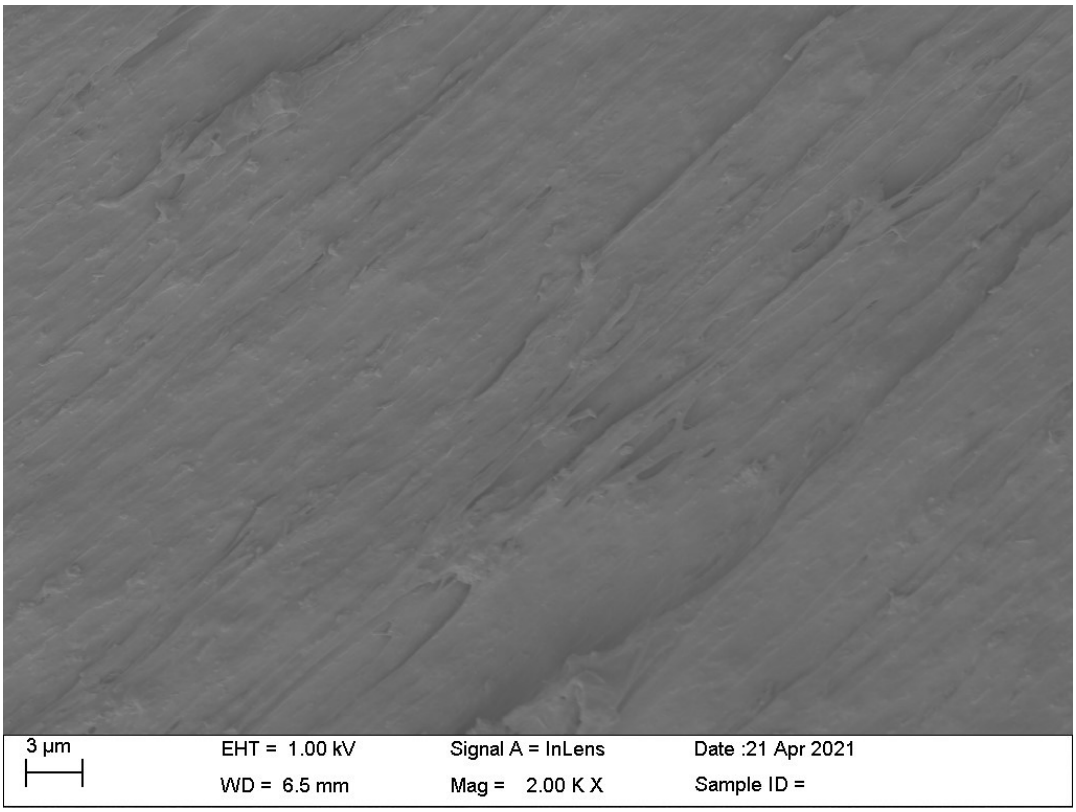

Figure 65: Sample 3, area 2, 2K magnification

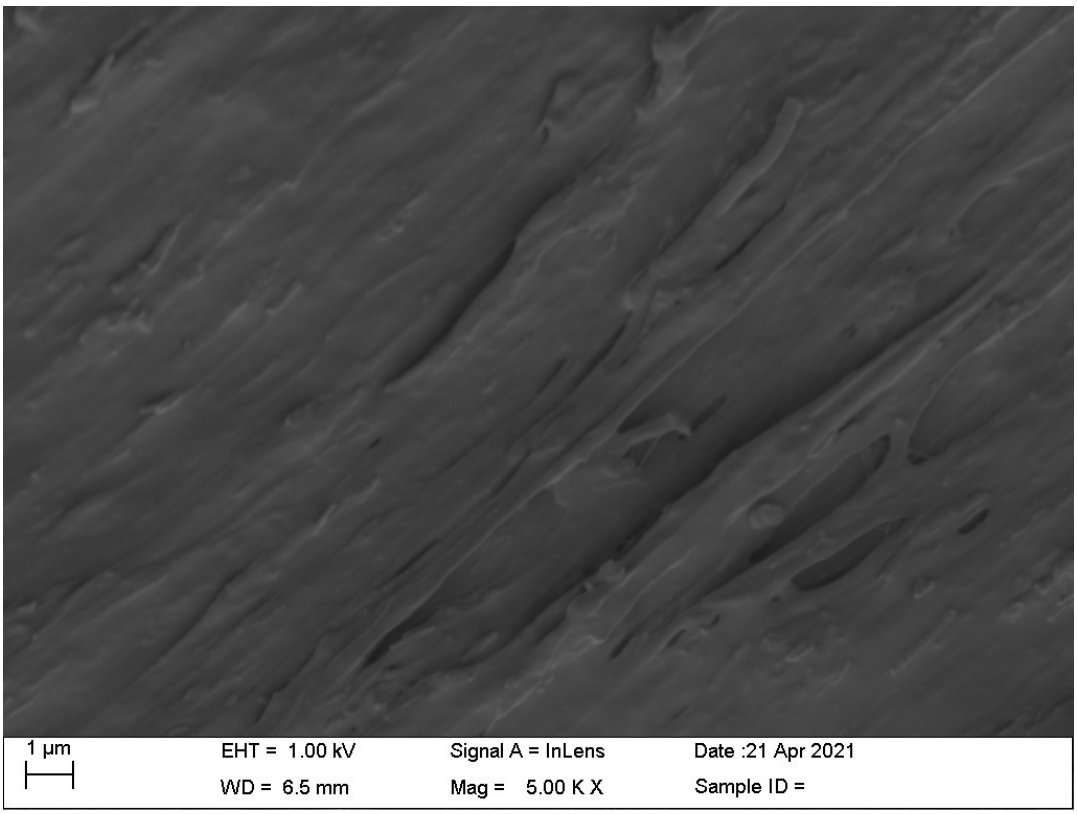

Figure 66: Sample 3, area 2, 5K magnification

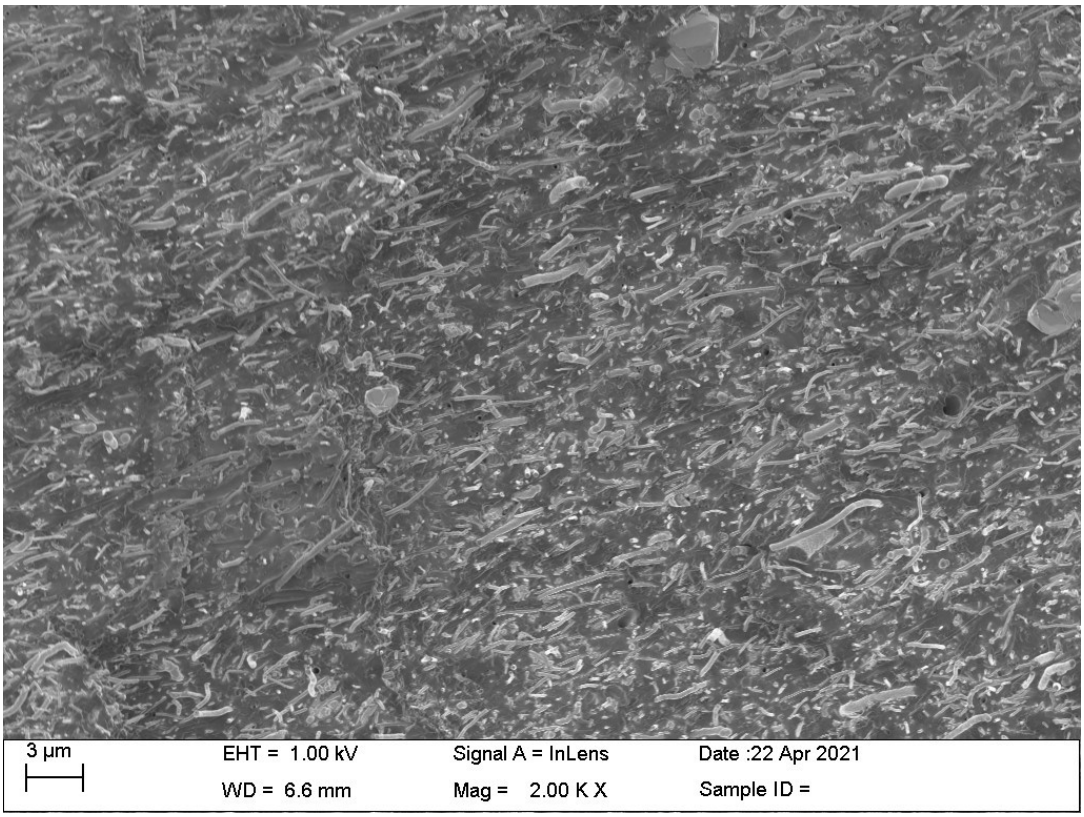

Figure 67: Sample 4, area 1, 2K magnification

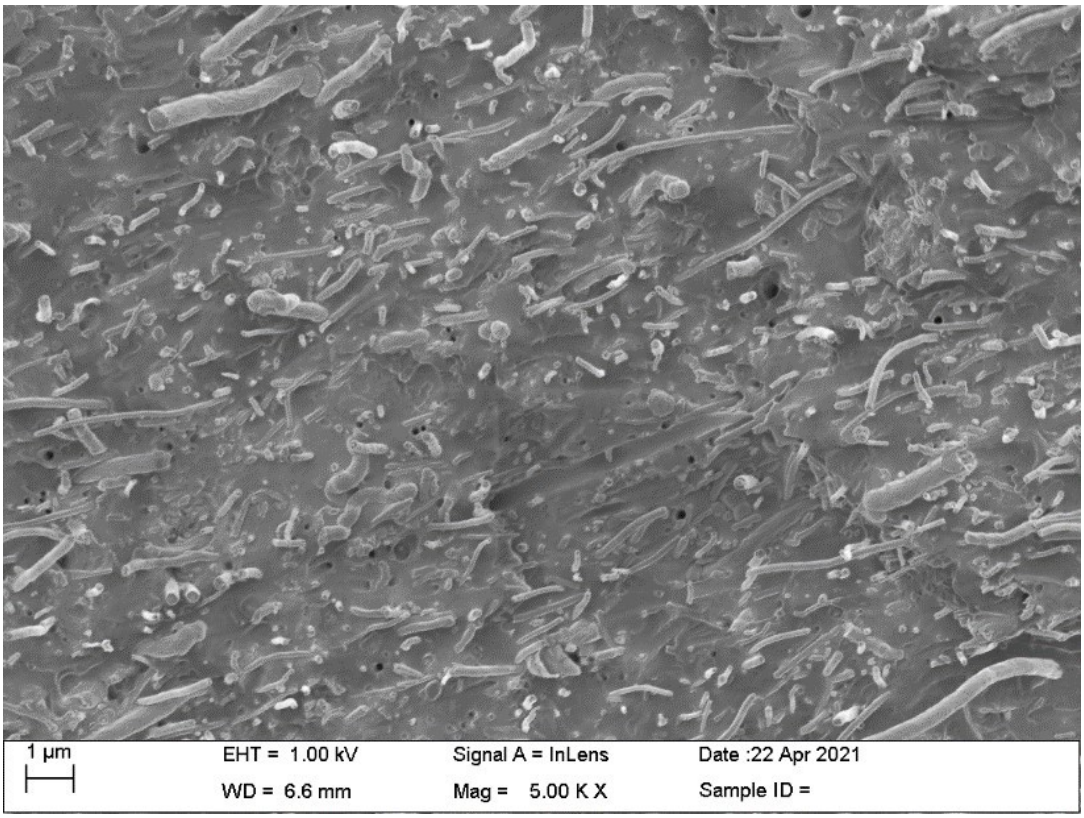

Figure 68: Sample 4, area 1, 5K magnification

APPENDIX B

APPENDIX B

ADDITIONAL MOLD FLOW SIMULATIONS

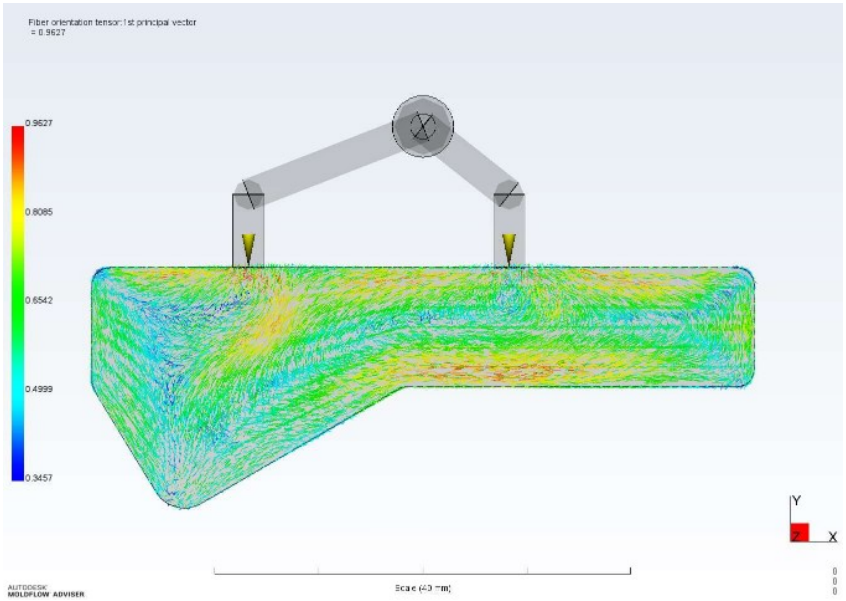

Figure 69: 2-Branch, mold flow simulation

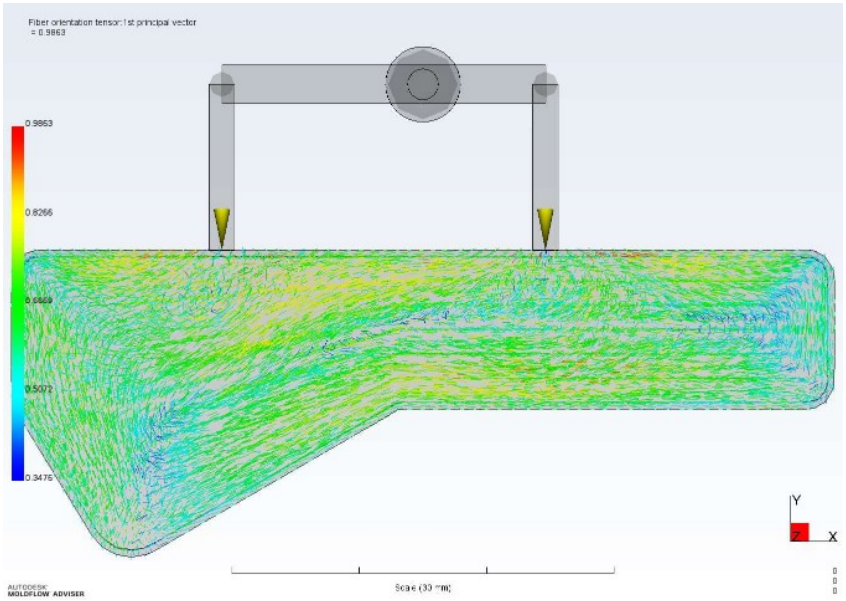

Figure 70: 2-Branch, mold flow simulation

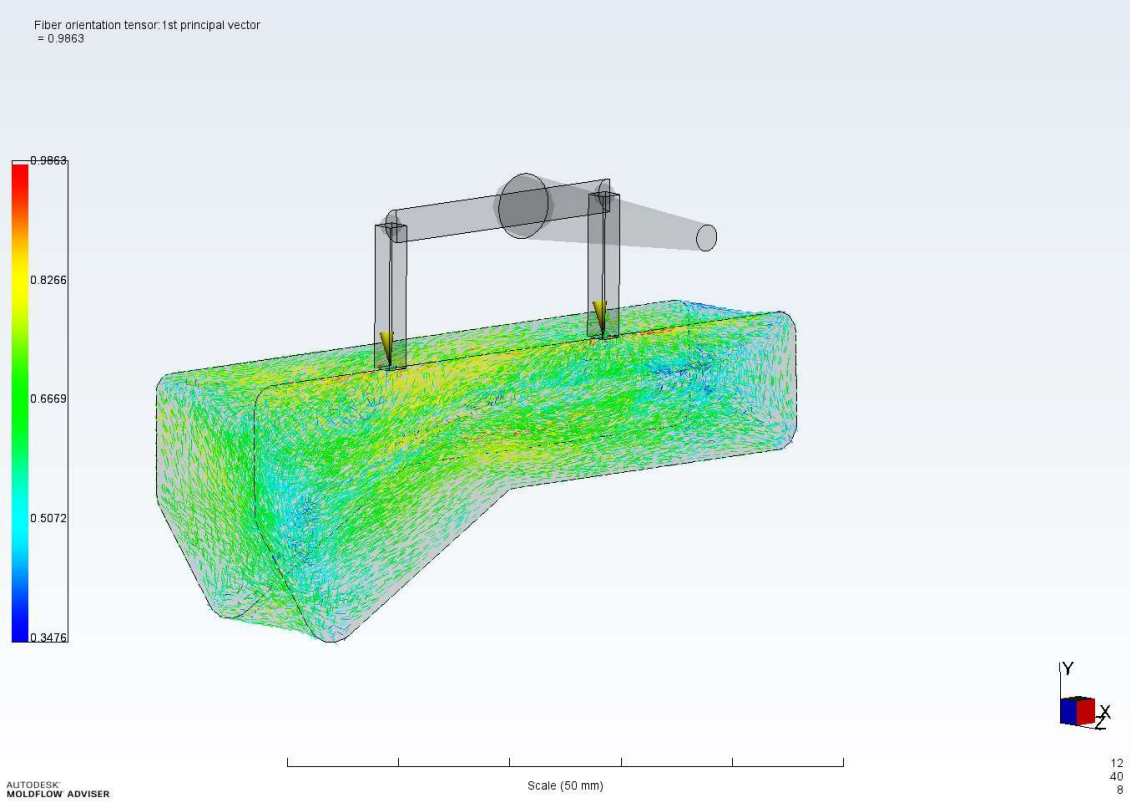

Figure 71: 2-Branch, mold flow simulation

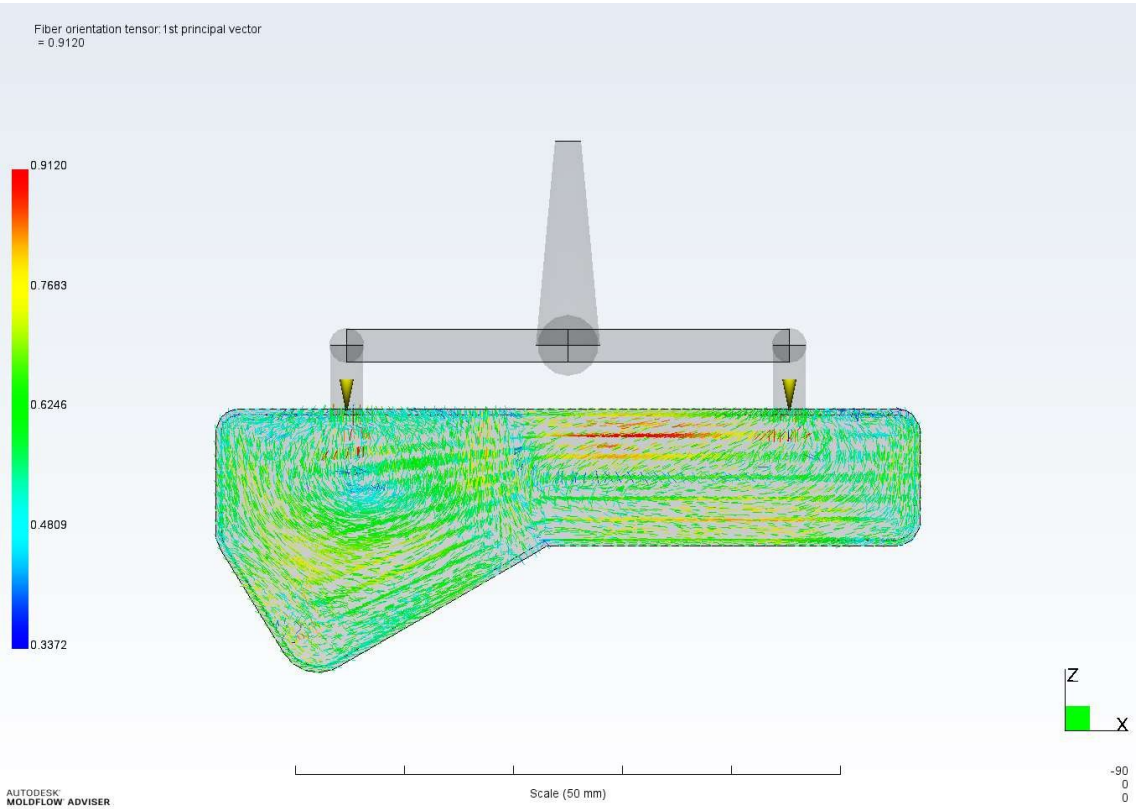

Figure 72: 2-Branch, mold flow simulation

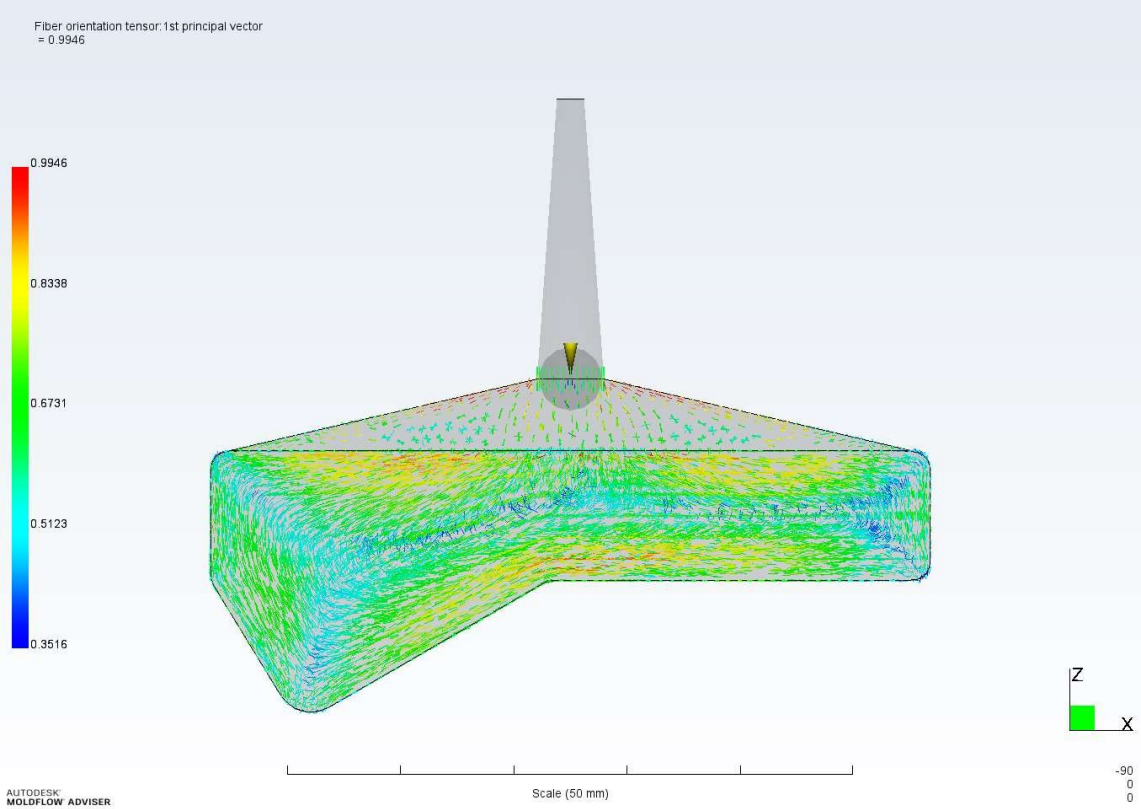

Figure 73: Fan configuration mold flow simulation

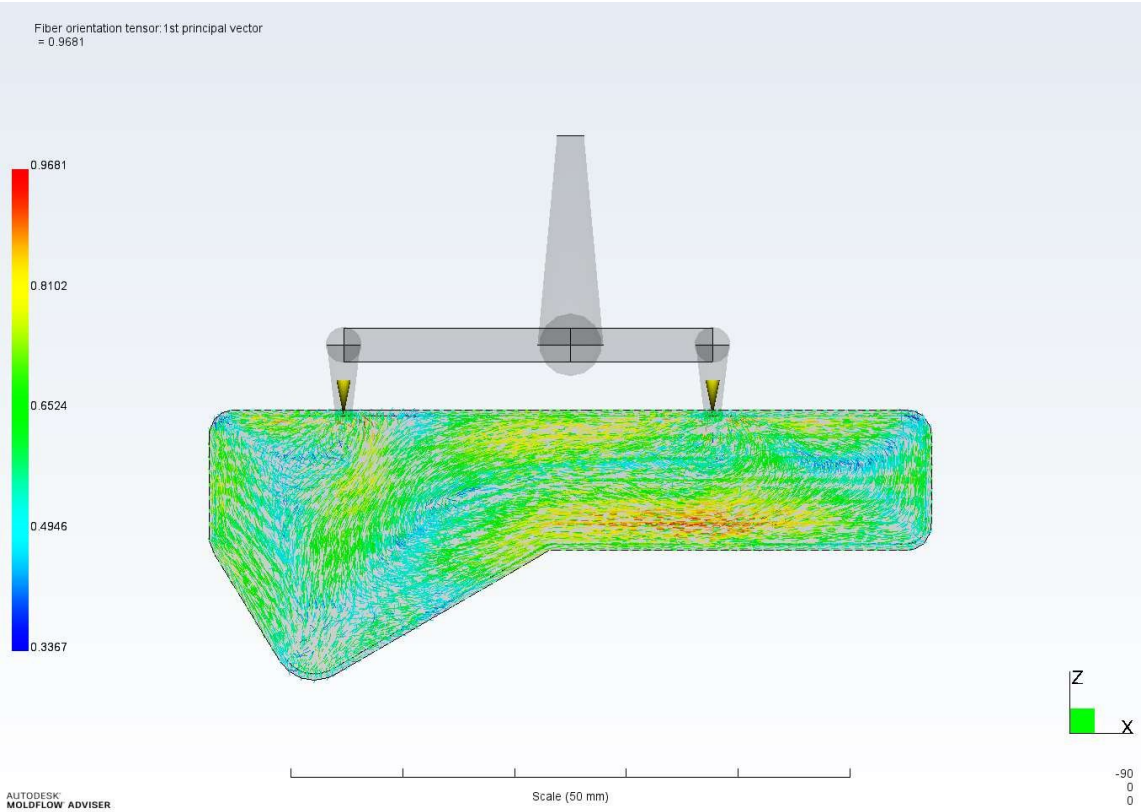

Figure 74: 2-Gate flow mold design

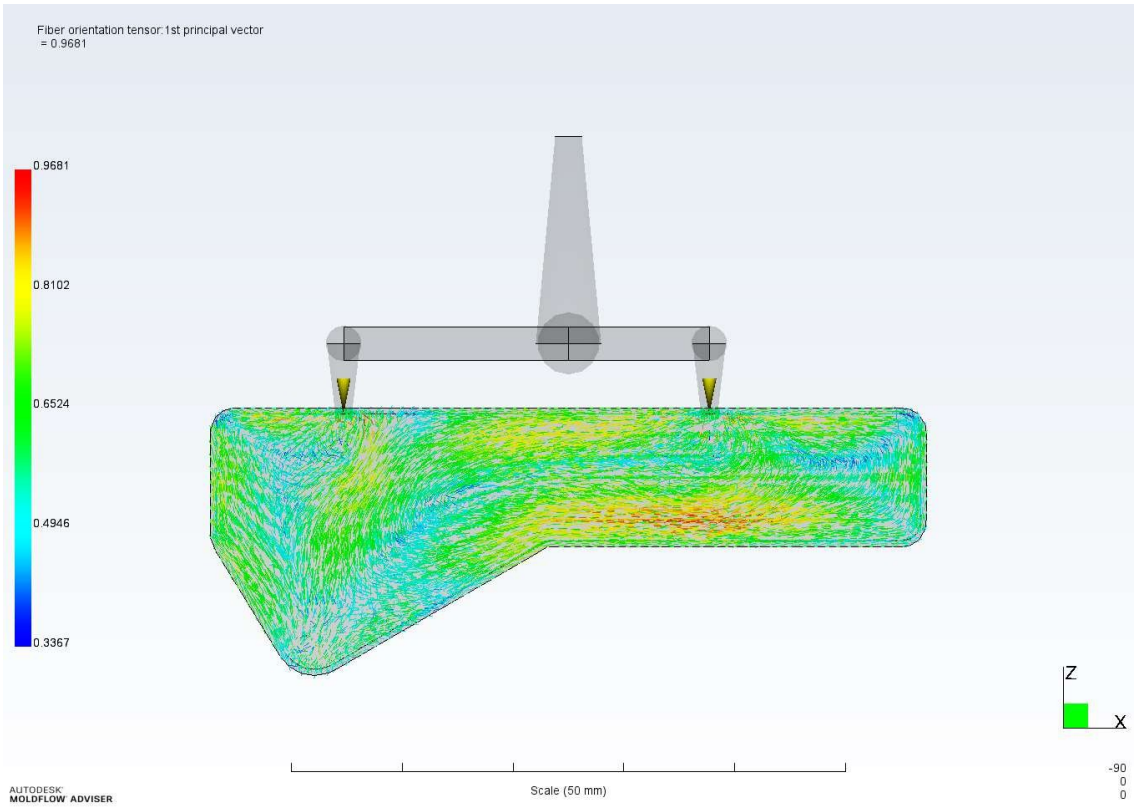

Figure 75: 2-Gate mold design

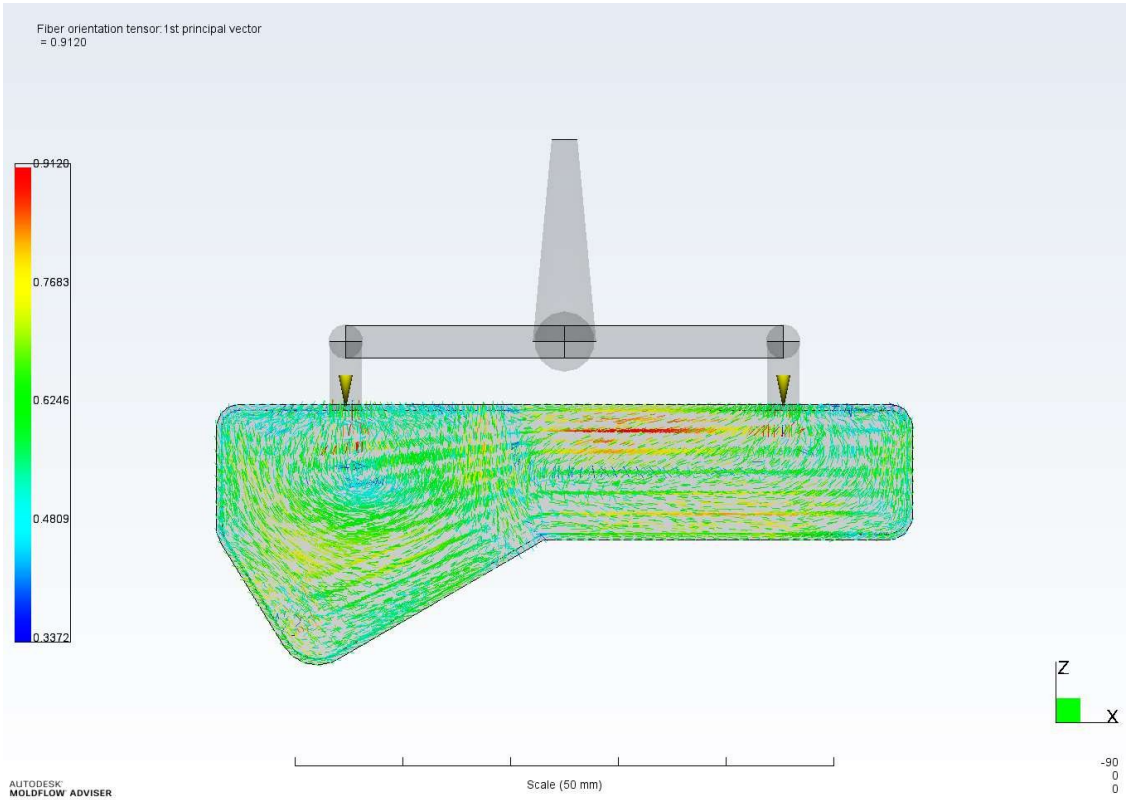

Figure 76: 2-Gate mold design

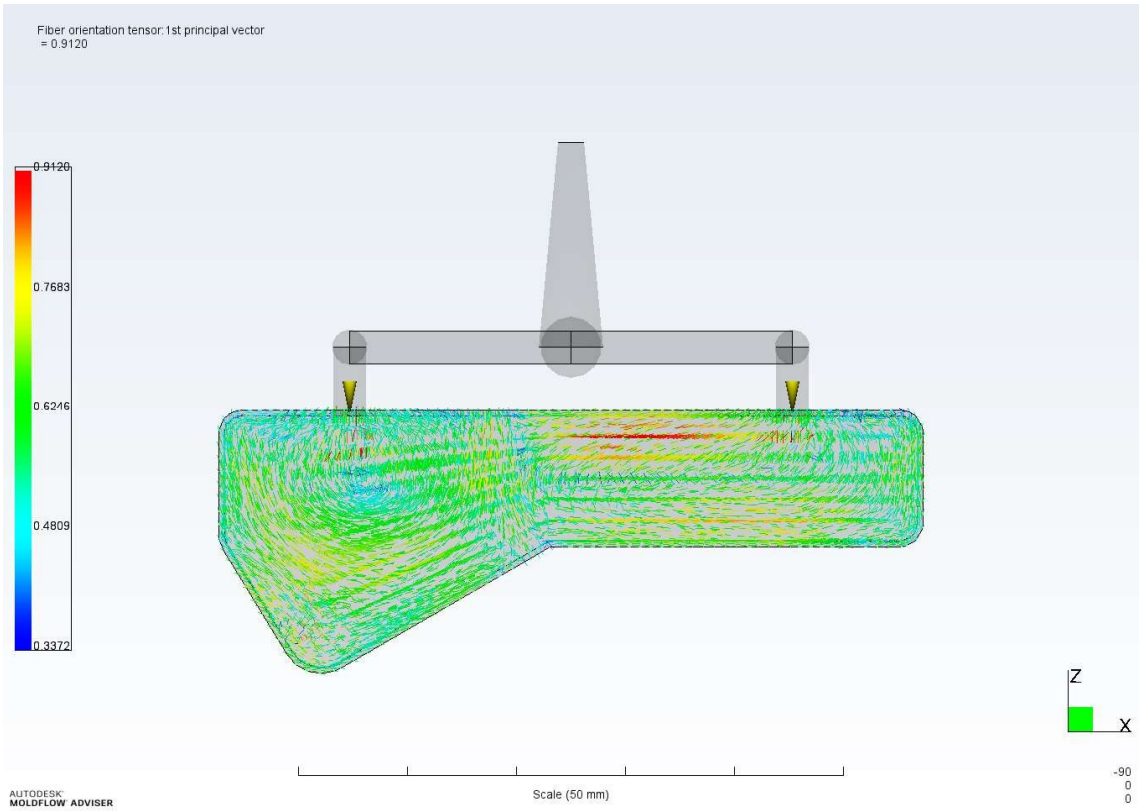

Figure 77: Two-gate mold deign

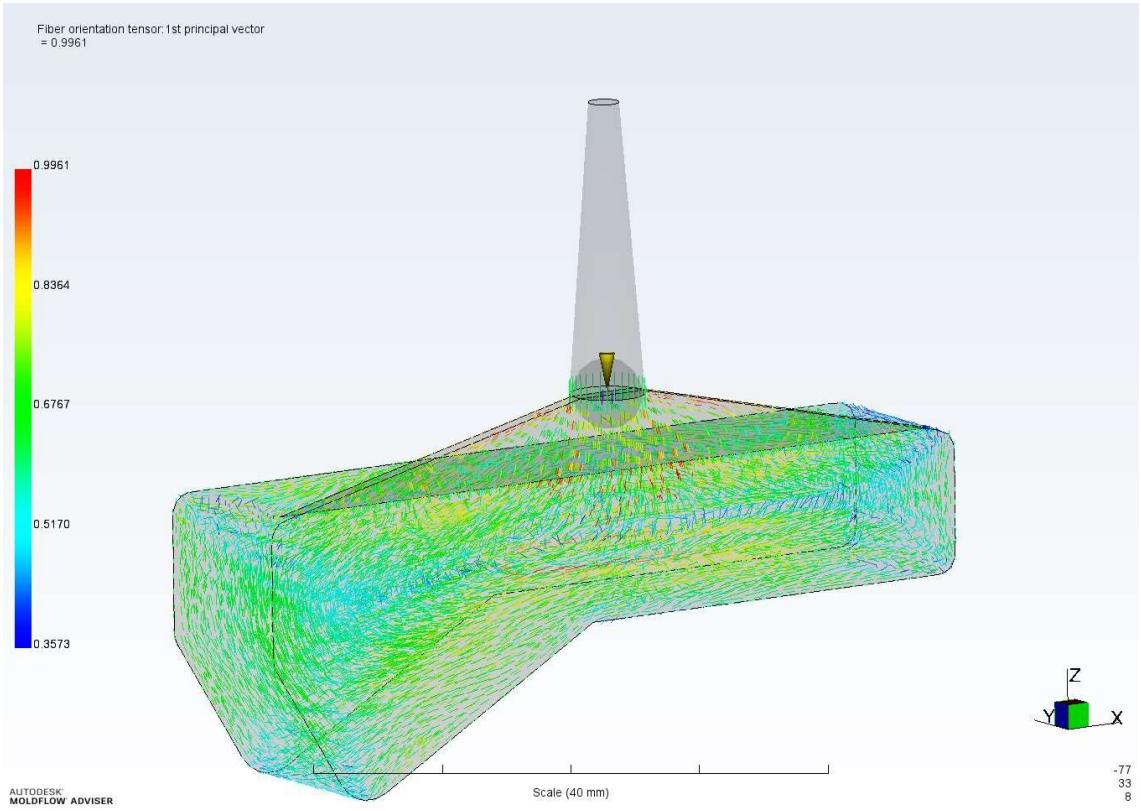

Figure 78: Fan mold simulation

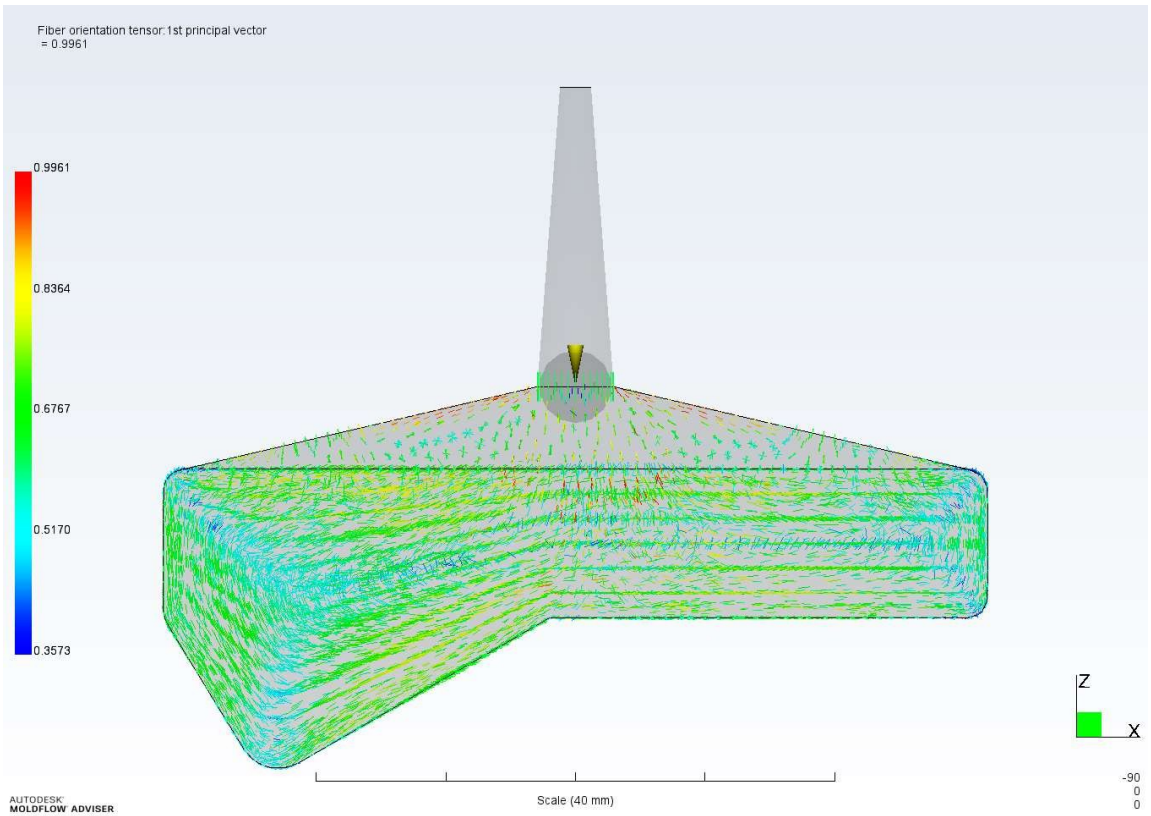

Figure 79: Fan mold flow design

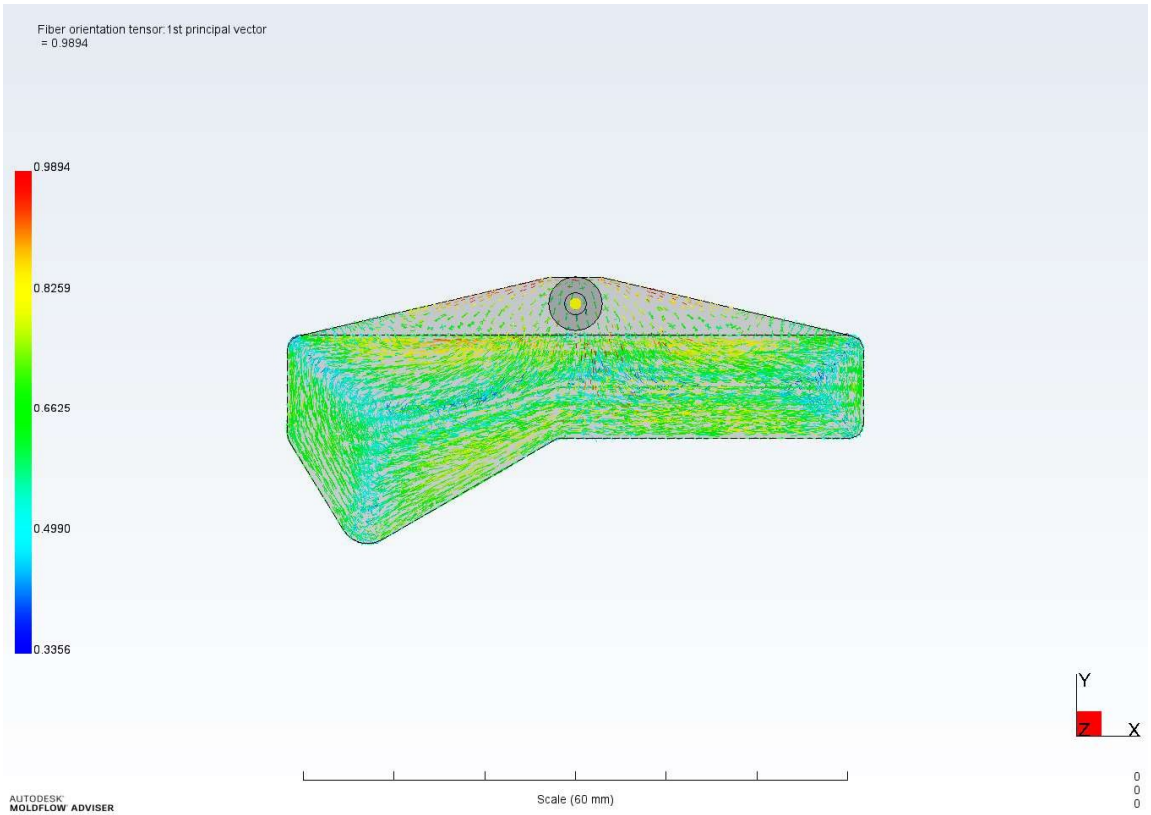

Figure 80: Fan mold design

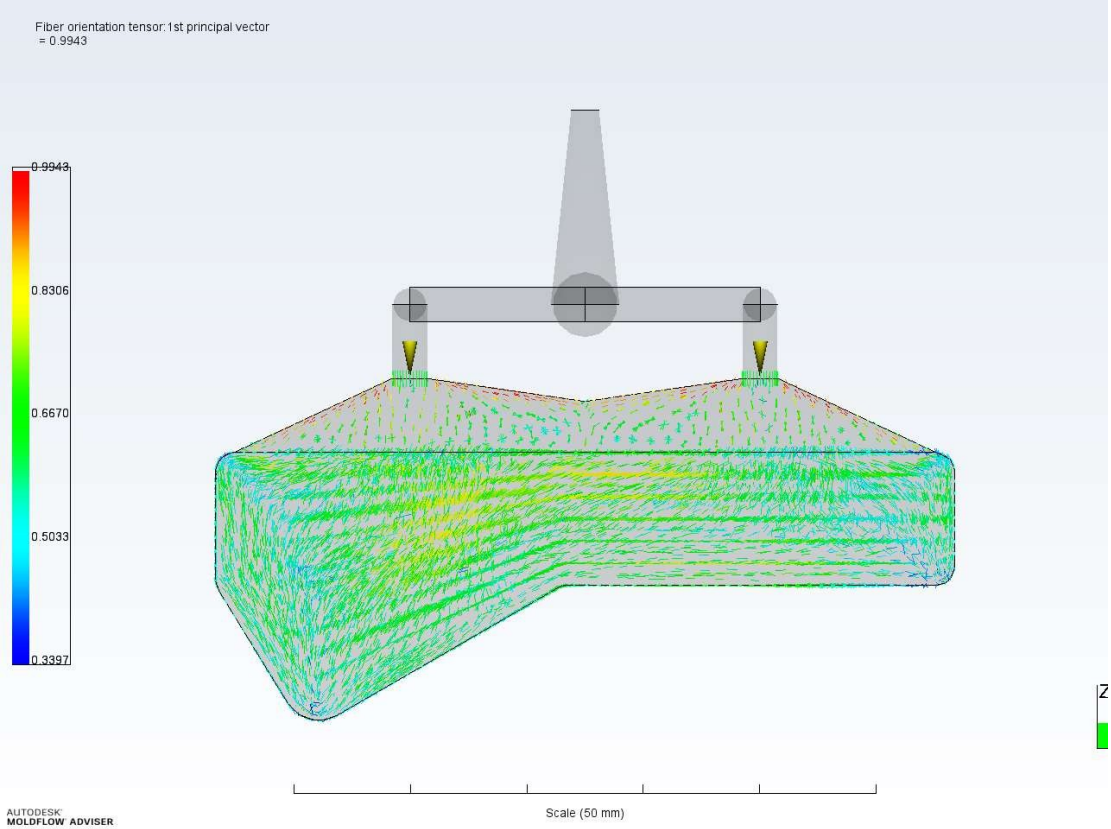

Figure 81: 2-Gate mold design

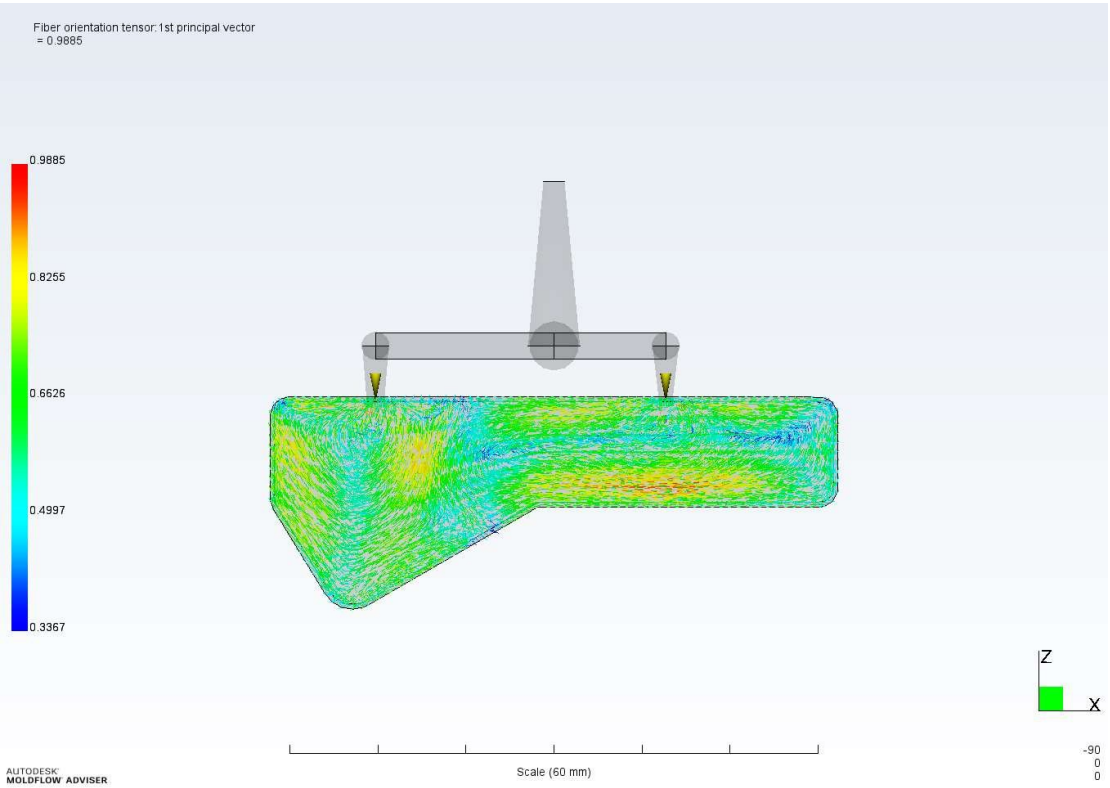

Figure 82: 2-Branch gate design

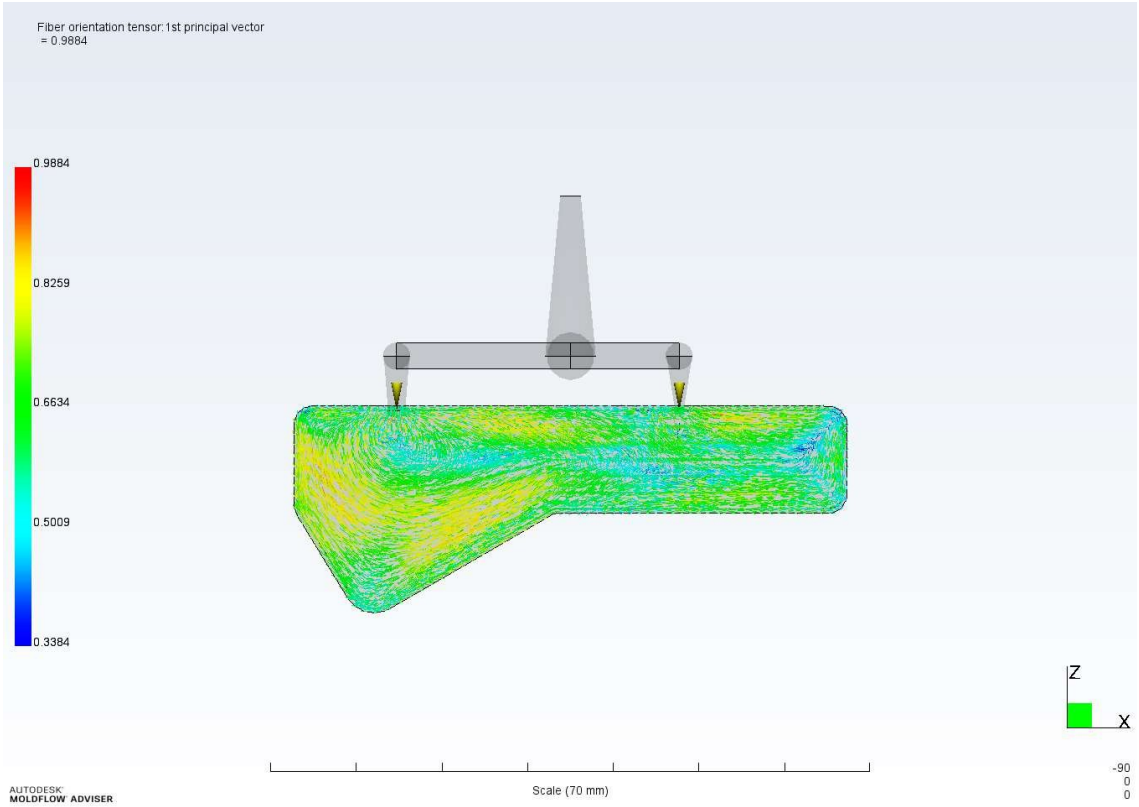

Figure 83: 2-gate mold design

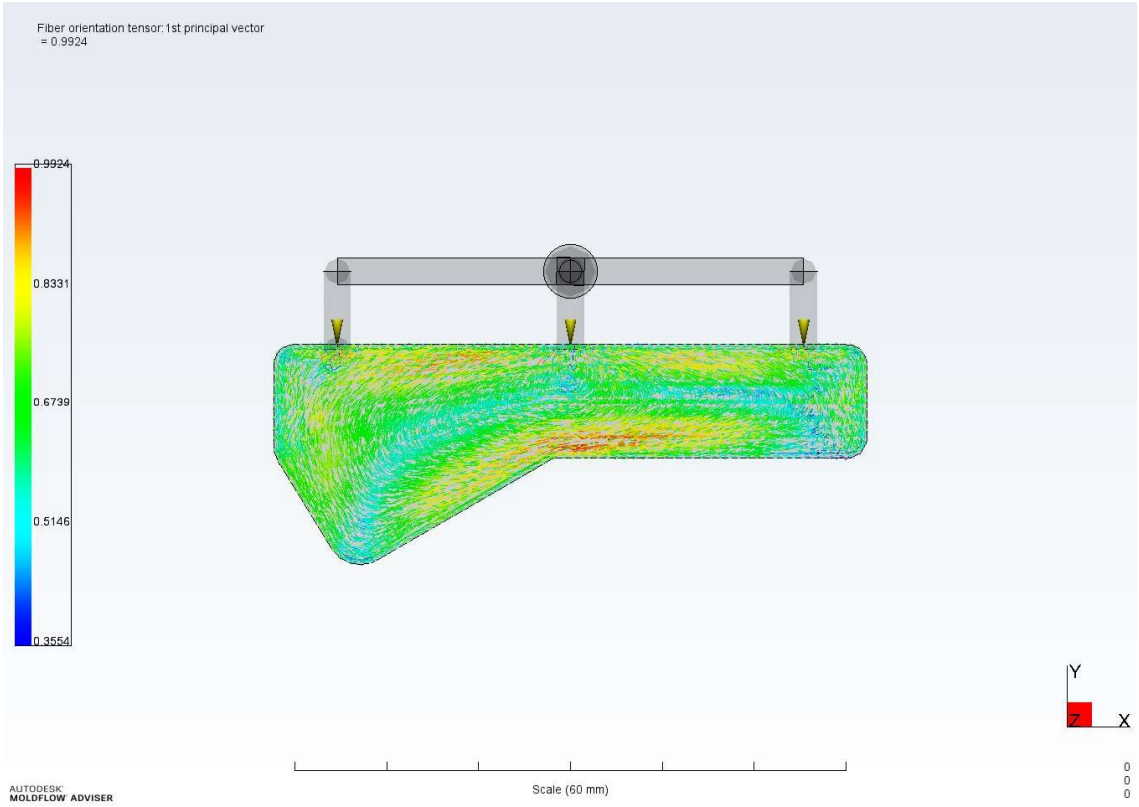

Figure 84: 3-Gate mold design

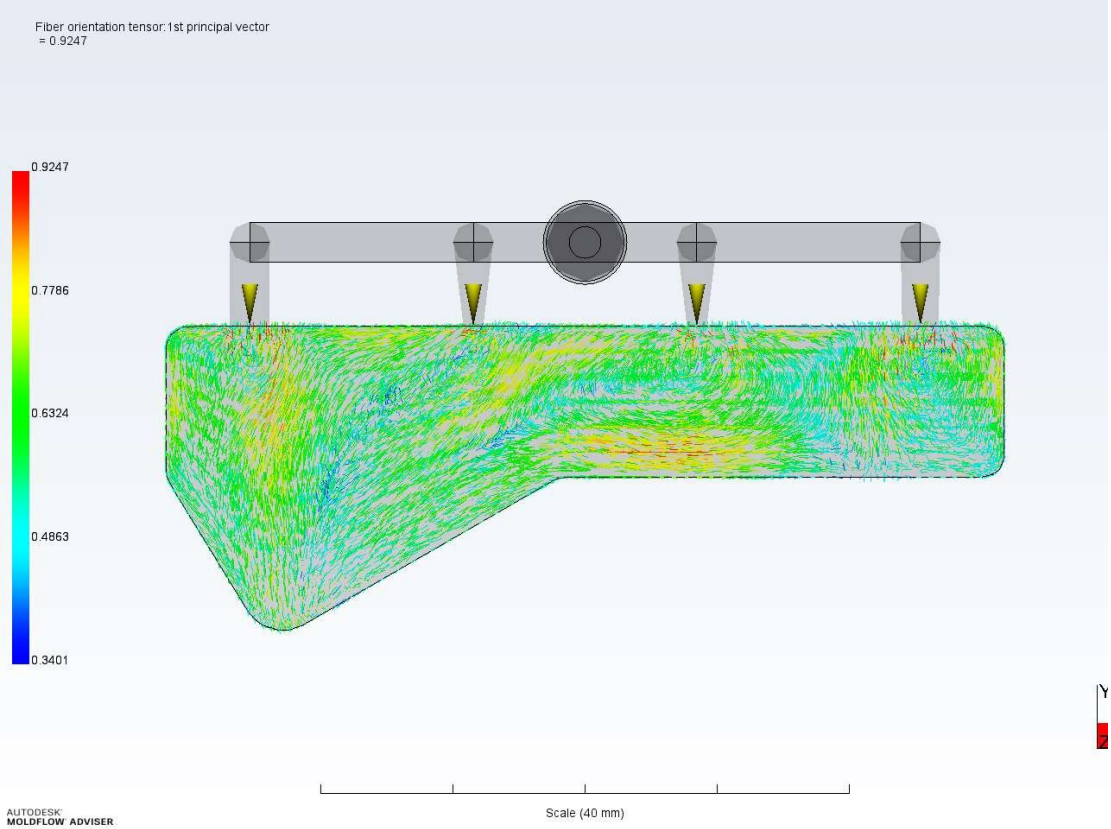

Figure 85: 4-Gate mold design

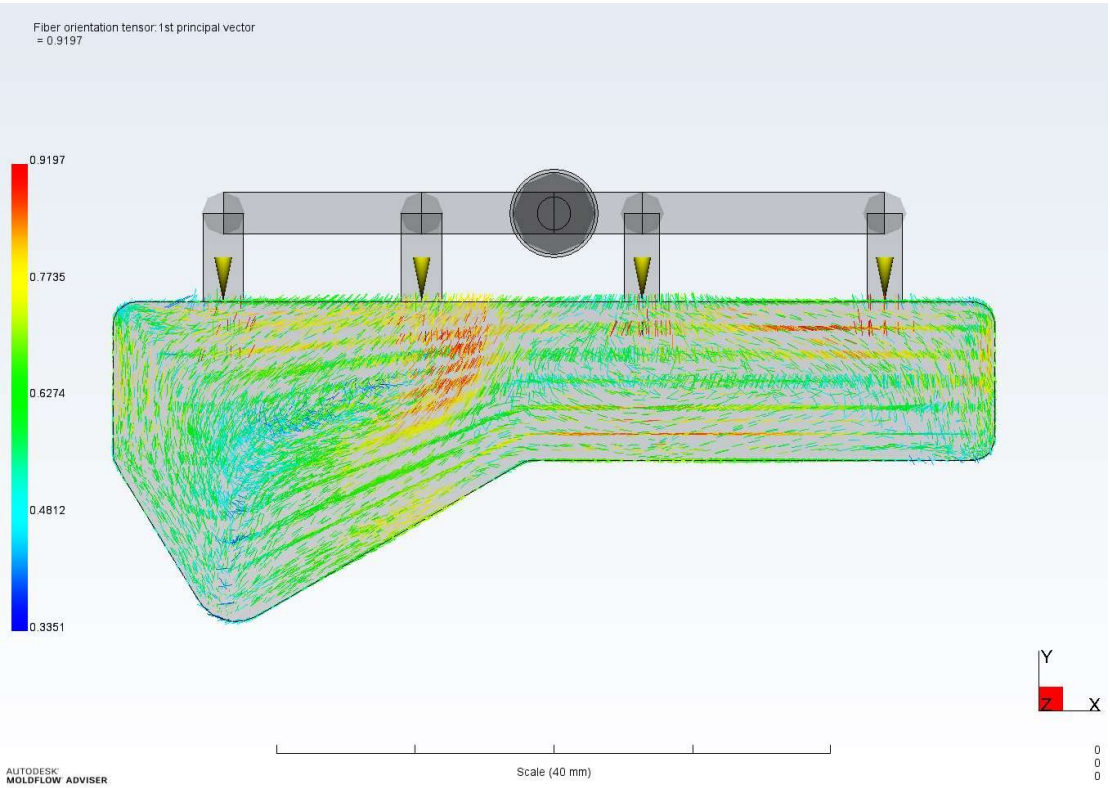

Figure 86: 4-Gate mold design

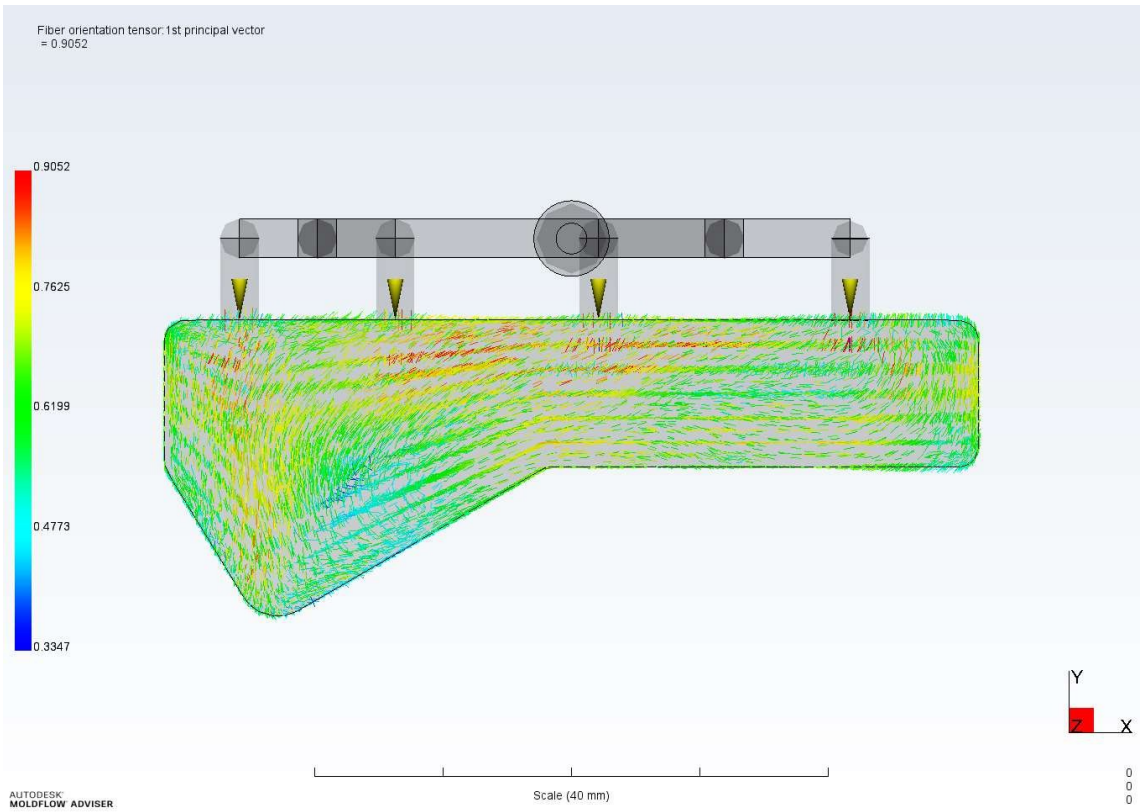

Figure 87: 4-Gate mold design

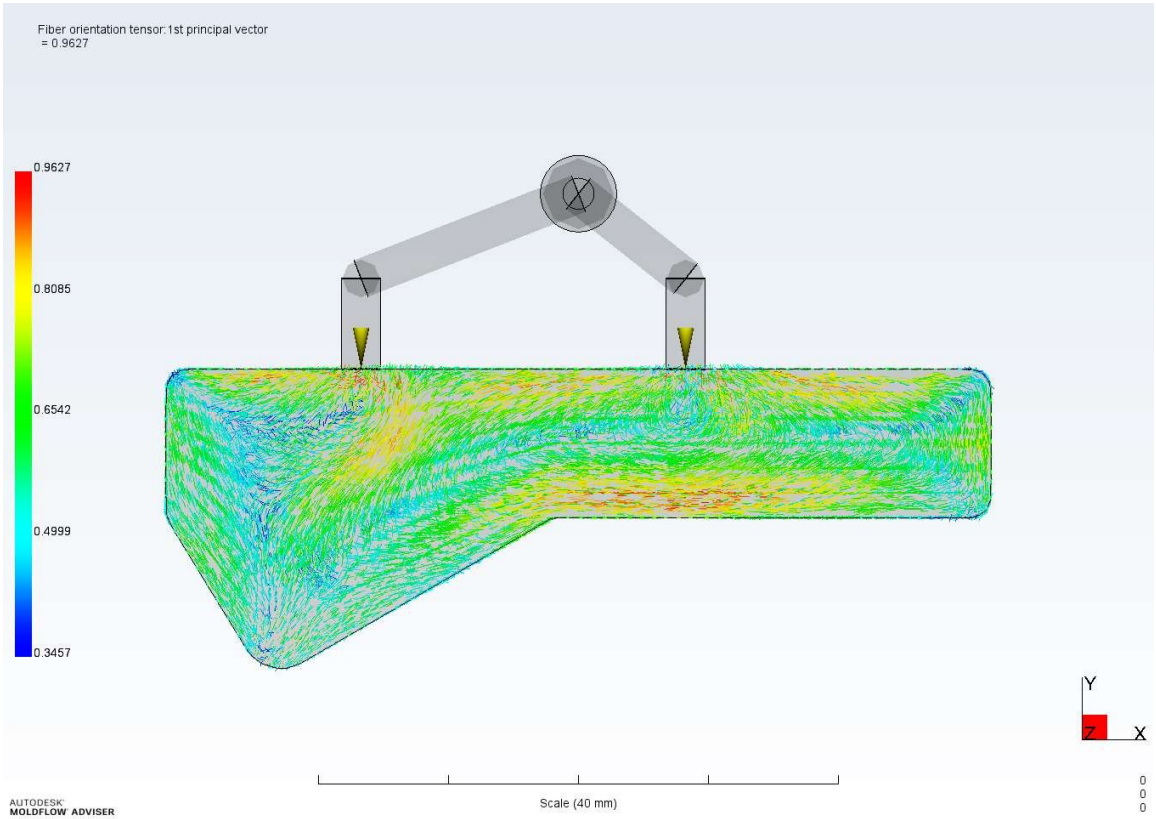

Figure 88: 2-Gate mold design

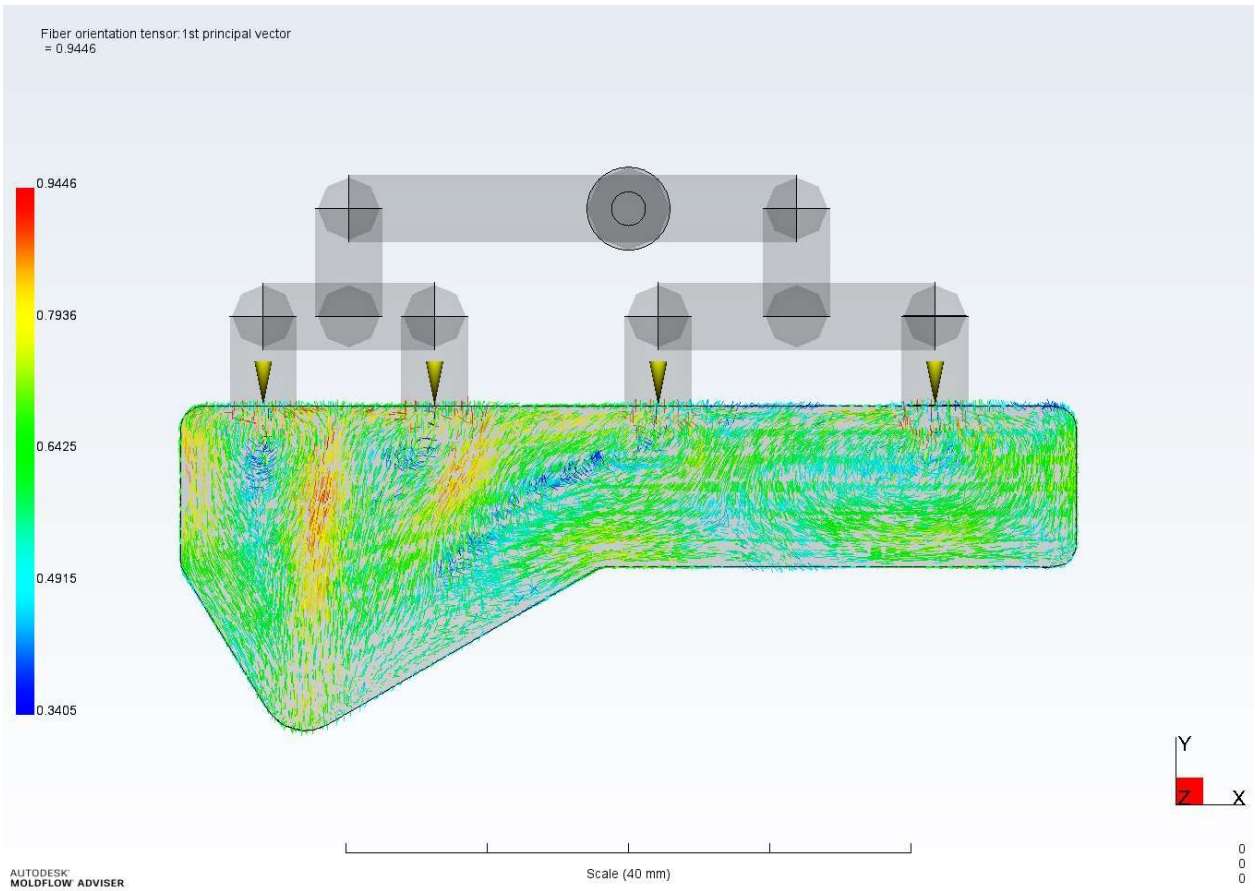

Figure 89: Final design, modified

BIOGRAPHICAL SKETCH

Jesse M. Aguilera was born on the June 19th, 1987 in the city of Chicago, Illinois, to Mr. Jesse and Belinda Aguilera. He graduated from La Vernia high school in 2005 and began working where the learned and became passionate about engineering and attending evening class at the community college in San Antonio, with engineering in mind.

He would later transfer to Austin Community College and obtained an Associates of Applied Science in computer aid drafting in the fall of 2014. Knowing the importance of education, he took his experience and in 2017, applied to The University of Texas Rio Grande Valley to continue his education in mechanical engineering. Here, he met great faculty and people that would change his life. He earned his Bachelor of Science in Mechanical Engineering in the Spring of 2020.

During his senior year of his undergraduate studies, he was given an opportunity to work with Dr. Constantine Tarawneh, the Associate Dean of Engineering at his center, the University Transportation Center for Railway Safety where he applied his knowledge from industry and academia, to become a more successful engineer, and to experience real life scenarios not found in textbooks or classrooms. The research led him to earn the Dwight D. Eisenhour Transportation Fellowship and obtain his Master of Science in Mechanical Engineering in the Spring of 2022. With great admiration and appreciation, Jesse remains forever to Dr. Tarawneh and the team at the UTCRS. Jesse can be reached at 244 Deer Ridge Drive, La Vernia, Texas 78121.